

# Subunit diversity of the nematode levamisole-sensitive acetylcholine receptor

Thomas B. Duguet  
Institute of Parasitology  
McGill University  
Montreal - Canada

2017

A thesis submitted to McGill University in partial fulfillment of the requirements of the degree of  
Doctor of Philosophy.

© Thomas B. Duguet 2017

## Abstract

Pentameric ligand-gated ion-channels (pLGICs) represent a large family of transmembrane proteins that play a fundamental role in synaptic neurotransmission throughout the animal kingdom. These essential mediators of neuromuscular movement appeared more than two billion years ago and through the central mechanism of gene duplication and loss, have led to a diverse family of modern-day pLGICs. The evolution of pLGICs has given rise to a complex population of heteromeric receptors, particularly in the clade V nematode species, closely related to the free-living model *Caenorhabditis elegans*. Among them, the levamisole-sensitive acetylcholine receptor (L-AChR) stands out, composed of five different subunits in *C. elegans*. The appearance of new subunits of this receptor continues through gene duplication. Expansion of the *unc-29* gene to four copies in the parasitic nematode of small ruminants, *Haemonchus contortus*, is proposed as a model of the process more generally. I was able to show that despite very similar sequences, the four copies have diverged in function, most clearly in their interaction with other subunits of the receptor. Interaction with  $\alpha$ -type subunits limits the role that non- $\alpha$  type subunits can play in a functional receptor and these evolved interactions break down when subunits of different species are combined into the same receptor. I was also able to define the structural organization of the *C. elegans* L-AChR and so demonstrate these interactions occur between subunits in physical contact. This work provides a foundation that can be used to identify the precise mechanisms that determine subunit diversification in this complex family of pLGIC receptors.

## Résumé

Les canaux ioniques pentamériques ligand-dépendants (pLGICs) font partie d'un vaste groupe de protéines transmembranaires jouant un rôle fondamental dans la neurotransmission synaptique au sein du règne animal. Ces acteurs essentiels des mouvements neuromusculaires sont apparus il y a plus de 2 milliards d'années et ont, par le biais de duplications ou pertes génétiques, donné naissance à la grande famille des pLGICs actuellement connus. L'évolution des pLGICs a permis l'émergence d'une population complexe de récepteurs hétéromériques, en particulier dans la clade V des nématodes apparentés à l'espèce modèle libre *Caenorhabditis elegans*. Parmi eux, le récepteur à l'acétylcholine sensible au lévamisole (L-AChR) se démarque de part la présence de cinq sous-unités différentes chez *C. elegans*. L'apparition des nouvelles sous-unités de ce récepteur semble être en progression *via* le phénomène de duplication de gènes. En effet, l'expansion du gène *unc-29* sous forme de quatre copies chez le nématode parasite des petits ruminants *Haemonchus contortus*, est proposé en tant que modèle de ce processus de manière plus générale. J'ai pu démontrer que malgré des séquences très similaires, ces quatre copies ont subi une divergence fonctionnelle particulièrement marquée au niveau de leurs interactions respectives avec les sous-unités voisines du récepteur. En principe, les interactions avec les sous-unités de type  $\alpha$  limitent le rôle que les sous-unités non- $\alpha$  peuvent jouer au sein de récepteurs fonctionnels. En revanche, la combinaison de sous-unités provenant de différentes espèces au sein d'un même récepteur permet d'annihiler ces relations et de mieux comprendre leur rôle respectif. J'ai également pu établir l'organisation structurale du L-AChR de *C. elegans* et démontré que les interactions entre sous-unités se déroulent parmi celles établissant un contact physique direct. Ce travail fournit une base solide qui permettra d'identifier les mécanismes précis qui déterminent la diversification des sous-unités au sein de la grande et complexe famille des pLGICs.

## Acknowledgements

Above all, I would like to express my warmest thanks to my supervisor Dr. Robin Beech, for his unstinting support throughout these years. I received so much from you: your confidence, your constant encouragement and above all an open door at all times. I am so grateful that you bet on me and believed in our project, in joy and good atmosphere. I would also like to thank my co-supervisor Cédric Neveu. You have also done a lot to make my project as successful as possible, strong with your precious advice and experience.

I will not forget that my adventure also started at INRA, in Nouzilly, France. Thus, I would like to take this opportunity to thank Dr. Claude Charvet for his great involvement and support during my student adventure. I also thank INRA members: Dr. Élise Courtot, Dr. Mohammed Issouf, Jacques Cortet and Christine Sauvé for their technical assistance during my journey in France.

The Institute of Parasitology was a second home to me. I would especially like to thank Dr. Timothy Geary for participating in my entry into the PhD program. His smiles and loud laughs were a real pleasure. I also thank Shirley Mongeau, Serge Dernovici, Gordie and Mike for their very useful administrative and technical support as well as for their precious kindness.

I also owe the accomplishment of my work to the former or current members of the Geary group: Dr. Vanessa Dufour, Dr. Lucien Rufener, Dr. Elizabeth Ruis-Lancheros, Dr. Lucienne Tritten, Dr. Cristina Ballesteros and Mark Kaji who provided valuable help when I needed it the most.

I would like to thank Dr. Sean Forrester and Micah Callanan from the University of Ontario, Institute of Technology for welcoming me and giving me the opportunity to achieve some of my research objectives.

Thank you to Dr. Joseph Dent and Dr. Claudia Wever, Department of Biology, McGill, for opening their lab and giving assistance with *Xenopus* housing, handling and surgery as well as for *C. elegans* microinjections.

I would also like to thank Dr. Paula Ribeiro and Dr. Sean Forrester as members of my advisory committee for their instructive recommendations throughout my PhD project.

Thank you Jessica, who always encouraged me despite your own challenges and for your solid love. Thank you Papa & Maman, the best parents in the world without whom nothing would have been possible. Thank you Manon, Monique, Claude and Colette for your constant love and support.

Thank you all for making me a new person.

## **Dedication**

To Bernard Duguet and his unfailing confidence in me until the end.

## Contribution of authors

All the experiments, data acquisition and analysis were performed by the author with the supervision of Dr. Robin Beech and Dr. Cédric Neveu. Laboratory space and resources were provided by Dr. Robin Beech, Dr. Timothy Geary, Dr. Sean Forrester, Dr. Joseph Dent and Dr. Cédric Neveu. The preparation and edition of all figures and tables presented in this thesis were also executed by the author.

Chapter II is based on the following published article. Only the work for which I was responsible is reported in this chapter and the text is completely rewritten. Figures presented in chapter II have directly been extracted, with permission, from the following publication:

Duguet, T. B., C. L. Charvet, S. G. Forrester, C. M. Wever, J. A. Dent, C. Neveu and R. N. Beech (2016). "Recent Duplication and Functional Divergence in Parasitic Nematode Levamisole-Sensitive Acetylcholine Receptors." *PLoS Neglected Tropical Diseases* 10(7): e0009826.

Dr. Robin Beech performed the bioinformatic and phylogenetic analysis of the nematode *unc-29* genes in the journal article (Duguet et al., 2016). Dr. Beech also contributed in the editing of this thesis.

All the results presented in chapter III and IV should be considered original contributions to the field of research and have not yet been submitted for publication. The conception and design of experiments from chapter III were made in collaboration with my supervisors. Chapter IV corresponds to a research project exclusively proposed and designed by the author.

- The original pTB207 plasmids (*Xenopus laevis* oocyte expression) containing the *Caenorhabditis elegans* L-AChR subunits cDNA sequences were a gift from Dr. Thomas Boulin.
- The insertion into pTB207 of *Haemonchus contortus* L-AChR subunits and accessory proteins corresponding cDNAs were originally performed and provided by Dr. Cédric Neveu and Dr. Claude Charvet.
- The *ttx-3::GFP* (*C. elegans* plasmid marker) was kindly provided by Dr. Joseph Dent (Department of Biology, McGill University)

## List of Abbreviations

- AbD: antibody diluent
- ACC: acetylcholine chloride channel
- ACh: acetylcholine
- AChR: acetylcholine receptor
- ACR (protein): acetylcholine receptor
- ATP: adenosine triphosphate
- AUP: animal use protocol
- BAPTA-AM: 1,2-bis(2-aminophenoxy)ethane-N,N,N',N'-tetraacetic acid tetrakis(acetoxymethyl ester)
- BEPH: bephenium
- BiP: binding immunoglobulin protein
- cDNA: complementary deoxyribonucleic acid
- CGC: *Caenorhabditis* Genetics Center
- CHRNA: acetylcholine receptor alpha subunit gene
- cRNA: complementary ribonucleic acid
- DEG: degeneration of certain neurons
- DES: degeneration suppressor
- DH $\beta$ E: dihydro- $\beta$ -erythroidine
- DMPP: dimethylphenylpiperazinium
- dNTP: deoxynucleoside triphosphate
- dTC: d-tubocurarine
- EC<sub>50</sub>: half maximal effective concentration
- EGL: egg laying defective
- ELIC: *Erwinia* ligand-gated ion-channel
- ELISA: enzyme-linked immunosorbent assay



- ER: endoplasmic reticulum
- EXP: expulsion defective protein
- GABA:  $\gamma$ -aminobutyric acid
- GFP: green fluorescent protein
- GGR: glycine-gated receptor
- GLIC: *Gloeobacter* ligand-gated ion-channel
- GluCl: glutamate chloride channel
- GlyR: glycine receptor
- 5HT: 5-hydroxytryptamine
- iGluR: ionotropic glutamate receptor
- L1-4: larval stage
- L-AChR: levamisole-sensitive acetylcholine receptor
- LEV (drug): levamisole
- LEV (protein): levamisole resistance
- LGIC: ligand-gated ion-channel
- M-AChR: morantel-sensitive acetylcholine receptor
- Meca: mecamlamine
- MOD: modulation of locomotion defective
- MOLO: modulator of levamisole receptor
- MPTL: monepantel
- N-AChR: nicotine-sensitive acetylcholine receptor
- NGM: nematode growth medium
- NIC: nicotine NMJ: neuromuscular junction
- NRA: nicotinic receptor associated protein
- OCT: optimum cutting temperature
- OIG: immunoglobulin domain-containing
- OXA: oxantel

- PAR: proline-alanine-arginine
- PBS: phosphate buffered saline
- PCR: polymerase chain reaction
- PFA: paraformaldehyde
- PIP<sub>2</sub>: phosphatidylinositol-4,5-biphosphate
- pLGIC: pentameric ligand-gated ion-channel
- pTB207: *in vitro* transcription vector (*Xenopus laevis* protein expression)
- PYR: pyrantel
- RIC: resistance to inhibitors of cholinesterase
- SE: standard error
- SOC: suppressor of clear
- TBD: tribendimidine
- TEVC: two-electrode voltage-clamp
- TM1-4: transmembrane domain
- *ttx-3* (promoter): abnormal thermotaxis
- UNC: uncoordinated phenotype

# Table of contents

ABSTRACT	2
RÉSUMÉ	3
ACKNOWLEDGEMENTS	4
DEDICATION	6
CONTRIBUTION OF AUTHORS	7
LIST OF ABBREVIATIONS	8
TABLE OF CONTENTS	11
<b>Chapter I: Introduction &amp; Literature Review.</b>	<b>1</b>
1.1 General introduction	1
1.2 Nematodes	3
1.2.1 <i>Caenorhabditis elegans</i>	4
1.2.2 <i>Haemonchus contortus</i>	6
1.3 Nervous system and Neurotransmission	8
1.3.1 <i>The C. elegans nervous system</i>	10
1.3.2 <i>The cholinergic system</i>	10
1.4 Pentameric Ligand-Gated Ion-Channels	11
1.4.1 <i>Structure</i>	11
1.4.2 <i>Ligand binding</i>	13
1.4.3 <i>Ion selectivity</i>	14
1.4.4 <i>Assembly</i>	15
1.4.5 <i>Chaperones</i>	16
1.5 Evolution of pLGICs	18
1.5.1 <i>Diversity</i>	18
1.5.2 <i>Gene duplication</i>	20
1.5.3 <i>Acetylcholine receptor subunits</i>	22
1.6 Levamisole-sensitive AChRs	24
1.6.1 <i>L-AChR research milestones</i>	24
1.6.2 <i>Diversity of L-AChR genes</i>	25
<b>Chapter II - Functional divergence of Hco-unc-29 subunit copies.</b>	<b>30</b>
2.1 Introduction	30
2.2 Results	31
2.2.1 <i>Reconstitution and characterization of L-AChRs with each Hco-UNC-29 copy.</i>	31
2.2.2 <i>Expression of H. contortus / C. elegans subunit admixtures in Xenopus oocytes.</i>	39

2.2.3 Expression of the <i>Hco-unc-29</i> paralogs in transgenic <i>C. elegans</i>	40
2.3 Discussion	46

### **Chapter III - Subunit interaction in the levamisole sensitive acetylcholine receptor from *H. contortus* and *C. elegans*.**

3.1 Introduction	48
3.2 Results	50
3.2.1 Admixtures in a <i>C. elegans</i> L-AChR subunit background	50
3.2.2 Admixtures in a <i>H. contortus</i> L-AChR subunit background	56
3.3 Discussion	61

### **Chapter IV - Quaternary structure of the *C. elegans* levamisole receptor.**

4.1 Introduction	64
4.2 Results	66
4.2.1 Construction and expression of dimers of L-AChR subunits	66
4.2.2 Construction and expression of trimers of L-AChR subunits	68
4.2.3 Identification of the pentameric structure of the <i>C. elegans</i> L-AChR	71
4.3 Discussion	74
Figure 4.6: Putative subunit arrangement of the <i>C. elegans</i> L-AChR	75

### **Chapter V: General Discussion.**

5.1 Hco-UNC-29 copies are functionally divergent	81
5.2 Sequence dependent mechanisms determine production of a functional L-AChRs	83
5.3 Assembly of the <i>C. elegans</i> L-AChR subunits form a unique quaternary structure	84
5.4 Remaining questions and prospects	86

### **Chapter VI: Material and methods.**

6.1 Animals	89
6.1.1 <i>Caenorhabditis elegans</i>	89
6.1.2 <i>Haemonchus contortus</i>	89
6.1.3 <i>Xenopus laevis</i>	89
6.2 AChR cDNA/cRNA library	90
6.2.1 Accession numbers	90
6.2.2 Linearization	90
6.2.3 In vitro RNA transcription	90
6.3 <i>Xenopus laevis</i> oocytes - electrophysiology	91
6.3.1 Oocyte extraction	91
6.3.2 Oocyte injection	91
6.3.3 Pharmacological compounds	91

6.3.4 <i>Two-electrode voltage clamp</i>	92
6.4 <i>Caenorhabditis elegans</i> - Transgenesis	93
6.4.1 <i>Molecular biology</i>	93
6.4.2 <i>Microinjection</i>	93
6.4.3 <i>Paralysis assay</i>	93
6.5 Immunohistochemistry	94
6.5.1 <i>Antibodies</i>	94
6.5.2 <i>Xenopus oocytes</i> - whole cell immunochemistry	94
6.5.3 <i>H. contortus</i> - cryosection immunochemistry	95
6.6 AChR subunit concatenation	95
6.6.1 <i>Dimers</i>	96
6.6.2 <i>Trimers</i>	97
6.6.3 <i>Tetramers</i>	98
5.6.4 <i>Pentamers</i>	98
<b>References</b>	<b>104</b>

# Chapter I: Introduction & Literature Review.

## 1.1 General introduction

Muscular control of movement is fundamental to animal life and emerged approximately 600 to 700 million years ago, leading to an explosion of bilaterian species that were able to explore their environment in three dimensions (Smith et al., 2013, Holland 2015). A critical component was a modification of chemoreceptors that signal through ion-flow so that they respond to chemical signals produced from other cells. Adaptation and diversification of these chemo-receptors ultimately led to a wide repertoire of synaptic signalling with neurotransmitters regulating membrane polarization of target cells. As movement directly coincides with the diversity of animal life, understanding the mechanisms controlling the diversification of neurotransmitter receptors is of fundamental importance.

Acetylcholine (ACh) was the first neurotransmitter discovered, in the early 20th century (Loewi et al., 1926) and plays a dominant role in neuromuscular coordination as a main agonist of both muscarinic (mAChRs) and nicotinic acetylcholine receptors (nAChRs). These latter have been the focus of intensive investigation since their discovery (Changeux 2012). Being structurally similar, nAChRs (also commonly named AChRs) are composed of five transmembrane subunits surrounding a central pore through which ions selectively pass into the cytosol of post-synaptic cells. Importantly, subunit composition is a key feature at the origin of the diversification of AChRs and other pentameric ligand-gated ion-channels (pLGICs) (Ortells et al., 1995, Dent 2006, Beech et al., 2015). Indeed most recent phylogenetic studies point out that homomeric receptors were likely at the origin of heteromeric receptors through a variety of diversification processes that are common to the whole pLGIC family (Ortells et al., 1995, Dent 2006, Beech et al., 2015). Although progress has been made in understanding the properties different subunits can confer on the receptor, the mechanisms controlling how subunits combine and how new subunits and new combinations arise remains poorly understood.

The major issue in the investigation of such phenomenon lies in the fact that most of the major metazoan AChR subunit types emerged approximately 600 to 700 million years ago (Ortells et al., 1995, Dent 2006, Dent 2010, Beech et al., 2014). Such a long period of evolution after the initial events has obscured those sequence residues that are responsible for subunit characteristics among many changes that have no significant effect. Recently duplicated subunits whose functional characteristics can be shown to be different would represent an ideal example to investigate these mechanisms in detail and the amino acids responsible.

A large variety of pLGIC subunits are found in the modern day that determine the ion selectivity and ligand binding properties of their receptors. Among the AChRs, two main subtypes of subunits are either called  $\alpha$  or non- $\alpha$  depending on their ability to form respectively the principal and complementary faces of the ACh binding site (Corringer et al., 2000). In nematodes, muscular AChRs are split in three major groups called N-, M- or L-type AChRs corresponding to their respective affinity to nicotine and the anthelmintics morantel and levamisole (LEV) (Martin et al., 1997, Robertson et al., 1999, Qian et al., 2006, Boulin et al., 2008, Courtot et al., 2015). The L-AChR is of particular interest as the most recent studies have revealed complex subunit composition suggesting maximal diversification (Boulin et al., 2008, Boulin et al., 2011, Buxton et al., 2014, Duguet et al., 2016). However, recent studies suggest that, in some parasitic nematode species, the same process continues in the form of newly duplicated genes (Neveu et al., 2010, Duguet et al., 2016). Indeed, the helminth genome initiative provides evidence of recent gene duplication and loss in the *unc-38* and *unc-29* families of L-AChR subunits, which seems to represent a common phenomenon of diversification among the whole Nematoda phylum (Beech et al., 2015).

Deciphering the conditions and mechanisms governing subunit gene duplications remains a requirement for understanding the establishment of pLGIC diversity within nematodes in particular. However, most duplication events are old so that gene sequences have diverged too much to determine functionally important residues. Fortunately, the identification of recently duplicated *unc-29* paralogs within the trichostrongylid nematodes and particularly in the parasitic nematode of small ruminants *Haemonchus contortus* (Neveu et al., 2010) shows that the duplication process is ongoing. More importantly, these new paralogs represent a good model for understanding the conditions and mechanisms responsible for diversification as well as their functional impact on the nematode biology.

In order to understand the relevance of such a model, it is critical to understand the general biology of nematodes. The free-living species *C. elegans* and the parasitic nematode *H. contortus* are here proposed as model organisms to study subunit duplication, as one possesses a single *unc-29* gene whereas the other expresses four paralogs, a phenomenon that is found more generally across the strongylid nematodes (Duguet et al 2016). In order to understand this in context, I will present a review of nematode biology, their neuromusculature and specifically the structure and function of the pLGIC neurotransmitter receptors. I will review what is known about gene duplication and accompanying changes in the pharmacological properties of pLGIC receptors and conclude this introduction with a

description of what is known to date in terms of the evolutionary changes and in the L-AChRs of different species of parasitic nematodes. 1.2 Nematodes

In the animal kingdom, insects and nematodes share a common ancestor of moulting animals, the ecdysozoa (Aguinaldo et al., 1997). Nematodes represent the second most abundant group of animals after insects with up to 10 millions estimated species of which only 26,000 have been reported so far and 100 are currently targeted for genome sequencing (Blaxter et al., 1998, Blaxter et al., 2015). Also called "round worms", the nematodes are characterized by a simple and conserved morphology despite a high diversity of species. Physiological functions such as the respiratory and circulatory systems are absent. The nematode body is non segmented and covered with a resistant cuticle and the digestive and muscular systems are present in tubular form (Basyoni et al., 2016). A nervous system often qualified as anatomically simple but neurochemically complex is present and ensures locomotion, reproduction, feeding, and other major biological functions (White et al., 1986, Basyoni et al., 2016).

Free living nematodes can complete their life cycle in large numbers in both aquatic and terrestrial environments (Floyd et al., 2002, Lee 2002). They play an important role in the equilibrium of soil ecosystems by recycling mineral and organic material (Lee 2002). Many species parasitize a variety of eukaryotic multicellular organisms including humans, insects, animals in general and plants. They are consequently a global problem for human health (Lustigman et al., 2012), and the reason for important economic losses for livestock production and agriculture (Abad et al., 2008, Roeber et al., 2013).

The phylum Nematoda has long been classified for their distinctive morphological properties (Durette-Desset et al., 1999, Lee 2002). However, recent phylogenetic studies have allowed a more detailed classification based on the sequencing of ribosomal RNA subunits (Blaxter et al., 1998, Parkinson et al., 2004, Mitreva et al., 2005, Holterman et al., 2006, Blaxter et al., 2015). The phylum is classified into five clades: clade I (Dorylaimia), clade II (Enoplia), clade III (Spirurina), clade IV (Tylenchina), clade V (Rhabditina) and are composed of free-living and parasitic nematodes targeting humans, animals or plants (Parkinson et al., 2004, Mitreva et al., 2005, Meldal et al., 2007, Blaxter et al., 2015) (Figure 1.1).



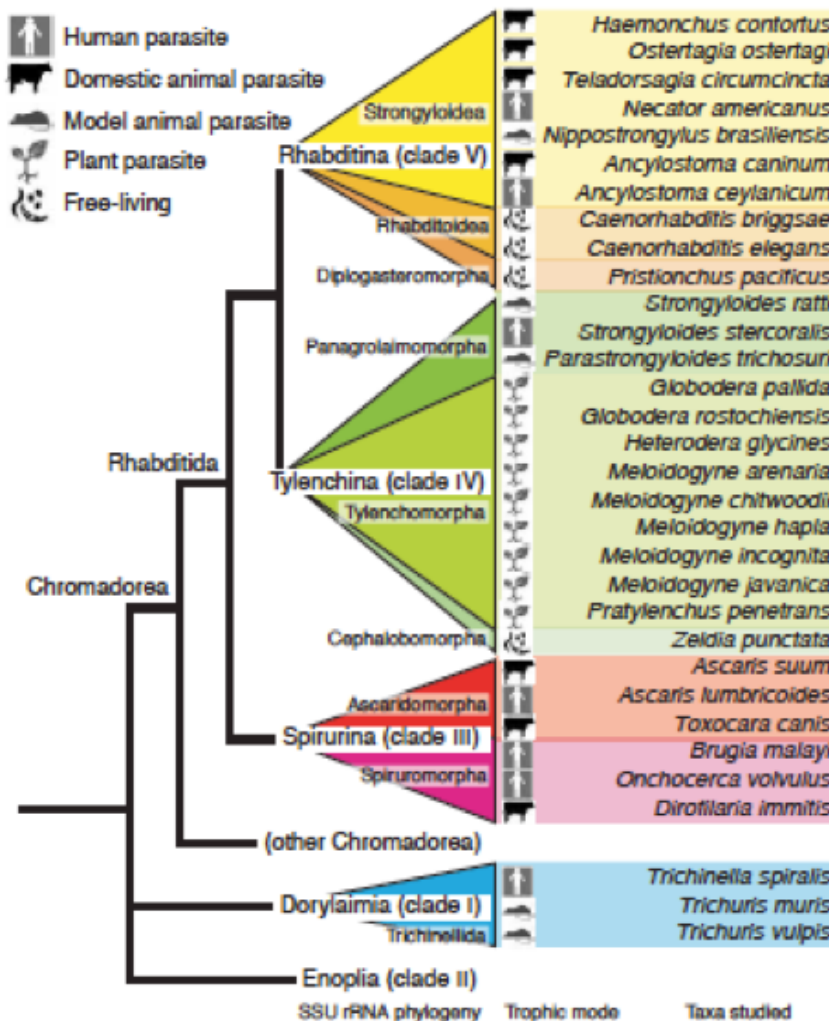


**Figure 1.1: Phylogeny of Nematoda phylum**

permission from Macmillan Publishers Ltd: [NATURE GENETICS] (Parkinson et al., 2004), copyright (2004)

### 1.2.1 *Caenorhabditis elegans*

□ The free-living, clade V nematode *Caenorhabditis elegans* is a key organism that has been proposed as a model for decrypting "classical problems of molecular biology" encountered in eukaryotic organisms as a whole, by the Nobel prize winner for Medicine (2002), Sydney Brenner (Brenner 1974, White et al., 1986, Brenner 1988, Hobert 2013). Specifically, *C. elegans* was chosen to study development, cell differentiation and organization of the neuromusculature. In fact, one of the first genetic screens carried out in *C. elegans* was to identify defects in the nervous system by screening with the anthelmintic levamisole (Lewis et al., 1980). This novel approach has allowed the identification and characterization of a large part of the L-AChR signalling system (Lewis et al., 1980)

and pioneered the use of a variety of pharmacological compounds for tracking molecular targets and understanding their biology (Jones et al., 2004, Mathew et al., 2016).

*Caenorhabditis* is a small nematode ; as adult forms are about 1mm long (Figure 1.2) ; that is easily cultivable at low cost and generate offspring rapidly. Its transparency makes localization of structures within the worm possible and its invariant number of somatic cells allows specific cells and cell types to be identified reliably. *C. elegans* was the first multicellular eukaryotic genome published, in 1998 (Consortium 1998), and this allowed genes to be identified and cloned rapidly. Moreover, advanced genetic techniques that are available offer the possibility to create transgenic worms to carry out functional analysis of genes from other organisms *in vivo*.

The life cycle of *C. elegans* is completed in 3 days when maintained at 25°C. Single animals can initiate a new generation of worms as most of the adult forms are self-fertilizing hermaphrodites, the rest being males. Adult hermaphrodite worms release eggs which rapidly undergo embryogenesis to give rise to L1 stage larvae. This step is followed by three successive moults (L2, L3, L4 larval stages). If external conditions are favourable, L4 larvae initiate their final development step toward the young adult stage, which become hermaphrodite. Alternatively, under less favourable conditions, L2 larvae develop into a "dauer" stage, which is a resistant form that can survive and rapidly change to L4 larvae when the environment becomes more favourable for the development of the worms (Corsi et al., 2015).

*C. elegans* is particularly effective as a model for a variety of parasitic nematode species that are directly related to human and animal health as well as crop damage, due to their phylogenetic proximity. As a model it has proved instrumental in gaining knowledge on effective control strategies and a better understanding of drug resistance mechanisms (Holden Dye et al., 2007, Mathew et al., 2016).

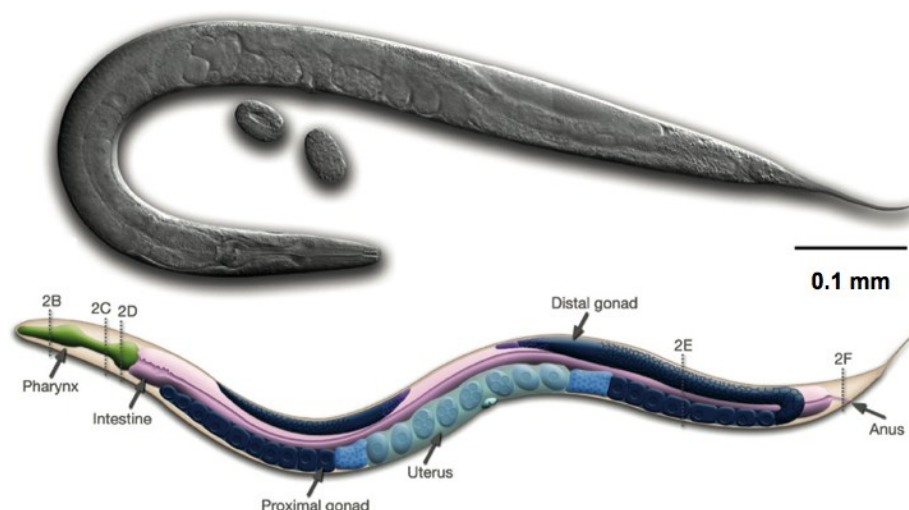


**Figure 1.2:** Adult hermaphrodite *Caenorhabditis elegans* with eggs (top) and anatomical organization (bottom) (<http://www.wormatlas.org>)

### 1.2.2 *Haemonchus contortus*

Transfer of knowledge from *C. elegans* to parasitic nematodes, particularly the parasite of sheep, *Haemonchus contortus*, has provided highly successful in identifying the molecular targets of many anthelmintic compounds including ivermectin (Cully et al., 1994, Forrester et al., 2003, Wolstenholme et al., 2005), LEV (Boulin et al., 2008, Williamson et al., 2009, Boulin et al., 2011, Buxton et al., 2014), monepantel (Rufener et al., 2010, Baur et al., 2015) and morantel (Courtot et al., 2015). Despite this success, in almost every case, subunit genes showed significant differences from that in *C. elegans* (Laing 2013). The development of a closely related parasitic nematode model, such as *H. contortus* is invaluable for understanding the importance of these differences.

The barber pole worm *H. contortus* is a major pest affecting livestock production worldwide (Emery et al., 2016). Being the most pathogenic gastrointestinal nematode infecting small ruminants, *H. contortus* is largely encountered in tropical and subtropical regions (O'Connor et al., 2006) and is widespread in all temperate zones (Herd 1986, van Wyk et al., 1997, Hoste et al., 2002, Almeida et al., 2010) and even sub-polar regions such as Sweden (Waller et al., 2004). The parasite feeds on blood, causing anemia and digestive trouble leading to loss of weight, low milk/meat/wool production (Suarez et al., 2009) as well as an alteration of reproductive capacities (Poppi et al., 1990) and sometimes the death of weaker individuals.

*Haemonchus contortus* is the largest strongylid parasite of ruminants (adult female: 1.5 to 3 cm in length), being part of the order Strongyloidea (Durette-Desset et al., 1999, Parkinson et al., 2004), the

male adults characterized by a small buccal apparatus and a large copulatory bursa. Other Strongyloidea include *Teladorsagia circumcincta* and *Trichostrongylus colubriformis* that are found in temperate regions (Parkinson et al., 2004, O'Connor et al., 2006). The Strongyloidea group is a close relative of *Caenorhabditis spp.* that are free-living nematodes of the Rhabditoidea group. Both belong to the clade V Rhabditina (Parkinson et al., 2004, Blaxter et al., 2015).

*H. contortus* has a direct lifecycle involving ruminant hosts (Figure 1.3). Adults live in the abomasum, female worms shed eggs, released onto the grazing field within faeces of the host. The eggs hatch to deliver larval stage 1 (L1). L1 and L2 both feed on organic matter in the environment. The infective larval stage 3 (L3) is ingested by the grazing host. L3 are highly mobile, resistant and can anchor to the mucosa of the host abomasum. L3s molt into L4 under stimulation of digestive fluids and then into L5 (juvenile stage). The prepatent period, L3 ingestion to first appearance of eggs in the feces, lasts 17 to 21 days (Zajac 2006). Finally adult male and female worms mate, producing 5000 to 10,000 eggs per day (Coyne et al., 1991). Extreme infection causes severe anemia due to blood feeding (Clark et al., 1962).

The genome of *H. contortus* has been recently sequenced, which represents the first strongylid genome to be published along with an important transcriptomic dataset (Laing et al., 2013, Schwarz et al., 2013, Laing et al., 2016). It was then followed by the publication of draft genomes from important strongylid species such as the pig nodule worm *Oesophagostomum dentatum* (Tyagi et al., 2015), the human hookworm *Necator americanus* (Tang et al., 2014) or the zoonotic hookworm *Ancylostoma caninum* (Schwarz et al., 2015), etc. Globally, clade V genomes are structurally similar and share lots of conserved genes, which validates the use of *C. elegans* as a comparison model for functional genomic studies (Gilleard 2013).

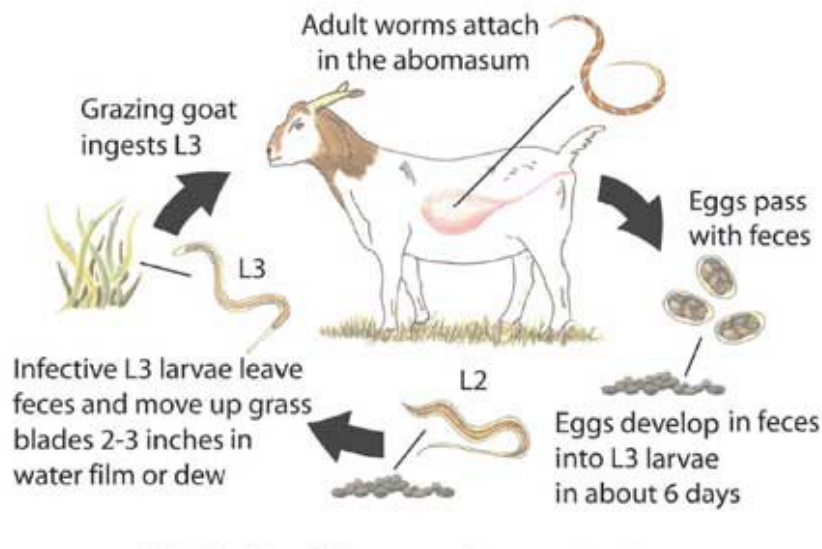


**Figure 1.3: Life cycle of *Haemonchus contortus*, the barber pole worm**  
(<http://www.aragriculture.org>)

### 1.3 Nervous system and Neurotransmission

The nervous system is one of the great fundamental physiological functions driving general behaviour throughout the Eumetazoa superfamily of animals. The fundamental signalling unit is the neurone (Renard et al., 2009), which conducts an electrical signal as the flow of charged ions and transmits and receives information through cell interconnections either in the form of an electrical gap junction between cells or a chemical synapse (Kandel et al., 2000). This thesis focuses on synaptic signalling at the neuromuscular junction (NMJ).

In vertebrates, a signal is propagated along the neuronal axon towards synaptic termini in the form of local disturbances of electrolytic gradients on either side of the neuronal plasma membrane, called an action potential. This rapid event occurs on a scale of 0.5 to hundreds of milliseconds and is driven by the inflow of  $\text{Na}^+$ , followed by the outflow of  $\text{K}^+$  through voltage-gated ion channels anchored within the neuronal membrane (Kandel et al., 2000). The membrane potential is normally fixed at -70 mV but the wave of depolarization- hyperpolarization, known as an action potential, progresses without loss of amplitude (Kandel et al., 2000). Unlike insects (Peron et al., 2009), nematodes, and particularly in *C. elegans*, neurotransmission is for a large majority based on diffusion of ions within cells and does not involve the transmission of action potentials (Mellem et al., 2008). Depolarization of the presynaptic

membrane provokes release of neurotransmitters contained in vesicles (Richmond 2005). This process is finely regulated by enzymatic breakdown of the neurotransmitters and/or re-uptake by pre- and postsynaptic cells as well as glia (Kandel et al., 2000).

Neurotransmitters principally activate specific post-synaptic receptors, which are divided into two main classes. Slow chemical neurotransmission is mediated by G-protein coupled receptors, sensitive to classical neurotransmitters including ACh, glutamate, serotonin and biogenic amines as well as neuropeptides (Green et al., 1994, Cottrell 1997), that lead to an indirect depolarization by activating second-messenger pathways (Vogliss et al., 2006). Fast acting neurotransmission is mediated by ionotropic glutamate receptors (iGluRs) and pLGICs belonging to the "cys-loop" receptors. Their permeability to either cations ( $\text{Na}^+$ ,  $\text{Ca}^{2+}$ ,  $\text{K}^+$ ) or anions ( $\text{Cl}^-$ ) leads to either depolarization (excitatory state) or hyperpolarization (inhibitory state), respectively (Kandel et al., 2000, Keramidas et al., 2004, Barry et al., 2005, Vogliss et al., 2006). pLGICs are activated by various fast-acting neurotransmitters such as ACh,  $\gamma$ -aminobutyric acid (GABA), biogenic amines, protons, among others and drive important functions such as reproduction (Rand 2007), feeding (McKay et al., 2004, Wolstenholme 2012), defecation and locomotion (Schuske et al., 2004).

Located at the NMJs, pLGICs are the preferential target of many drugs (Holden Dye et al., 2007, Martin et al., 2012) due to their rapid physiological response (Aceves et al., 1970, Aubry et al., 1970). The importance of pLGICs can be summarized by their control of locomotion where pLGICs mediate control indirectly, at the neuronal junction and directly, at the neuromuscular junction, (Jorgensen 1995, Schuske et al., 2004). Nematode movement is characterized by sinusoidal waves (Gray et al., 1964), corresponding to cycles of contraction and relaxation. Interneurones control backward or forward movement and motor neurones directly command individual muscles (Schuske et al., 2004). Thus, on one side, an excitation signal from cholinergic neurones leads to the release of ACh and contraction of muscles. On the opposite side, muscles relax in response to GABAergic motor neurones, that are in turn stimulated by cholinergic pre-synaptic motor neurones (Jorgensen 1995). This contraction-relaxation balance is a fundamental mechanism driving normal nematode movement and so the balance between the muscular ACh and GABA gated pLGICs is critical for maintaining body muscle activity. The details of how this is achieved is of primary interest for understanding movement and the potential for these as effective drug targets.

### 1.3.1 The *C. elegans* nervous system

The model nematode *C. elegans* possesses a relatively simple nervous system (Brenner 1974) compared to vertebrates, that is entirely mapped. A total of 302 neurones are connected *via* 7000 chemical synapses, 2000 NMJs and 600 gap junctions (White et al., 1986). Most of the neurone cell bodies are grouped in the head around the pharynx, in the ventral midline and the tail (White et al., 1986). Different neuronal organizations such as the circumpharyngeal ring of interneurons and motor neurone processes are found in the head and manage sensory and motor information (Albertson et al., 1976, White et al., 1976). Chemoreceptive and sensory organs such as amphids and phasmids respectively in the head and the tail are represented by groups of specialized neurones (White et al., 1986).

The overall innervation of the worm body is organized as parallel groups of processes coming from the nerve ring running either longitudinally (nerve cords) or circumferentially (commissures connecting nerve cords), all adjacent to the hypodermis. The ventral nerve cord contains interneurone processes and motor neurone bodies innervating wall muscles of both sides (White et al., 1976) via the intermediate NMJs.

### 1.3.2 The cholinergic system

Acetylcholine is a fundamental neurotransmitter that was first identified as an inhibitor of cardiac activity and later as an activator of skeletal muscles within the peripheral nervous system of vertebrates (Loewi et al., 1926). ACh is also a major actor of the animal autonomous nervous system and principal neurotransmitter in several cerebral areas within the central nervous system (Kandel et al., 2000).

In nematodes such as *C. elegans*, ACh is one of the most abundant neurotransmitters and is released by a majority of neurones (Pereira et al., 2015). The role of ACh in nematodes was first identified using the human intestinal worm *Ascaris lumbricoides* where it also mediates excitatory neurotransmission (Delcastillo et al., 1963, Del Castillo et al., 1967). The first large scale genetic screen for mutants affecting the *C. elegans* nervous system was based on the ACh receptor agonist, LEV (Lewis et al., 1980). Decades later, a precise description of *C. elegans* cholinergic signalling includes the ACh biosynthesis pathway in pre-synaptic neurones, its vesicular transport and release to the synapses followed by binding on post-synaptic acetylcholine receptors (Rand 2007, Pereira et al., 2015).

Although primarily an excitatory neurotransmitter at the neuromuscular junction (Rand 2007, Pereira et al., 2015), ACh is also found at the neuronal junctions (Hobert 2013, Pereira et al., 2015) where it can

play an inhibitory role, for example, in the pharyngeal nervous system (Putrenko et al., 2005). Major functions such as locomotion, feeding and egg-laying involve the cholinergic system and more precisely the action of ACh on the corresponding ionotropic receptors (Rand 2007).

The most recent descriptions of the *C. elegans* cholinergic system have revealed a complex population of homomeric and heteromeric ACh-gated pLGICs (AChRs) made up of a variety of related subunits, particularly at the NMJs (Touroutine et al., 2005, Jones et al., 2007, Boulin et al., 2008, Jones et al., 2008). These AChRs are similar to those found in vertebrates where extensive research provides detailed knowledge of their structure, function, regulation and assembly (Thompson et al., 2010, Fu et al., 2016). This also means that new knowledge gained from the nematode AChRs will be directly relevant to our understanding of this class of receptors in general.

## 1.4 Pentameric Ligand-Gated Ion-Channels

The post-synaptic ligand-gated ion-channels (LGICs) are found universally in vertebrates, invertebrates and have also been identified in some prokaryotic species (Connolly et al., 2004, Tasneem et al., 2005, Jones et al., 2008, Jones et al., 2010). These transmembrane ion-channels are activated by chemical messengers such as neurotransmitters and selectively allow cations ( $\text{Na}^+$ ,  $\text{K}^+$ ,  $\text{Ca}^{2+}$ ) or anions ( $\text{Cl}^-$ ) to pass into the post-synaptic cells through their central pore. LGICs can also be activated and/or modulated by various allosteric ligands, blockers, ions and variations of plasma membrane potential.

The LGIC superfamily groups four major classes of ion-channels: the cys-loop, pentameric LGICs (pLGICs), iGluRs, the ATP, and  $\text{PIP}_2$ -gated ion-channels. pLGICs mediate the majority of excitatory and inhibitory ionotropic neurotransmission (Lester et al., 2004, Barry et al., 2005). In vertebrates, a variety of pLGIC ligands have been characterized, including acetylcholine,  $\gamma$ -aminobutyric acid ( $\text{GABA}_A$ ,  $\text{GABA}_C$ ), 5-hydroxytryptamine (serotonin), glycine, zinc and protons (Lester et al., 2004). Invertebrate receptors are predominantly gated by acetylcholine, GABA, serotonin, histamine, glutamate and protons (Lester et al., 2004, Jones et al., 2008, Jones et al., 2010).

### 1.4.1 Structure

The major functions of pLGICs rely on changing electrolytic gradients across cellular membranes under the activation of specific ligands, which supposes a structural adaptation of the receptors for



ligand binding and ion diffusion. pLGICs are composed of five subunits anchored in the plasma membrane of post-synaptic cells. Subunits can be identical and so form homopentamers or different subsets of subunits can co-assemble to form heteropentamers (Corringer et al., 2000, Hanna et al., 2000). Subunits are essentially composed of a large N-terminal extracellular ligand-binding domain, four  $\alpha$ -helical transmembrane domains (TM1-4) and a long intracellular loop located in between the TM3 and TM4 (Thompson et al., 2010, Tsetlin et al., 2011) (Figure 1.4). A distinguishing feature of the pLGIC family is the strong conservation of their overall structure. The molecular structure of a variety of receptors from vertebrates, invertebrates and bacteria, in closed or ligand-bound states have been interpreted, through electron microscopy, X-ray crystallography or *in silico* modelling. Indeed, this approach represents an effective strategy for predicting key features of receptors such as ligand binding and the residues involved in subunit interfaces. Indeed the 3D structure of the different sub-families of pLGICs have been reported including the AChRs from the electric ray, *Torpedo californica*, the snail *Lymnaea stagnalis* (Brejc et al., 2001, Unwin 2005), the human  $\alpha 4\beta 2$  (Morales-Perez et al., 2016)  $\alpha 7$  (Amiri et al., 2005), the *C. elegans* GluCl $\alpha$  receptor (Hibbs et al., 2011), the prokaryotic GLIC (Bocquet et al., 2009) and ELIC channels (Hilf et al., 2008), the mouse 5-HT $_3$  receptor (Kesters et al., 2013, Hassaine et al., 2014), the human GABA $_A$  receptor (Miller et al., 2014) or the human GlyR (Du et al., 2015).

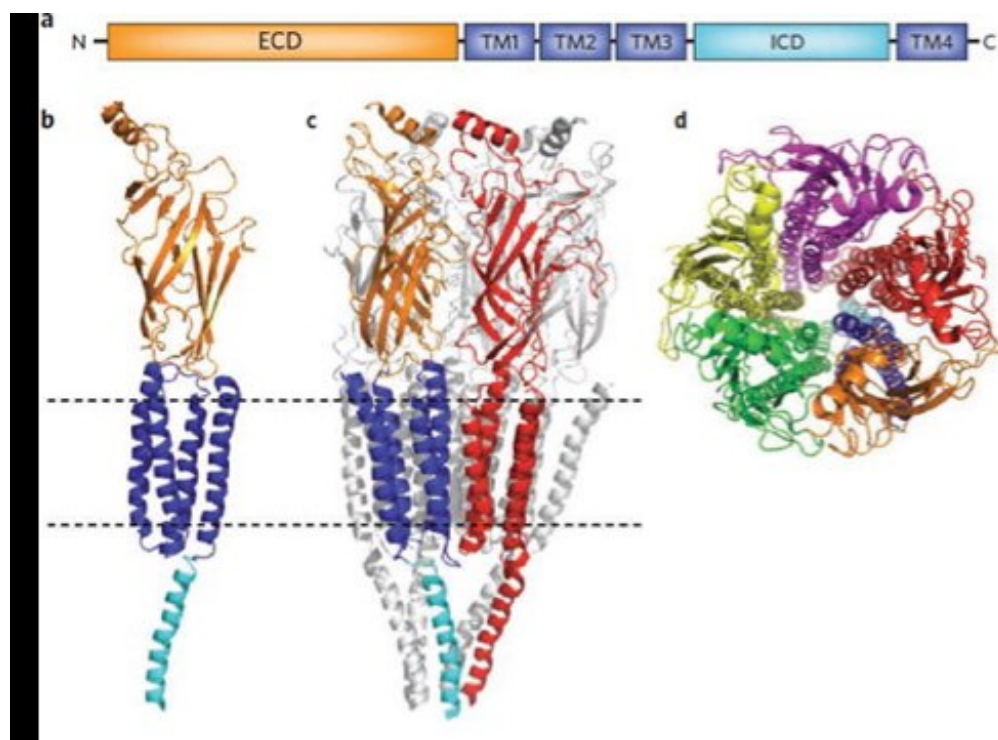


**Figure 1.4: pLGIC structure.**

(a) Secondary structure of subunits: extracellular domain (ECD), transmembrane domains (TM), intracellular domain (ICD) ; (b) Tertiary structure of a AChR subunit ; (c) whole AChR receptor ; (d) Top view of a AChR with the central ion pore.

permission from Macmillan Publishers Ltd: [NATURE CHEMICAL BIOLOGY] (Akabas 2011), copyright (2011)

**1.4.2 Ligand binding**

The N-terminal extracellular domain of pLGIC subunits represents approximately half of the protein, from which the ligand-binding sites are formed. Activating neurotransmitter molecules bind to the interface between two adjacent subunits of the pLGIC in a hydrophobic binding pocket of their extracellular domains (Corringer et al., 2000, Brejc et al., 2001). The principal subunit contributes three binding loops, A, B and C and the complementary subunit, loops D, E and F enclosing the bound ligand (Figure 1.5). The hydrophobic pocket, formed typically from tyrosine and tryptophan residues, coordinates the ligand and allows interaction with surrounding amino acid residues that ultimately leads to channel opening.

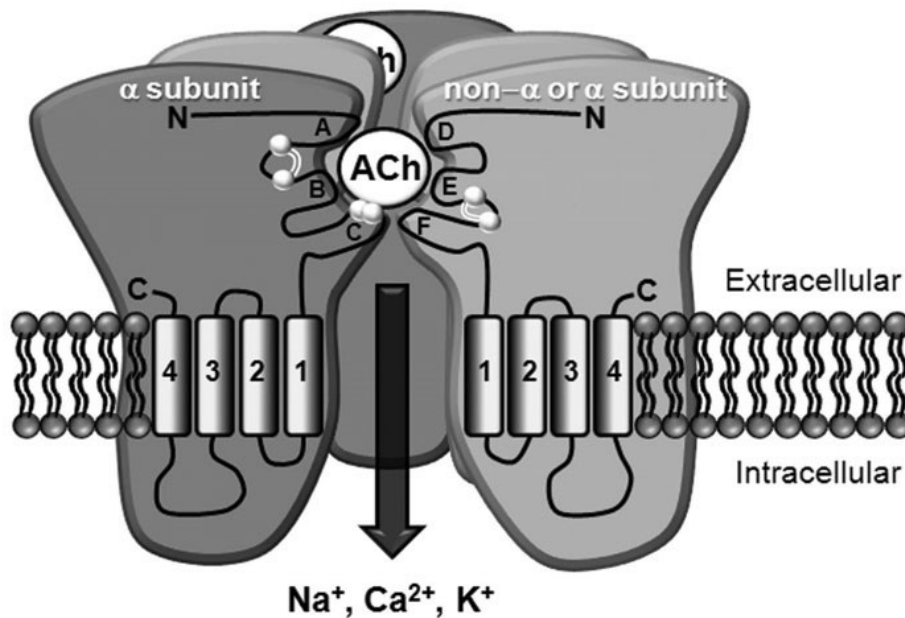


**Figure 1.5: Schematic representation of the ACh binding site of a heteromeric AChR (Jones et al., 2010)**

With permission of Springer [Springer ebook] (Jones et al., 2010), copyright (2010)

Homomeric receptors can, in theory, bind five independent ligands but, in reality, channel opening proceeds through an asymmetrical occupation of two or possibly three sites that produce an unstable state that transitions toward a stable, active state (Rayes et al., 2009, Mowrey et al., 2013). This can be achieved because binding of the first ligand molecule can alter affinity for a second and third ligand. This cooperative binding can be estimated through the Hill equation, which determines the level of cooperativity within multi-subunit proteins such as allosteric enzymes or ion-channels (Yifrach 2004). In contrast, heteromeric receptors contain subunits that are structurally distinct and create binding sites with different binding characteristics. For example, the vertebrate AChR  $\alpha$  subunits can occupy both principal and complementary positions, whereas the  $\beta$ ,  $\gamma$  and  $\delta$  subunits can only act as a complementary subunit (Corringer et al., 2000). Indeed,  $\alpha$  subunits contains two vicinal cysteines in loop C that are critical for maintaining the structure of the ACh-binding pocket (McLane et al., 1991). As pairs of  $\alpha/\alpha$  and  $\alpha/\text{non-}\alpha$  subunits can form functional ligand binding sites, the nature of subunits and their stoichiometry within the heteromeric receptors can directly influence their pharmacological profile. The human  $\alpha 4\beta 2$  receptor is found in the brain and subunits can assemble to form two receptors:  $(\alpha 4)_3(\beta 2)_2$  or  $(\alpha 4)_2(\beta 2)_3$  exhibiting different sensitivities to ACh, nicotine and variable permeability to  $\text{Ca}^{2+}$  (Nelson et al., 2003, Zhou et al., 2003). The quaternary structure of  $(\alpha 4)_2(\beta 2)_3$  has been solved recently through X-ray crystallography (Morales-Perez et al., 2016).

The "cys-loop" LGICs take their name from a particular amino acid sequence motif located in the N-terminal extracellular domain of each subunit. It corresponds to a loop made up of 13 amino acids flanked by two cysteines forming a disulphide bond. This loop plays a critical role in receptor gating and inter-subunit assembly (Green et al., 1997). Notably, the prokaryotic cys-loop homologs that have been described so far do not contain the cys residues in a homologous position within the sequence (Tasneem et al., 2005).

#### *1.4.3 Ion selectivity*

Ion exchange is another essential functional feature of ion-channels. The pentameric structure of pLGICs creates a funnel-shaped transmembrane (TM) region that controls ion flow through specific amino acids that allow only specific cations ( $\text{Ca}^{2+}$ ,  $\text{K}^+$ ,  $\text{Na}^+$ ) or anions ( $\text{Cl}^-$ ) to pass through the central pore.

The TMs of each subunit are formed from  $\alpha$  helices and anchor the receptor in the lipid bilayer of the cells. Within the receptor, the central pore is formed of a inner ring of the second transmembrane

domaine (TM2) from each subunit whereas TMs 1, 3 and 4 form outer complex that is directly in contact with lipids (Miyazawa et al., 2003, De Planque et al., 2004). The TM2 plays a critical role in gating mechanisms as it forms a selective filter for ions (Keramidas et al., 2004). Indeed, the TM2s forms a funnel where the inner diameter gradually reduces toward the gate of the channel. The TM2 contains mostly non-polar amino acids but charged residues are present along the  $\alpha$  helix (Keramidas et al., 2004). These rings of charged residues added to a narrow diameter directly contribute to ion-selectivity. In the case of heteromeric receptors such as AChRs, the presence of multiple subunit subtypes changes the composition of the TM2s which would explain the important differences observed regarding  $\text{Ca}^{2+}$  permeation (Girod et al., 1999, Thompson et al., 2010).

The intracellular domain corresponds to a large loop located between the TM3 and TM4. Initial studies attributed a role of "portal" for ion entry or exit (Unwin 1993, Miyazawa et al., 1999). In addition, recent works have also demonstrated a potential relationship with channel conductance (Hales et al., 2006). Indeed, the intracellular loop contains important charged amino acids affecting the ion flow between the cytoplasm and the gate of the receptor. In addition, a complex communication exists between the intracellular domain and other cytosolic proteins such as protein kinases, which can directly influence the desensitization rate of the receptors, the surface expression or the sensitivity to various ligands (Talwar et al., 2014). Other post-translational modifications such as glycosylation and palmitoylation may also play a role in assembly of subunits and trafficking of the receptor from the endoplasmic reticulum to the plasma membrane (Wanamaker et al., 2003, Alexander et al., 2010).

#### *1.4.4 Assembly*

The fine degree of neurotransmission control achieved by pLGIC mediated signalling involves control over subunit composition and presentation of receptors at the synaptic interface. Post-synaptic cells regulate subunit synthesis, folding, assembly and transport of the receptor to the plasma membrane (Fu et al., 2016). Proteolysis of mis-folded subunits and unassembled receptors occurs through the endoplasmic reticulum-associated degradation system (Vembar et al., 2008) and ultimately, only 25 to 30 % of synthesized subunits are assembled into functional receptors (Wanamaker et al., 2003).

Subunits are synthesized in the endoplasmic reticulum (ER) and must meet structural requirements prior to their transport to the plasma membrane *via* the Golgi apparatus. The N-terminal domain of subunits contains critical amino acids and glycosylation sites regulating the assembly and trafficking of receptors to the cell surface (Sumikawa et al., 1994, Avramopoulou et al., 2004). The short extracellular C-terminal tail, beyond the fourth transmembrane domain may be essential for the

assembly of subunits and their expression at the cell surface, as described for the human 5-HT<sub>3</sub> receptor (Butler et al., 2009) and muscular AChR (Ealing et al., 2002).

The assembly of subunits is a complex process involving a variety of accessory proteins. Mostly residing in the ER, subsets of chaperons involved in subunit assembly can vary dramatically depending on the organism and the pLGIC subtypes (Millar et al., 2008, Fu et al., 2016). For example, in vertebrates, BiP is a "heat shock protein" located in the ER that interacts specifically with AChR subunit monomers (Wanamaker et al., 2003) and associates with unfolded GABA<sub>A</sub> receptor subunits (Di et al., 2013). On the other hand, calnexin is an ER-membrane chaperone notably involved in controlling subunit folding and assembly of several pLGICs subtypes (Gelman et al., 1995, Keller et al., 1996, Han et al., 2015). Interestingly, the requirement of accessory proteins in nematodes seems to be exclusively related to AChRs (Gottschalk et al., 2005) as no proteins assisting the biosynthesis of anionic pLGICs have been reported. Moreover, for certain types of pLGICs, different chaperones are involved at every step of the receptor biosynthesis, from the assembly/folding of subunits to the export and regulation of expression at the plasma membrane (Millar 2003, Gottschalk et al., 2005).

#### 1.4.5 Chaperones

Within the ER, the pLGIC subunits undergo proper folding and co-assembly with subunit partners to form immature ion-channel complexes. Among the pLGIC-related ER-chaperones, RIC-3 (resistance to inhibitors of acetylcholinesterase 3) is a transmembrane protein exhibiting multi-faceted but nonetheless essential functions for receptors biosynthesis and is mostly associated with cation-selective ion-channels. Indeed, the vertebrate RIC-3 acts primarily on folding and assembly of the 5-HT<sub>3</sub> receptor (Walstab et al., 2010) and seems to enhance channel expression of the human homomeric  $\alpha 7$  receptor while inhibiting other AChR subtypes (Castillo et al., 2005, Alexander et al., 2010). More broadly, a recent study also suggests that the phosphorylation of the *C. elegans* RIC-3 may be essential in the fine regulation of muscular activity (Safdie et al., 2016). In nematodes, RIC-3 is one of the most described accessory proteins among a group of chaperons involved in the assembly of a variety of AChRs exclusively (Halevi et al., 2002, McKay et al., 2004, Francis et al., 2005, Gottschalk et al., 2005, Lansdell et al., 2005) including the L, N, M-AChRs respectively sensitive to levamisole, nicotine and morantel (Boulin et al., 2008, Boulin et al., 2011, Buxton et al., 2014, Courtot et al., 2015, Abongwa et al., 2016) (Figure 1.6). Interestingly, the *Xenopus laevis* RIC-3 seems also able to interact with nematode AChRs such as the N-AChR from *C. elegans* (Bennett et al., 2012). Particularly for the L-AChRs, a complex network of accessory proteins have been identified (Martin et al., 2012) among

which the ER proteins NRA-2 and NRA-4 seem to influence the subunit composition of receptors (Almedom et al., 2009).

From the ER to the plasma membrane other chaperones regulate the trafficking of newly synthesized receptor such as the golgi protein UNC-50 (Eimer et al., 2007) and UNC-74 (Haugstetter et al., 2005), a thioredoxin-like protein residing in the ER (Boulin et al., 2008). Interestingly, UNC-50, UNC-74 along with RIC-3 remain critical accessory proteins for the successful reconstitution of L-AChRs in *Xenopus* oocytes (Boulin et al., 2008, Boulin et al., 2011, Martin et al., 2012).

Chaperons can also interact with receptors exposed at the plasma membrane and subsequently play a role in clustering receptors at the synapses For example, the secreted LEV-9 and the transmembrane protein LEV-10 both bind to the nematode L-AChRs (Gally et al., 2004, Gendrel et al., 2009). On the other hand, MOLO-1 is a recently identified transmembrane protein, which positively modulates L-AChR gating (Boulin et al., 2012) and OIG-4 (Rapti et al., 2011), EGL-15 as well as SOC-1 (Gottschalk et al., 2005) all play a role in stabilizing the receptors and ensure a proper distribution and concentration on the membrane.

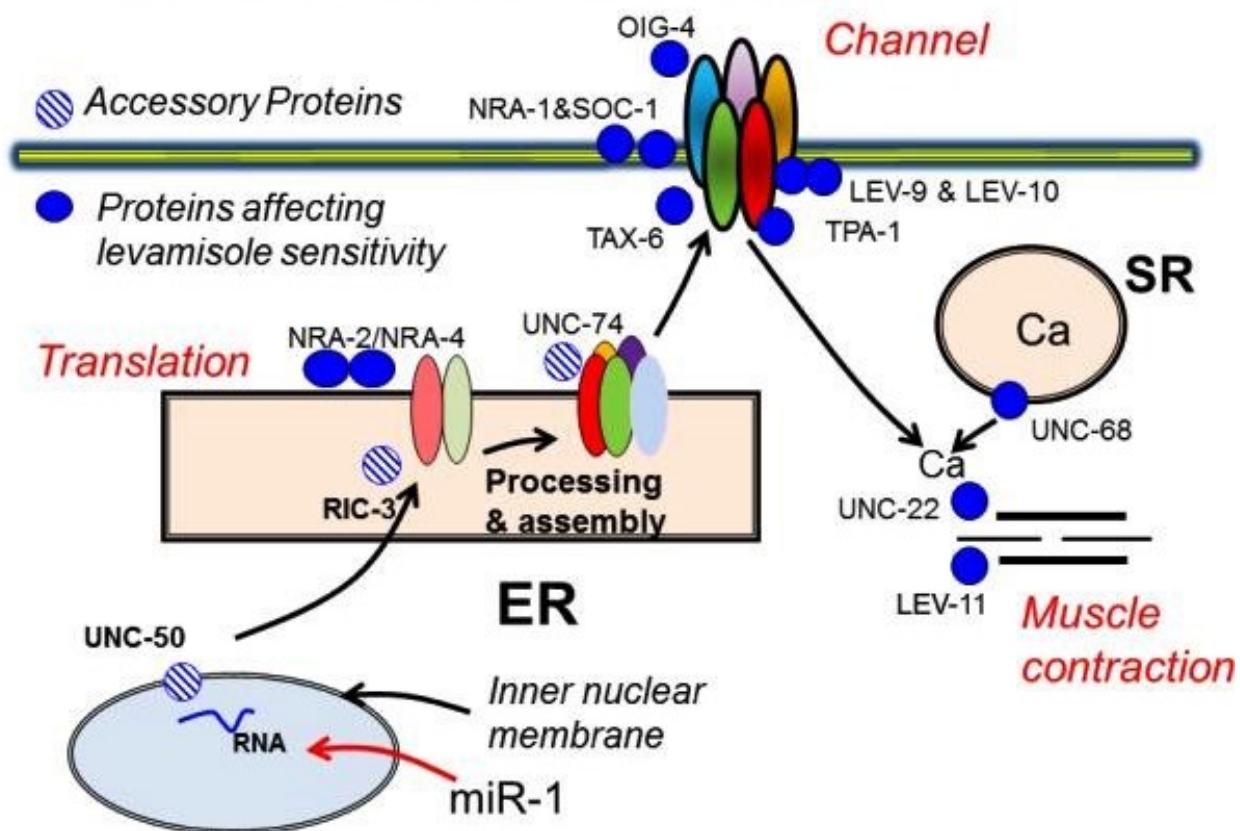


**Figure 1.6: *C. elegans* L-AChR biosynthesis (Martin et al., 2012)**

*With permission from ELSEVIER [TRENDS IN PARASITOLOGY] (Martin et al., 2012), copyright (2012)*

## 1.5 Evolution of pLGICs

The origin of pentameric ligand-gated ion-channels can be traced to before the emergence of multicellular organisms and they were likely involved in ancient signalling systems, as pLGIC-like proteins can be observed in some Gram-negative bacteria, playing the role of detectors of external molecules (Stock et al., 1977, Tasneem et al., 2005, Dent 2010). Overall, phylogenetic studies show that all metazoan subunit subtypes were already present in the ancestor of bilateria prior to the Cambrian explosion, approximately 600 million years ago (Dent 2006, Dent 2010). Since then, the evolution of pLGICs has been punctuated by major events of diversification involving notably gene duplications to produce the multiple receptors observed today, particularly in nematodes (Beech et al., 2015). One of the major events that dramatically increased the number of pLGICs corresponds to the rise of heteromeric receptors from the ancestral forms likely represented by homomeric forms (Ortells et al., 1995, Dent 2006, Dent 2010). Indeed, this phenomenon is related to the emergence of complementary subunits exhibiting the ability to form receptors with tuneable characteristics and has greatly contributed in diversifying the pLGIC types (Jones et al., 2008, Millar et al., 2009, Jones et al., 2010). Finally, similar diversification events have also allowed dramatic changes that affect ligand binding, channel conductance, ion-selectivity to create a diverse panel of receptor classes particularly adapted to new and specific functions (Beech et al., 2015).

### 1.5.1 Diversity

The pLGIC family groups a variety of neurotransmitter-gated ion-channels that are differentiated by their subunit composition, which directly influences the functional and pharmacological properties of the receptor. The diversity of subunits in the whole animal kingdom can be explained by a collection of genes encoding principal and complementary subunits, the number of genes being dramatically different between the major animal branches. Indeed, the human genome contains 45 genes encoding cationic receptors gated by ACh and serotonin and anionic channels gated by GABA and glycine

(Jones et al., 2008). In contrast, insects conserve a relatively restricted number of subunit genes with no more than 23 and 21 genes respectively reported in the model insect species *Drosophila melanogaster* (Littleton et al., 2000) or the honeybee *Apis mellifera* (Jones et al., 2006). Among these insect genes, some encode cationic subunits forming AChRs, both anionic and cationic GABA-gated and anionic receptors responding to glutamate and histamine. The diversity of nematode pLGIC subunits is remarkable, particularly in *C. elegans*, which possesses the highest number of subunit genes with a total of 102 reported so far (Jones et al., 2008).

The cationic AChR subunit genes remain certainly the largest group of pLGICs subunits (Mongan et al., 1998, Jones et al., 2007, Williamson et al., 2007, Holden-Dye et al., 2013) involved in the formation of many different receptors driving major biological functions in nematodes. The *C. elegans* genome contains up to 29 genes encoding AChR subunits (Mongan et al., 1998, Jones et al., 2007). The main gene groups are composed of either  $\alpha$ -type subunits (*unc-38* and *acr-8* groups) or non- $\alpha$  (*unc-29* group) or both (*acr-16*, *acr-26* and *deg-3* groups) (Jones et al., 2007) (Figure 1.7).

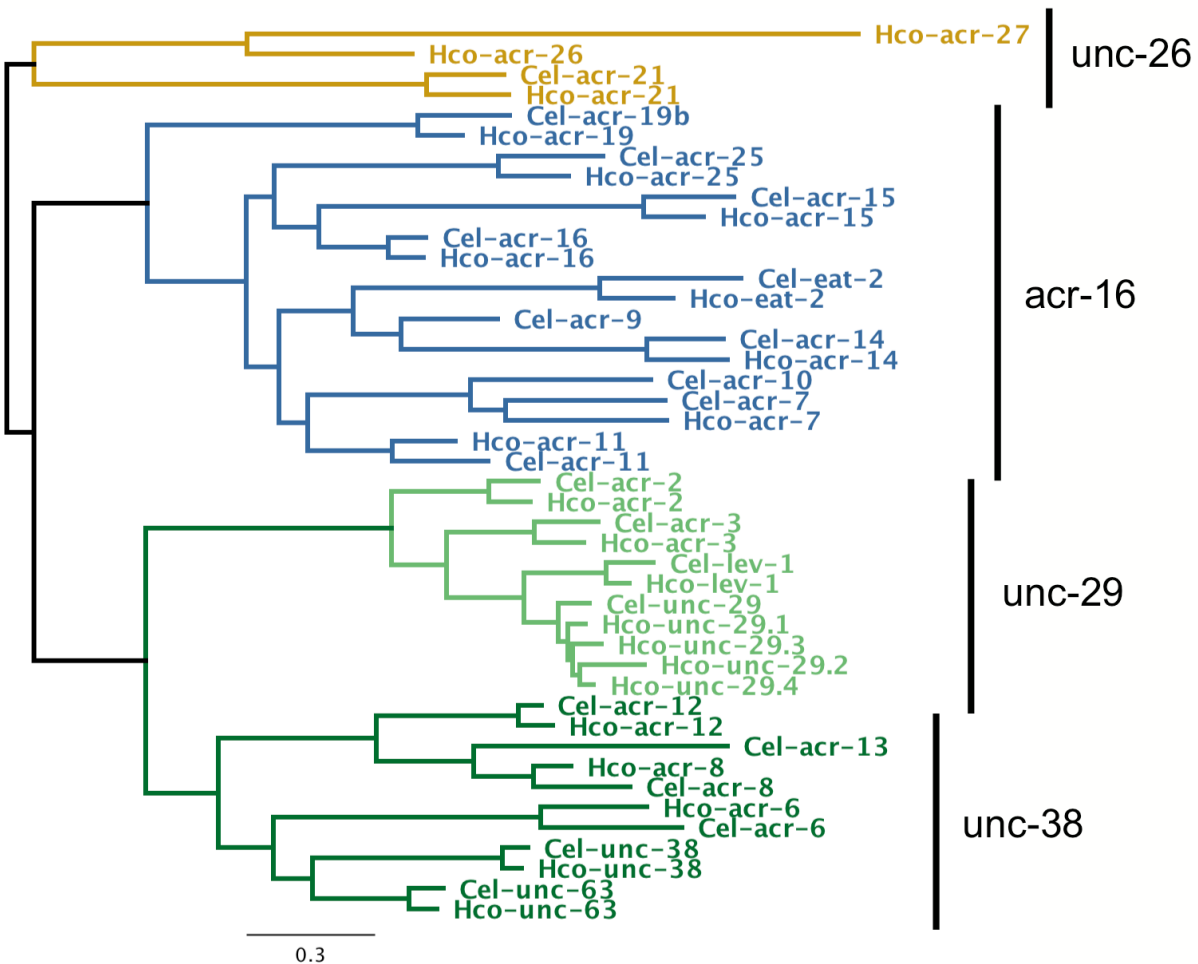




**Figure 1.7: Maximum likelihood phylogeny of AChR subunits from *C. elegans* and *H. contortus*.** Based on a protein sequence alignment excluding the signal peptide, intracellular loop and C-terminal tail. Scale bar represents substitution per site.

The clade I nematode *Trichinella spiralis* and the clade III species *B. malayi*, both possess a restricted number of pLGIC subunit genes compared to *C. elegans*. All the different main gene subgroups are represented in both species but *T. spiralis* and *B. malayi* only have 8 and 9 AChR subunit genes respectively (Williamson et al., 2007). The reason for the limited number of subunits is different between the clade I and clade III nematodes. Gene expansion is observed in the nematodes following divergence from clade I. It seems that the clade I nematodes persist with an original smaller set of subunits, while the clade III nematodes have lost subunits present in their common ancestor with the clade V nematodes (Neveu et al., 2010, Beech et al., 2014, Duguet et al., 2016).

The actual distribution of subunit genes observed in nematodes involve complex evolutionary mechanisms that correspond to the adaptation of species to specific biological contexts. Understanding these processes from the origin of pLGICs to the current day family of receptors will provide insight into the mechanisms responsible and the details of cell physiology that leads to an environment in which the diversification and appearance of new receptors classes is favoured.

### 1.5.2 Gene duplication

The appearance of duplicated genes, otherwise known as paralogs, is believed to be a principal process responsible for the origin of biochemical diversity (Ohno 1970). There are many possible consequences of duplicated genes that include a general increase in expression levels, an alteration in location and timing of expression, a change in biochemical function and the separation of tasks for a multifunctional protein among the gene copies (Hahn 2009, Beech et al., 2015). Two specific scenarios are particularly relevant for expansion of the nematode pLGICs family.

First, a change in the location and/or timing of subunit expression can lead to new biology. For example, subunits *unc-29* and *lev-1* are found within the muscular L-AChR, whereas the paralogous copies, *acr-2* and *acr-3*, are found in the motor neuronal ACR-2R of *C. elegans* (Jospin et al., 2009). Similarly, the *glc-1* and *avr-15* genes encoding glutamate-gated chloride channels (GluCl)s subunits in *C. elegans* take both their origin from a duplication that occurred after the split of *C. elegans* from *Caenorhabditis briggsae* (Beech et al., 2015). Being notably involved in the sensitivity to the anthelmintic ivermectin (Dent et al., 2000), *avr-15* is mostly expressed in pharyngeal muscles (Dent et

al., 1997) whereas *glc-1* expression is observed in a variety of tissues and from embryos to adult stages (Ghosh et al., 2012), suggesting a divergent biological function.

Second, changes in subunit function can involve binding of new ligands, a switch in ion selectivity, differences in subunit interactions leading from homomeric to heteromeric receptors and as a consequence changes in ligand affinity and gating properties. Indeed, the large library of pLGIC subunits offers a variety of cases exhibiting changes in function that are subsequent to gene duplication events. For example, ion-selectivity remains a major feature of pLGICs as it directly contributes in maintaining excitation or inhibition of post-synaptic cells. However, a switch of electrical properties has been reported and highlights a phenomenon that dramatically changes receptor function. For example, the GABA-gated *C. elegans* EXP-1 (expulsion defective protein) homomeric receptor belongs to the ligand-gated chloride channel (LGCC) family and is involved in enteric muscle contraction (Beg et al., 2003). While sharing similarity with the nematode GABA-gated chloride channels, this receptor contains the anion-selectivity amino acid motif "PAR" (Jensen et al., 2005) within the TM2, which indicates a switch into cation selectivity.

Ligand specificity represents another important feature that can be the subject of particular evolutionary processes. For example, the affinity for glutamate appears to be very ancient as it is shared by GluClIs found in the Ecdysozoan (Cully et al., 1994, Cully et al., 1996), Molluscan (Kehoe et al., 2009) and Platyhelminths species (Dufour et al., 2013). However, a recent study revealed that from these three group of organisms, the amino acids involved in glutamate binding are different and suggests a polyphyletic origin of these ancient pLGICs that all converged towards glutamate recognition (Lynagh et al., 2015). Similarly, calculation of the substitution rate along the phylogenetic branches leading to the nematode LGCC-like subunit groups MOD-1 (serotonin-gated), GGR-3 (GABA/Glycine-gated) and ACC-1 (acetylcholine chloride channels)(Jones et al., 2008), shows a significant increase particularly for residues in close contact with the ligand (Beech et al., 2015). In other words, this suggests a propensity for a switch in ligand specificity and a convergent evolution towards binding new molecules.

Another common fate of subunit evolution is the ability to form new interactions with adjacent subunits to form, in some cases, heteromeric receptors that are required for maintaining a function. For example, the *unc-29* clade provides subunits forming the neuronal ACR2R and the L-AChR which are complex heteromeric receptors composed of both  $\alpha$  and non- $\alpha$  subunit types (Boulin et al., 2008, Jospin et al., 2009). The muscular nematode  $\alpha$ -type ACR-26 and non- $\alpha$  ACR-27 AChR subunits both belong to the ACR-16 clade and are absent from free-living and parasitic nematodes (Bennett et al., 2012, Courtot et

al., 2015). In *H. contortus*, ACR-26 and ACR-27 form an obligate heteromeric channel called M-type AChR responding to ACh and the anthelmintic morantel but none of these subunits assemble on their own to form homomeric channels (Courtot et al., 2015). In contrast, other subunits can participate in forming heteromeric receptors while adjusting pLGIC function. For example, within the unique group of invertebrate acetylcholine-gated chloride channels (ACCs), the *C. elegans* ACC-1 and ACC-2 subunits form homomeric channels responding to ACh in *Xenopus laevis* oocytes (Putrenko et al., 2005). However, ACC-3 subunit forms obligate heteromeric receptors when combined with ACC-1 and induces a faster desensitization of the receptor whereas the ACC-4 subunit seems to combine with both ACC-2 and ACC-3 but this association seems to negatively regulate ACC-2 expression (Putrenko et al., 2005).

The conditions favouring the persistence of duplicate genes and the sequence changes that follow these events and lead to specific functional changes remains poorly understood as most of the pLGIC subunits appear hundreds of millions of years ago followed by long periods of subsequent sequence change. Examples of more recent duplication are needed to establish a model for deciphering the diversification mechanisms. In this thesis I am proposing that duplicate copies of the non-alpha *unc-29* L-AChR subunit in the sheep parasite, *H. contortus*, can serve as such a model.

### 1.5.3 Acetylcholine receptor subunits

The nematode AChR subunits are particularly diversified and may be classified into six groups, the *deg-3*, *acr-26*, *acr-16*, *acr-8*, *unc-38* and *unc-29*, each taking the name of a well characterized gene (Jones et al., 2007). The *deg-3*, *unc-38* and *acr-8* groups are exclusively composed of  $\alpha$  type subunits (Mongan et al., 1998, Jones et al., 2007). The *unc-29* group contains only non- $\alpha$  type subunits, whereas *acr-16* and *acr-26* include both types (Jones et al., 2004, Jones et al., 2007, Bennett et al., 2012, Courtot et al., 2015) (Figure 1.7). Each group traces back to one or two subunits inherited from the common ancestor with insects that have then undergone expansion within the nematodes (Dent 2006, Beech et al., 2015). The genes composing these groups can therefore be quite different between nematode clades and also among species from the same clade (Jones et al., 2007, Williamson et al., 2007, Holden-Dye et al., 2013). Important AChRs from each clade have been successfully reconstituted in *Xenopus* oocytes and characterized. The *deg-3* group contains subunit genes that are unique to nematodes and some of them, such as *Cel-acr-23*, *Cel-acr-20* and *Hco-mtpl-1* are involved in sensitivity to anthelmintics from the amino-acetonitrile derivatives family (Rufener et al., 2009, Rufener et al., 2013, Baur et al., 2015). Interestingly, other genes appear to be unique to specific groups

of nematode species such as the *acr-26* ( $\alpha$ ) and *acr-27* (non- $\alpha$ ), which encode subunits forming a morantel-sensitive receptor in *H. contortus* (Bennett et al., 2012, Courtot et al., 2015). Indeed, both genes have been detected in human/animal parasitic nematodes but seem absent from free-living and plant parasitic nematode species (Courtot et al., 2015).

The muscular ACR-16 forms a homomeric receptor defined as an N-AChR for its particular sensitivity to nicotine (Touroutine et al., 2005, Boulin et al., 2008, Abongwa et al., 2016) and is expressed by nematodes from clade III to clade V (Holden-Dye et al., 2013). Subunits from the *acr-8*, *unc-38* and *unc-29* subunits combine to form an L-AChR that is specifically sensitive to levamisole. The N-AChR and L-AChR of *C. elegans* are both found within the same synaptic junctions and both respond to acetylcholine and activate muscle contraction, forming a redundant ACh signalling pathway (Richmond et al., 1999). It is surprising that while ACR-16 forms a homopentamer, the L-AChR of *C. elegans* requires five different subunits and so represents the maximum diversity of subunits possible and yet both perform similar physiological roles in the same physical location. As yet, we have no explanation for why this might be the case.

The emergence of diversity within the *acr-8*, *unc-38* and *unc-29* clades predates the origin of ecdysozoans as the most recent phylogenetic studies show that insects possess an *unc-38*-like  $\alpha$ , a *unc-29*-like non- $\alpha$  subunit and that the *acr-8* group existed before the split between insects and nematodes (Beech et al., 2015). In other words, this may indicate that the ancestors of ecdysozoans were already able to form heteromeric receptors. In the common ancestor of nematodes, gene duplications gave rise to *unc-38*, *unc-63* and *acr-6* and *acr-8* and *acr-12* in the two  $\alpha$  subunit clades (Beech et al., 2015) (Figure 1.7). A similar expansion of the *unc-29* group produced four non- $\alpha$  subunits, *unc-29*, *lev-1*, *acr-2* and *acr-3* (Beech et al., 2015) (Figure 1.7). Gene duplications continued throughout the evolution of the Nematoda phylum as illustrated by the *acr-13* gene (also called *lev-8* within the *acr-8* group), which appeared after separation from clade I and has subsequently been lost from all but the rhabditid worms in clade V and the pig parasite *Ascaris suum* in clade III (Holden-Dye et al., 2013, Beech et al., 2015).

The particular interest of these groups of subunit genes relies on their ability to form receptors exhibiting complex and unique subunit composition that play different functional roles such as the *C. elegans* muscular L-AChR, that contains *unc-38*, *unc-63*, *acr-13*, *lev-1* and *unc-29* and motor neuronal ACR-2R that contains *unc-38*, *unc-63*, *acr-12*, *acr-2* and *acr-3* (Boulin et al., 2008, Jospin et al., 2009). The recent identification of four paralogs of *unc-29* within the trichostrongylid nematodes and particularly in *H. contortus*, together with multiple independent duplications of *unc-29* throughout the

strongylid nematodes indicates that the process of diversification through gene duplications within the L-AChR clade is still ongoing (Neveu et al., 2010, Duguet et al., 2016). It is interesting to speculate whether these recent duplications represent events similar to those that created the four members of the *unc-29* clade early in nematode evolution and, if so, they provide an ideal opportunity to investigate the mechanisms that determine this process in general.

## 1.6 Levamisole-sensitive AChRs

The identification and functional characterization of the nematode L-AChR represents over half a century of research and has remained a strategic receptor for understanding neuromuscular control and anthelmintic activity and resistance in targeted nematode species (Martin et al., 2012). Many different approaches have combined to provide a remarkably detailed picture of this receptor.

### 1.6.1 L-AChR research milestones

Levamisole is one of the first generations of veterinary anthelmintics broadly introduced to the market in the late 1960's (James et al., 2009) and mostly used as a broad-spectrum deworming agent, particularly efficient against sheep, pig, cattle lung and gastrointestinal worms such as *H. contortus* and other trichostrongylid nematodes (Thienpont et al., 1966, Walley 1966). As a drug specifically known to target AChR signalling, LEV was used to screen for resistant mutants in the, then, newly available *C. elegans* model for genetic analysis (Brenner 1974, Lewis et al., 1980). This work led to the discovery of 12 loci among which are five genes that encode AChR subunits: the 3  $\alpha$ -type *unc-63*, *unc-38*, *acr-13* and 2 non- $\alpha$ -type *lev-1* and *unc-29* (Figure 1.7). Throughout the subsequent decades, several studies demonstrated the co-assembly of some of these subunits and their expression in muscular tissues (Fleming et al., 1997, Richmond et al., 1999, Culetto et al., 2004, Towers et al., 2005). Attempts to reconstitute a functional *C. elegans* L-AChR in *Xenopus* oocytes, were largely unsuccessful, leading to receptors that conducted only minimal currents (Fleming et al., 1997, Richmond et al., 1999, Culetto et al., 2004, Towers et al., 2005). A major breakthrough was achieved using the five AChR subunits, UNC-63, UNC-38, ACR-13, LEV-1, UNC-29 along with three chaperons RIC-3, UNC-74, UNC-50 (Boulin et al., 2008), which led to robust ACh induced currents. This study paved the way for a renewed research interest in the L-AChR subunit genes and receptors from a variety of strategic parasitic nematode species.

### 1.6.2 Diversity of L-AChR genes

A new era of parasitic nematode genome sequencing has made it possible to directly clone specific genes reliably, which together with injection and expression of heterologous cRNA in *Xenopus laevis* oocytes to express functional pLGICs has generated information on the L-AChR of several different nematode species (Bianchi et al., 2006, Millar 2009). In each case, parasitic nematodes for which an L-AChR has been reconstituted are different in subunit composition from the *C. elegans* model (Williamson et al., 2007, Holden-Dye et al., 2013, Buxton et al., 2014, Li et al., 2015, Duguet et al., 2016). Unlike *C. elegans*, these parasite subunits may combine in several combinations to produce a variety of different receptors that display different pharmacological properties (Martin et al., 2012).

The first parasitic L-AChR reconstituted was from the clade III pig parasite *A. suum*. While the same L-AChR subunits, with the exception of *lev-1*, present in *C. elegans* are also found in the *A. suum* genome, only subunits *unc-38* and *unc-29* have been examined so far (Williamson et al., 2009). Two receptor subtypes could be reconstituted depending on ratio of cRNA injected in oocytes (Figure 1.8). The receptor produced with *unc-29* in excess of *unc-38* responds preferentially to LEV and pyrantel (PYR), an anthelmintic from the tetrahydropyrimidine family. Conversely, with *unc-38* in excess of *unc-29*, the receptor responds primarily to nicotine and oxantel, another member of the pyrantel group. Interestingly, in contrast with the *C. elegans* L-AChR reconstitution, the co-expression of accessory proteins was not required (Williamson et al., 2009).

The clade V strongylid nematode *O. dentatum* possesses the *unc-63*, *unc-38*, *acr-8* and *unc-29* L-AChR subunit genes (Buxton et al., 2014). Again, several different subunit combinations form functional receptors in *Xenopus* oocytes, each with different pharmacological characteristics. A minimal subunit combination required to form a functional receptor from *O. dentatum* subunits includes only UNC-63 and UNC-29, which induces larger responses to PYR than to LEV (Buxton et al., 2014) (Figure 1.8). Also, including UNC-38 generates a receptor responding to ACh and strongly to PYR but  $\text{Ca}^{2+}$  permeability remained very low. In contrast, including ACR-8 produces a larger response to ACh and the receptor becomes sensitive to LEV. A receptor composed of all UNC-63, UNC-38, ACR-8 and UNC-29 subunits produced the biggest response to ACh and LEV (Buxton et al., 2014) (Figure 1.8). The conductance of this receptor subtype (35 pS) expressed in oocytes (Buxton et al., 2014) corresponds to the conductance obtained from *in vivo* muscular electrophysiology (Robertson et al., 1999). It would appear that while functional receptors can be produced from combinations lacking

certain subunits, this may be an artefact of *Xenopus* oocytes and that the receptor produced from the full complement of subunits represents the receptor found *in vivo*.

The genome of *H. contortus* encodes a similar subunit complement to *O. dentatum* (Laing et al., 2013, Laing et al., 2016). Indeed, *unc-63*, *unc-38* and *acr-8* were identified and cloned for the purpose of L-AChR reconstitution in *Xenopus* oocytes (Fauvin et al., 2010, Neveu et al., 2010). *H. contortus* lacks the  $\alpha$ -type subunit *acr-13* whereas this subunit in *O. dentatum* is not essential, it is in the *C. elegans* L-AChR (Boulin et al., 2008) (Figure 1.8). In *C. elegans*, *acr-8* is expressed mostly in the L1 larval stage but seems normally excluded from formation of a functional receptor despite evidence it is able to complement *acr-13 in vivo* (Hernando et al., 2012). Of particular interest for my thesis research, the trichostrongylid nematodes *H. contortus*, *T. circumcincta* and *T. colubriformis*, each encode four paralogous copies of *unc-29* that have appeared since divergence from the *Caenorhabditis* group, named *unc-29.1*, *unc-29.2*, *unc-29.3* and *unc-29.4* (Neveu et al., 2010).

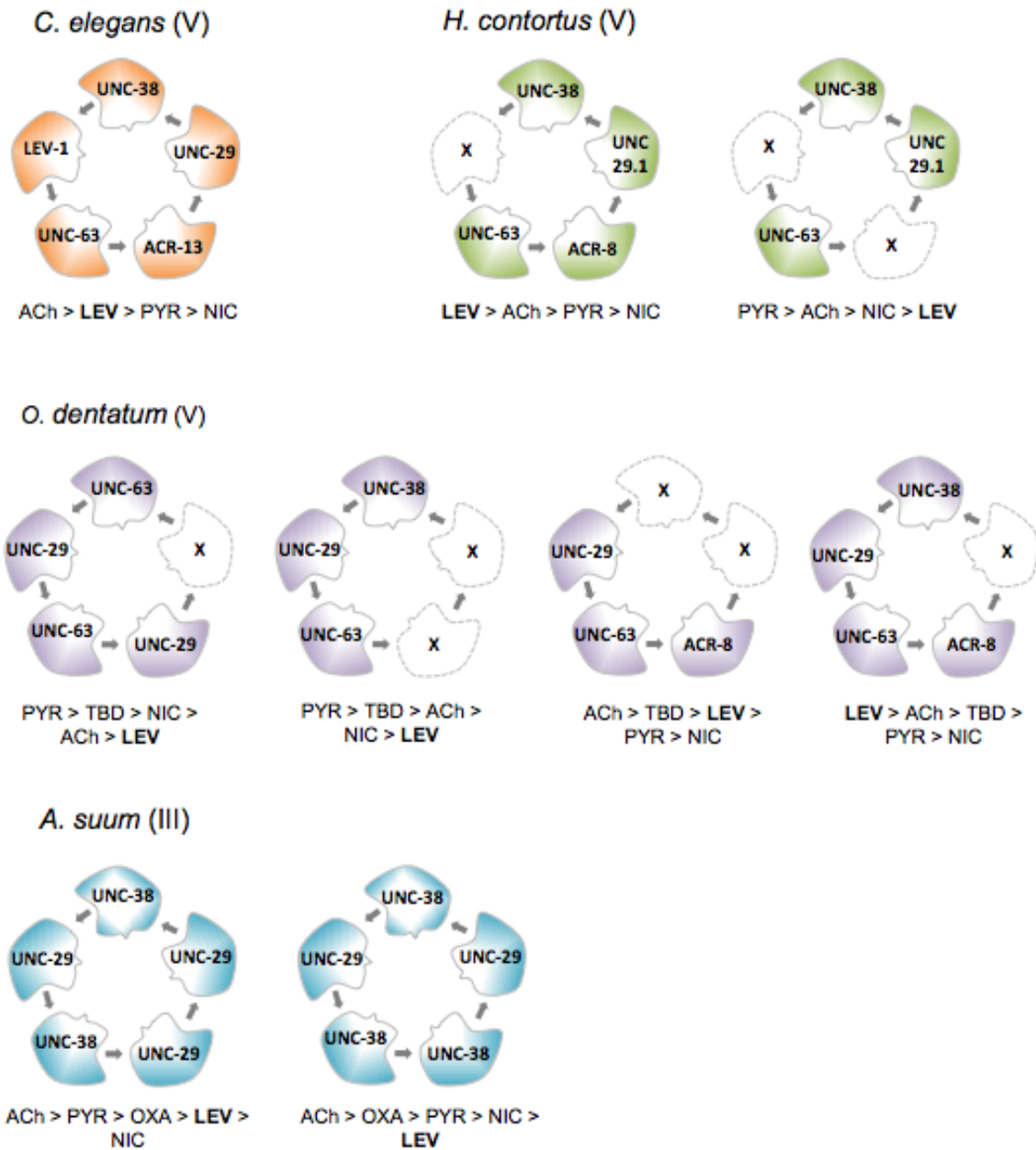


**Figure 1.8: L-AChRs reconstituted in *Xenopus* oocytes and their respective pharmacology.** adapted from (Boulin et al., 2008, Williamson et al., 2009, Boulin et al., 2011, Buxton et al., 2014). Brackets indicate nematode clade. Agonists correspond to acetylcholine (ACh), tribendimidine (TBD), nicotine (NIC), pyrantel (PYR), oxantel (OXA) and levamisole (LEV)



### 1.6.3 Duplication of *unc-29* - a new model

The origin of pLGICs remains largely obscure as their emergence predates the Cambrian explosion and most likely the split of eukaryotes and prokaryotes (Tasneem et al., 2005, Dent 2006). The identification of specific sequence changes following duplication that are responsible for changes in function, and ultimately the persistence of the new subunit types, is greatly limited.

The recent duplication of the *unc-29* gene was first identified in trichostrongylid nematodes where both genomic and transcriptomic information allowed the successful cloning of the corresponding genes (Neveu et al., 2010). A phylogenetic analysis of the *unc-29* genes present in clade III and clade V nematodes revealed the presence of at least 9 recent duplication events of *unc-29* within the Strongylida suggesting the duplications in *H. contortus* are representative of a wider phenomenon (Duguet et al., 2016). The four *H. contortus* paralogs share approximately 74 % protein sequence identity with their ortholog from *C. elegans* (Figure 1.9) and from 74 % to 92 % amino acid identity between paralogs (Neveu et al., 2010). This compares to 61% identity between the two non-alpha subunits of *C. elegans*, *lev-1* and *unc-29*.

The four copies of *unc-29* meet the first criteria required for a good model of pLGIC subunit diversification in that sequence divergence is limited between copies and that they are representative of a larger phenomenon of *unc-29* gene duplication in the strogylid nematodes. Through the work described in this thesis I show, in chapter II, that the functional characteristics of each copy have indeed changed and, in chapter III, that the ability of different subunit combinations to combine into functional receptors represents one major difference in functionality. In chapter IV, I demonstrate that only one specific quaternary arrangement of the five different subunits in the *C. elegans* L-AChR produces a functional channel. Taken together, this work shows that the duplication of *unc-29* subunits in the trichostrongylid nematodes fulfills the requirements of an effective model of pLGIC subunit duplication and divergence and provides the necessary details on the physical interaction between subunits in the *C. elegans* L-AChR. This lays the foundation for future work to specifically identify the mechanisms and specific amino acid changes that determine this process.

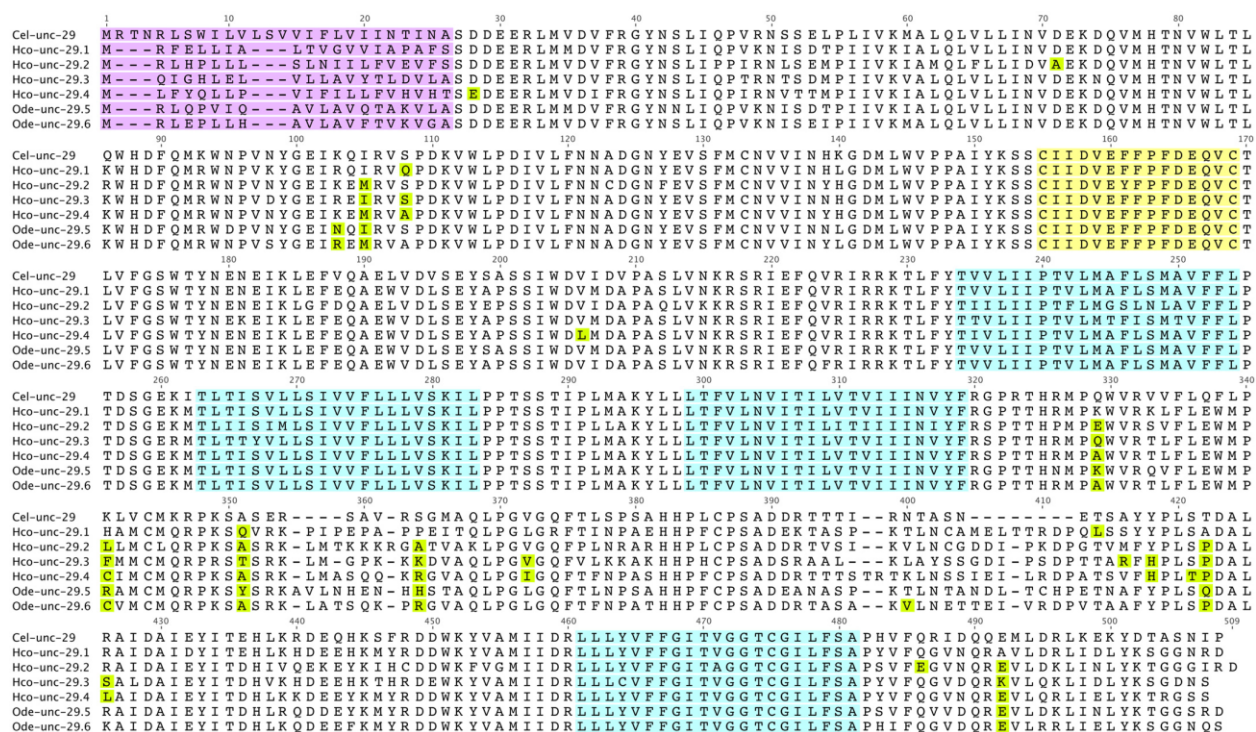


**Figure 1.9: Alignment of *C. elegans*, *H. contortus* and *O. dentatum* UNC-29 proteins.** Colors represent signal peptide (pink), the cys-loop (yellow), the transmembrane domains (blue) and positively selected residues (green). Adapted from (Duguet et al., 2016).

## Chapter II - Functional divergence of *Hco-unc-29* subunit copies.

### 2.1 Introduction

The major classes of nematode pentameric ligand-gated ion-channels trace their origins back to the period prior to the cambrian explosion from which the major classes of animal life appeared (Smith et al., 2013). Since movement is critical to animal life, the role that the diversification of pLGICs played in this process is of great concern. Over the last 600 million years, gene duplication and subsequent specialization of subunits has produced a great diversity of cell-to-cell signalling mechanisms as well as the emergence of new heteromeric receptors from presumably homomeric ancestral receptors (Ortells et al., 1995, Dent 2006, Dent 2010, Beech et al., 2015).

These events are old, followed by a long period of evolution that limits our ability to identify the critical mutational events responsible for functional change and the mechanisms responsible.

Interestingly, the duplications of the *unc-29* gene in trichostrongylid nematodes are a rare example of ongoing gene expansion and represent a potentially ideal model for investigating the mechanistic details of this critical process.

In order to establish whether duplications of *unc-29* could serve as model, it is critical to determine if the limited sequence divergence among the four paralogs corresponds to experimentally verifiable functional change. The approach used here is to replace each *unc-29* paralog, in turn, and determine whether this leads to any identifiably different physical characteristics of the receptors produced. This is done in transgenic *C. elegans*, to complement the function of the native *C. elegans unc-29* and in various admixtures of the *H. contortus* L-AChR1 and *C. elegans* L-AChR. There is no assumption that the reconstituted receptors correspond to any real receptor produced by the parasite *in vivo*. The technique is used simply to determine any physical characteristics associated specifically with the paralogous UNC-29 proteins. Although each copy of UNC-29 retained generally similar characteristics, and could functionally replace the *C. elegans* UNC-29 *in vitro* and *in vivo*, I was able to demonstrate that each had distinguishing functional characteristics in terms of ligand affinity and channel response. The most striking difference was that the subunit UNC-29.2 was able to reconstitute a functional receptor in combination with other *C. elegans* subunits but not those from *H. contortus*. This could suggest that compatibility between subunits is a feature that evolves rapidly and involves coadaptation with other subunits of the receptor.

## 2.2 Results

### 2.2.1 Reconstitution and characterization of L-AChRs with each *Hco-UNC-29* copy.

The presence of four distinct functional copies of *unc-29* would suggest they may each produce a different L-AChR that would be functionally divergent. To explore this possibility, different subunit combinations were used to reconstitute receptors in *Xenopus* oocytes and characterized by electrophysiology.

The previously described L-AChR1 containing subunits *Hco-unc-63*, *Hco-unc-38*, *Hco-acr-8*, *Hco-unc-29.1* (Boulin et al., 2011) was considered a positive control for the other combinations. Sequential replacement of *Hco-unc-29.1* by each of *Hco-unc-29.2*, *Hco-unc-29.3* and *Hco-unc-29.4* in the cRNA mixture was carried out. For clarity, a nomenclature of these new subunit combinations was adopted as follows. The original L-AChR1 (Boulin et al., 2011) is referred to as L-AChR1.1. Replacement of *Hco-UNC-29.1* with *Hco-UNC-29.2*, *Hco-UNC-29.3* and *Hco-UNC-29.4* in turn are referred to as L-AChR1.2, L-AChR1.3 and L-AChR1.4 (Figure 2.1). These four subunit combinations were individually expressed in *Xenopus* oocytes. After 4 days,  $\mu$ A range currents were recorded on exposure to 100  $\mu$ M ACh (Figure 2.1 A-C) and the LEV response at equimolar concentration corresponded to  $125.4 \pm 13.0$  % of the ACh currents for the L-AChR1.1 (Figure 2.1A, G). The relative affinity ( $EC_{50}$ ) obtained for ACh was  $2.4 \pm 0.2$   $\mu$ M and LEV,  $4.9 \pm 0.4$   $\mu$ M (Figure 2.1G, Table 2.1). These results were consistent with those of Boulin *et al.* (Boulin et al., 2011).

The injection of the cRNA mix corresponding to L-AChR1.2 did not generate any detectable currents with either 100  $\mu$ M of ACh or LEV application (Figure 2.2). These data were repeated (n=18) by testing at least three independent oocyte batches under the same conditions. Since the other paralogs were able to assemble with the remaining subunits (see below), it may be the case that UNC-29.2 also assembles into a receptor that is non-functional. If so, then the presence of UNC-29.2 may interfere with the ability of UNC-29.1 to produce a functional receptor and effectively "poison" the receptor similar to the effect of the truncated *H. contortus* UNC-63b (Boulin et al., 2011). Alternatively, if a functional receptor could be produced by co-assembly of both UNC-29.1 and UNC-29.2, the functional characteristics of this new receptor should be distinct. To test these hypotheses, the L-AChR1.1 was used as a model template in the presence of increasing amounts of *Hco-unc-29.2* cRNA at ratios of 0.2, 1 and 5 times compared to *Hco-unc-29.1* cRNA. These mixes were injected in oocytes but the different ratios did not reveal any detectable change in the pharmacology of the L-AChR1.1 (Figure 2.3, Table

2.2). Concentration-responses assays were performed with both ACh and LEV but the respective  $EC_{50}$  remained unchanged (Figure 2.3, Table 2.2). While not conclusive, these data provide no evidence that UNC-29.2 can co-assemble with the other L-AChR subunits.

In contrast, reconstitution of two new L-AChRs was achieved by expressing L-AChR1.3 and L-AChR1.4. Measurable currents were observed with 100  $\mu$ M ACh (Figure 2.1B, C). However, the maximum response to both ACh and LEV were significantly different from each other and constituted one of the specific pharmacological signature of these two receptors compared to the L-AChR1.1 (Figure 2.1B, C). Indeed, the L-AChR1.3 LEV response of  $65.2 \pm 9.9\%$  of the ACh current at 100  $\mu$ M made LEV a partial agonist of this receptor (Figure 2.1B, C, Table 2.3). In contrast, L-AChR1.4 responded to LEV similarly to ACh at the same concentration with a relative current of  $94.7 \pm 2.9\%$  (Figure 2.1B, C, Table 2.3). Concentration-response assays with ACh and LEV on both the L-AChR1.3 and L-AChR1.4 found the potency for ACh was similar to L-AChR1.1, with an  $EC_{50}$  of about 3.2  $\mu$ M (Figure 2.1G-I, Table 2.1). The  $EC_{50}$  for LEV was slightly lower for L-AChR1.4 than L-AChR1.3 with  $1.15 \pm 0.1$   $\mu$ M and  $2.5 \pm 0.35$   $\mu$ M respectively (Figure 2.1G-I, Table 2.1).

A panel of both cholinergic agonists and antagonists were used to evaluate channel response. Among these, dimethylpiperazine (DMPP), a cholinergic agonist, produced lower currents than both ACh and LEV but remained a common agonist of L-AChR1.1, L-AChR1.3 and L-AChR1.4 (Figure 2.1A-C, Table 2.3). Anthelmintics such as pyrantel (PYR), buphenium (BEPH) and nicotine (NIC) produced very weak responses compared to ACh at the same concentration (Figure 2.1A-C, Table 2.3).

Antagonist d-tubocurarine (dTC) (100  $\mu$ M) completely inhibited the ACh currents from all three *H. contortus* L-AChRs (Figure 2.1 D-F, Table 2.3), whereas the non-competitive antagonist dihydro- $\alpha$ -erythroidine (DH $\alpha$ E) (10  $\mu$ M), showed a very low inhibition of ACh response (Figure 2.1D-F, Table 2.3). Finally, the allosteric antagonist mecamylamine (Meca) (30  $\mu$ M) induced almost complete inhibition of the L-AChR1.1 and L-AChR1.4, corresponding, respectively, to  $99.9 \pm 0.1\%$  and  $96.4 \pm 1.9\%$  of the AChR response (Figure 2.1D-F, Table 2.3). The action of Meca was characteristically different on the L-AChR1.3, with only  $56.9 \pm 3.2\%$  inhibition of ACh-evoked currents (Figure 2.1E, Table 2.3), a clear signature of the L-AChR1.3 pharmacology.

Altogether, three new receptors were reconstituted in *Xenopus* oocytes: Hco-UNC-29.1, Hco-UNC-29.3 and Hco-UNC-29.4 that were characterized by very high affinity for ACh and LEV and each possessed distinctive pharmacological properties that made each receptor unique. The failure of L-

AChR1.2 to reconstitute a functional channel remains an unanswered question but is surprising given the high level of similarity between copies.

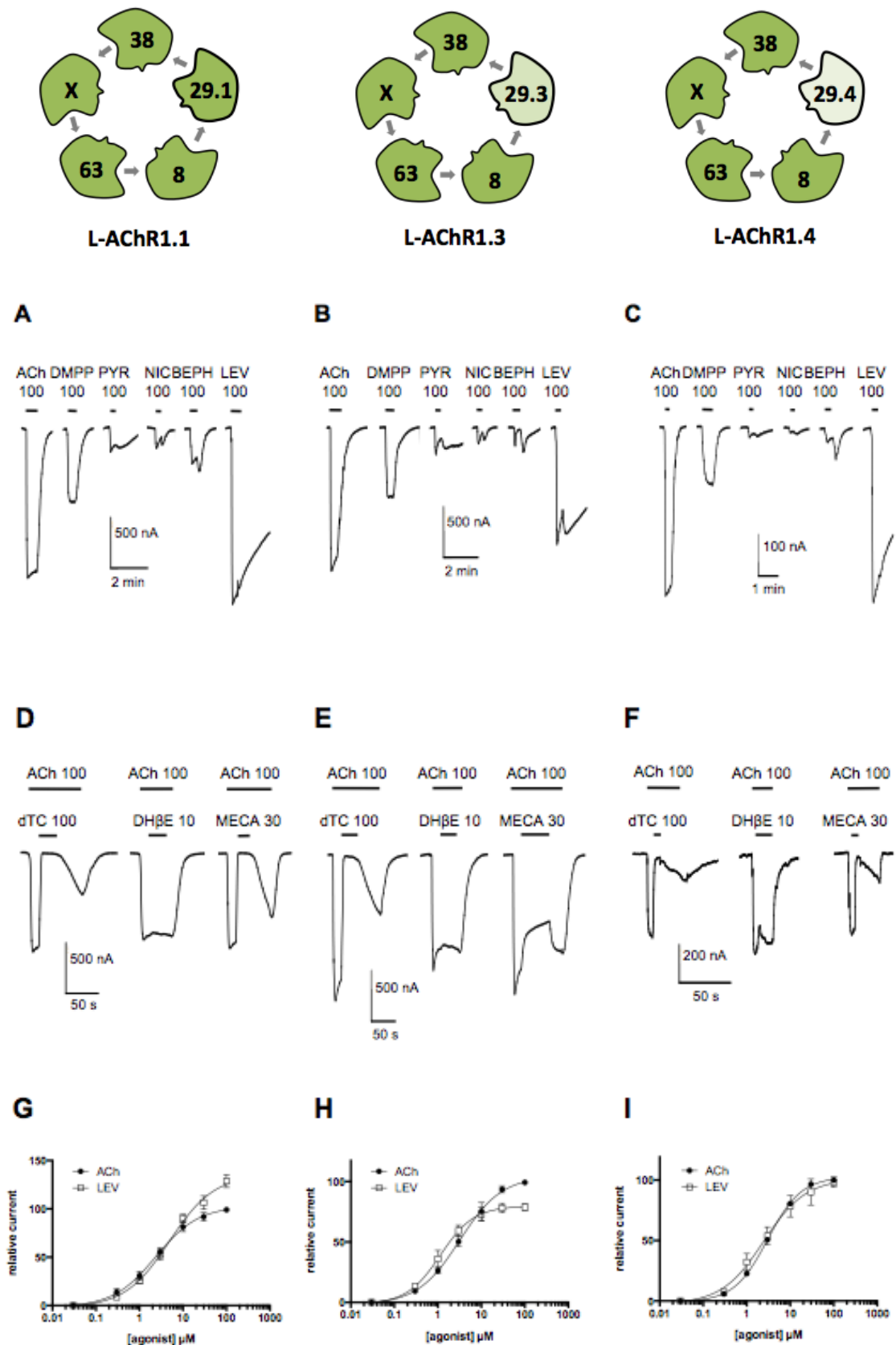


Figure 2.1: Response of *H. contortus* reconstituted receptors in *Xenopus* oocytes

Two-electrodes voltage-clamp experiments were performed on oocytes injected with *Hco-unc-63*, *Hco-unc-38*, *Hco-acr-8*, and *Hco-ric-3.1*, *Hco-unc-74*, *Hco-unc-50* cRNAs. *Hco-unc-29.1*, *unc-29.3* and *unc-29.4* were combined independently with the cRNA mixture. A), B) and C) Representative recording traces from single oocytes perfused with 100  $\mu$ M of the following cholinergic agonists: acetylcholine (ACh), Dimethylpiperazinium (DMPP), Pyrantel (PYR), Nicotine (NIC), Bephenium (BEPH) and Levamisole (LEV). D), E) and F) Representative recording traces from single oocytes continuously perfused with 100  $\mu$ M ACh. Oocytes were perfused with the following cholinergic antagonists: D-tubocurarine (dTC, 100  $\mu$ M), Dihydro- $\beta$ -erythroidine (DH $\beta$ E, 10  $\mu$ M) and Mecamylamine (MECA, 30  $\mu$ M). Black horizontal bars show the time period of agonist and or antagonist application. G), H) and I) Concentration-response curves for the L-AChR1.1, L-AChR1.3 and L-AChR1.4 for ACh (black circles) and LEV (white squares). All responses are normalized to 100  $\mu$ M ACh, which corresponds to the saturating dose. The ACh and LEV 50% effective concentration ( $EC_{50}$ ) values as well as Hill coefficients are indicated in Table 2.1. Maximum responses to agonists and antagonists are shown in Table 2.3. Error bars represent SE. Receptor diagrams do not correspond to the real subunit position and stoichiometry, "X" represents the unidentified L-AChR subunit present twice in the receptor.

	ACh			LEV		
	$EC_{50}$ ( $\mu$ M)	Hill	n	$EC_{50}$ ( $\mu$ M)	Hill	n
<b>L-AChR1.1</b>	$2.38 \pm 0.16$	$0.88 \pm 0.05$	8	$4.91 \pm 0.44$	$0.84 \pm 0.05$	8
<b>L-AChR1.3</b>	$3.19 \pm 0.22$	$0.89 \pm 0.05$	7	$1.15 \pm 0.08$	$1.13 \pm 0.09$	6
<b>L-AChR1.4</b>	$3.03 \pm 0.04$	$1.12 \pm 0.04$	4	$2.48 \pm 0.35$	$0.90 \pm 0.12$	4

**Table 2.1: ACh and LEV response profiles of the reconstituted L-AChR1.1, L-AChR1.3 and L-AChR1.4. Values  $\pm$  standard error.**



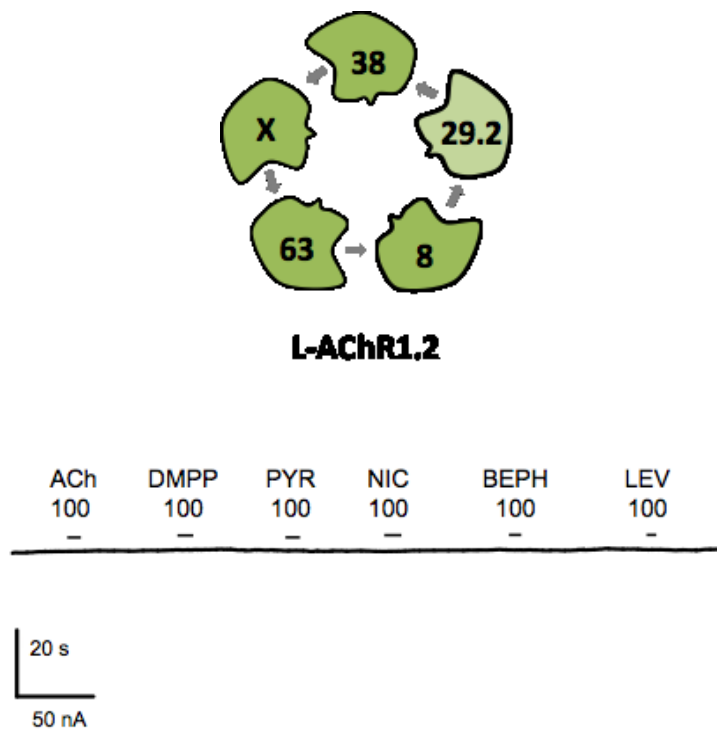


**Figure 2.2: Reconstitution and pharmacological characterization of L-AChR1.2 in *Xenopus* oocytes.** Two-electrode voltage-clamp were applied on *Xenopus* oocytes injected with *Hco-unc-63*, *Hco-unc-38*, *Hco-unc-29.2* cRNAs along with the *Hco-unc-50*, *Hco-unc-74* and *Hco-ric-3.1* cRNA encoding accessory proteins. Diagram representing top view of the putative receptor. The trace is a representative recording from single oocytes perfused with 100  $\mu$ M of the following cholinergic agonists: acetylcholine (ACh), Dimethylpiperazinium (DMPP), Pyrantel (PYR), Nicotine (NIC), Bephenium (BEPH) and Levamisole (LEV). Black horizontal bars show the time period of agonist application.

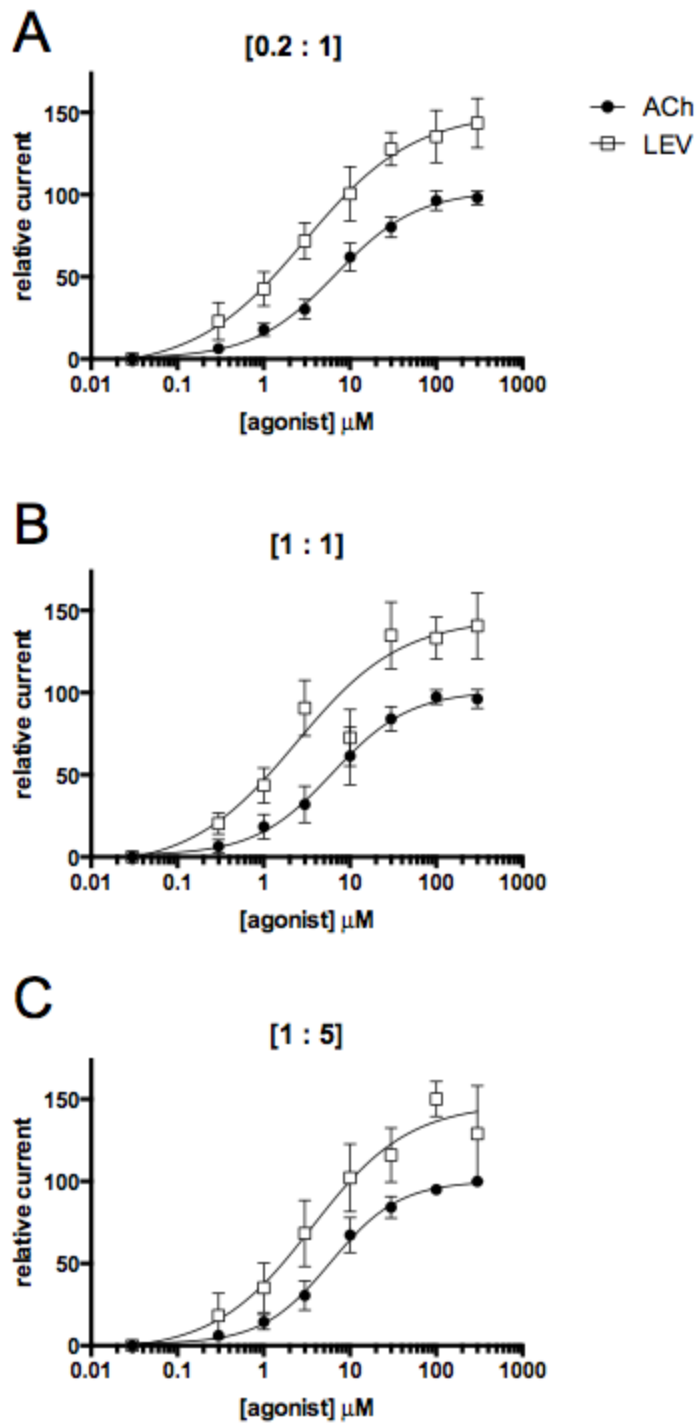


**Figure 2.3: Changing ratio of *Hco-unc-29.1* : *Hco-unc-29.2* cRNA in *Xenopus* oocytes.** cRNA mixture corresponding to the L-AChR1.1 was prepared and *Hco-unc-29.2* cRNA was added to the mixture at 0.2, 1, 5 times the concentration of *Hco-unc-29.1* cRNA. cRNA preparation were injected in *Xenopus* oocytes and TEVC experiments were performed. Graphs show dose-response curves with ACh (black circles) and LEV (white squares) for each ratio. All responses are normalized to 100  $\mu\text{M}$  ACh, which corresponds to the saturating dose. The ACh and LEV 50% effective concentration ( $\text{EC}_{50}$ ) values as well as Hill coefficients are indicated in Table 2.2. Errors bars represent SE.

	ACh			Lev		
<b>cRNA Ratio</b>	<b>EC<sub>50</sub> (μM)</b>	<b>Hill</b>	<b>n</b>	<b>EC<sub>50</sub> (μM)</b>	<b>Hill</b>	<b>n</b>
<b>[1:0.2]</b>	6.82 ± 0.69	0.91 ± 0.08	6	3.05 ± 0.49	0.69 ± 0.09	6
<b>[1:1]</b>	6.33 ± 0.92	0.96 ± 0.13	7	2.41 ± 0.52	0.71 ± 0.13	7
<b>[1:5]</b>	5.96 ± 0.57	1.09 ± 0.1	6	3.7 ± 0.84	0.77 ± 0.13	6

**Table 2.2: ACh and LEV response profiles for increasing addition of UNC-29.2 to the L-AChR1.1 from Figure 2.3. Values ± standard error.**

	L-AChR1.1		L-AChR1.3		L-AChR1.4	
<b>Agonists</b>	<b>Max. Current ± S.E. (%)</b>	<b>n</b>	<b>Max. Current ± S.E. (%)</b>	<b>n</b>	<b>Max. Current ± S.E. (%)</b>	<b>n</b>
Acetylcholine	100	12	100	11	100	8
DMPP	41.98 ± 1.41	9	36.93 ± 3.93	8	31.63 ± 1.00	8
Pyrantel	11.85 ± 0.99	12	13.79 ± 1.26	9	7.32 ± 0.98	7
Nicotine	4.7 ± 1.05	12	6.79 ± 1.46	8	1.52 ± 0.47	6
Bephenium	13.92 ± 1.70	12	9.59 ± 0.83	7	6.45 ± 0.84	7
Levamisole	125.4 ± 3.76	12	65.18 ± 3.50	8	94.71 ± 2.93	8
<b>Antagonists</b>	<b>Max. inhibition ± S.E. (%)</b>	<b>n</b>	<b>Max. inhibition ± S.E. (%)</b>	<b>n</b>	<b>Max. inhibition ± S.E. (%)</b>	<b>n</b>
D-tubocurarine	99.63 ± 0.35	11	99.98 ± 0.02	6	97.52 ± 1.09	7
DHβE	15.98 ± 2.16	11	23.55 ± 1.94	7	16.51 ± 5.73	6
Mecamylamine	99.91 ± 0.09	8	56.87 ± 3.18	5	96.4 ± 1.92	8

**Table 2.3: Pharmacological response of L-AChR1.1, L-AChR1.3 and L-AChR1. S.E: standard error.**

### 2.2.2 Expression of *H. contortus* / *C. elegans* subunit admixtures in *Xenopus* oocytes.

Subunit composition of the *C. elegans* and *H. contortus* differs in that the *C. elegans* L-AChR requires ACR-13, while no *acr-13* ortholog has been identified in *H. contortus*. The *H. contortus* L-AChR1 does not require LEV-1 and four different copies of *unc-29* are present in *H. contortus*. To test whether the Hco-UNC-29 copies retained their fundamental role as an *unc-29* subunit and replace Cel-UNC-29 in the *C. elegans* L-AChR, a similar approach proposed by Sloan *et al.*, (Sloan *et al.*, 2015) was applied. Indeed, admixtures of cRNA were prepared combining *Cel-unc-63*, *Cel-unc-38*, *Cel-acr-13* and *Cel-lev-1* along with each *Hco-unc-29* cRNA copy in turn as well as the cRNAs *Hco-unc-50*, *Hco-unc-74* and *Hco-ric-3.1* encoding L-AChR ancillary proteins (Boulin *et al.*, 2008, Boulin *et al.*, 2011). The native *C. elegans* L-AChR exhibited similar maximum responses to both acetylcholine ACh and LEV at 100  $\mu$ M as reported by Boulin *et al* (Boulin *et al.*, 2008) (Figure 2.4). This also confirmed that *H. contortus* accessory proteins were able to function properly between species. The omission of *Cel-unc-29* led to no significant current confirming this subunit is essential. Replacing *Cel-unc-29* with *Hco-unc-29.1* produced a receptor generating an average of 500 nA currents with 100  $\mu$ M ACh (Figure 2.4). Replacement with *Hco-unc-29.3* or *Hco-unc-29.4* led to similar responses to ACh with currents below 200 nA and, perhaps surprisingly *Hco-unc-29.2* also produced currents in response to ACh, although, the lowest, with an average of  $28.6 \pm 5.2$  nA (Figure 2.4). The relative response to 100  $\mu$ M LEV was almost identical for all four receptors containing the *H. contortus* *unc-29* copies (Figure 2.4). These data confirm that each of the Hco-UNC-29 copies can functionally replace Cel-UNC-29 in *Xenopus* oocytes, although with different efficiencies. Despite the low currents observed with Hco-UNC-29.2, these results confirm that this copy is functional and suggests that interactions between UNC-29.2 and other subunits within the L-AChR are responsible for its inability to produce a functional receptor.

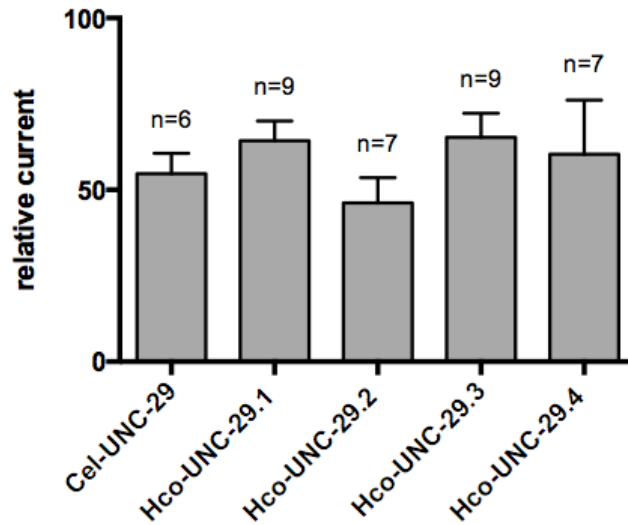


**Figure 2.4: LEV response relative to 100  $\mu$ M ACh currents of *H. contortus* / *C. elegans* subunit admixtures reconstituted in *Xenopus* oocytes**

Two electrode voltage clamp experiments were performed on oocytes injected with *Cel-unc-63*, *Cel-unc-38*, *Cel-acr-13*, *Cel-lev-1* cRNAs and co-expressed with *H. contortus* accessory proteins, *ric-3*, *unc-50* and *unc-74*. The addition of cRNAs encoding *Cel-unc-29*, *unc-29.1*, *unc-29.2*, *unc-29.3* or *unc-29.4* were tested independently. LEV response values were normalized to those elicited after perfusion of 100  $\mu$ M ACh. Error bars indicate SE.

### 2.2.3 Expression of the *Hco-unc-29* paralogs in transgenic *C. elegans*

Each *H. contortus* paralog was able to reconstitute a functional receptor in *Xenopus* oocytes but in order to test if this same ability occurs *in vivo*, each copy was expressed as a transgene under control of the body muscle *myo-3* promoter, in a *C. elegans* mutant background carrying a defective *unc-29* gene and exhibiting LEV resistance (Fleming et al., 1997). Expression of transgenes may lead to very high levels of expression (Mello et al., 1995) and distorted ratios of pLGIC subunits have been shown to alter the functional characteristics of reconstituted receptors (Williamson et al., 2009, Rufener et al., 2010, Charvet et al., 2012). A phenotypic assay that depends on normal regulation of movement, such as thrashing, may be sensitive to the precise nature of the reconstitute receptor and its ability to function within narrow parameters. For this reason, sensitivity to LEV was evaluated by measuring the fraction of moving transgenic animals over time after exposure. This phenotype depends only on whether a receptor is produced that is sensitive to LEV and allows cations to enter the muscle cell and would not require the receptor to function accurately in the regulation of coordinated movement.

Exposure of wild-type N2 worms to 200  $\mu$ M LEV produced a very quick paralysis that was complete after less than an hour of treatment, whereas the *unc-29(e1072)* mutant worms were still moving over

two hours after exposure (Figure 2.5). Transfection of the *unc-29(e1072)* strain with *Cel-unc-29* elicited a complete rescue of the LEV sensitive phenotype, with kinetics of paralysis very similar to the wild-type N2 animals (Figure 2.5). An increased sensitivity to LEV was observed for all *unc-29(e1072)* worms transfected with *unc-29* paralogs from *H. contortus*, which were almost completely paralyzed after 2 hours of exposure to the anthelmintic (Figure 2.5). These results confirm the observations made in *Xenopus* oocytes that all four copies of *H. contortus unc-29* are functional within the *C. elegans* L-AChR and have each retained their ability to combine into an L-AChR responsive to LEV.

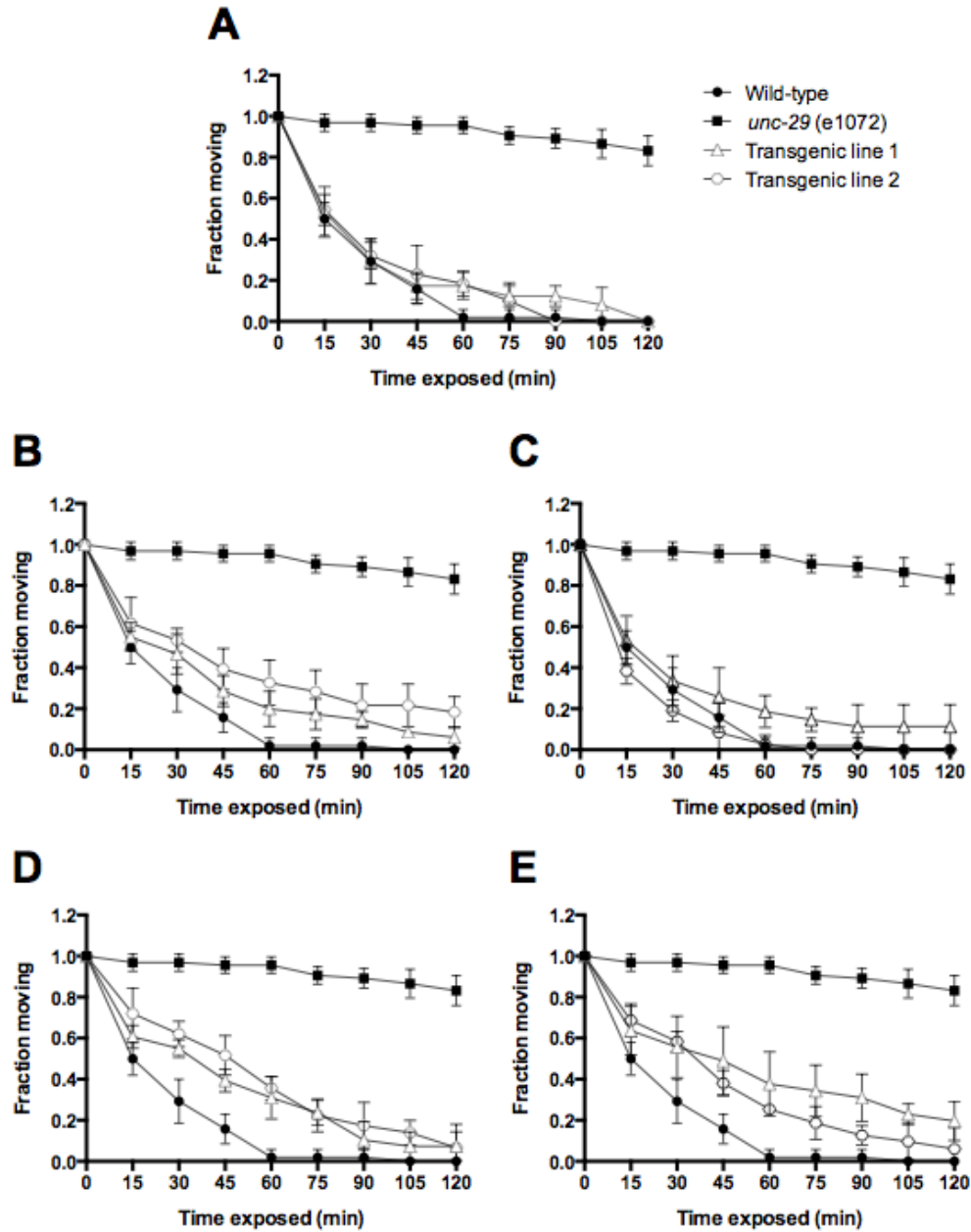


**Figure 2.5: Rescue of LEV sensitivity in transgenic *C. elegans***

*Hco-unc-29* gene copies were transfected into *C. elegans unc-29*(e1072) mutant strain (CB1072). The number of moving animals under exposure to 200  $\mu$ M LEV every 15 min are shown on the Y axes. N2 Bristol wild-type (black circles) and CB1072 *unc-29*(e1072) (black squares) controls are shown for comparison. Two independent transfected worm lines (white circles and triangles) were examined for each experiment. This assay was repeated three times on 12 animals per worm line. **A**) Transfection of *Cel-unc-29*. **B-E**) Transfection of *unc-29.1*, *unc-29.2*, *unc-29.3* and *unc-29.4* respectively. Data are plotted as mean  $\pm$  SE. A Two-way ANOVA with Bonferroni's multiple comparison post test was performed. In every case, both transfected lines were significantly more LEV sensitive than the CB1072 *unc-29*(e1072) mutants ( $p < 0.001$ ).

#### 2.2.4 *In situ* localization of Hco-UNC-29.1 and Hco-UNC-29.2

The heterologous expression of AChR subunits identified *unc-29.2* as unusual in that no functional receptor could be reconstituted along with the other subunits from *H. contortus*, unlike *unc-29.1*. No evidence was seen in reconstituted receptors that the subunits competed with each other for incorporation into a receptor but if this is a consequence of functional adaptation, it becomes important to understand if the subunits are co-expressed. To investigate this point, specific polyclonal antibodies were generated against both Hco-UNC-29.1 and Hco-UNC-29.2 peptides, designed from the intracellular domain. This loop is highly variable and is located between the TM3 and TM4 domains. The specificity and lack of cross-reactivity of both sets of antibodies were verified by ELISA. Immunofluorescence assays on *Xenopus* oocytes that were previously injected with either L-AChR1.1 or L-AChR1.2 were used to confirm the reactivity and specificity of the antibodies against the whole, mature subunit protein (Figure 2.6).

Localization of both Hco-UNC-29.1 and Hco-UNC-29.2 was performed on transversal 10 µm sections of male and female adult *H. contortus* (Figure 2.7E, F and M, N). The immunolabelling of myosin heavy chain identified body muscles of male and female worms and the uterus muscles of females with both subunits (Figure 2.7G, H and O, P). Then, a closer observation also revealed fluorescent signals from the uterus muscles of females. For both subunits and worm sexes, the signals were localized in the same area and any unspecific staining as observed in the intestinal lumen was identifiable using the peptide pre-adsorbed antibodies.

In conclusion, the localization of Hco-UNC-29.1 and Hco-UNC-29.2 confirms the potential role of these respective subunits in the worm locomotion and a unsuspected function in the reproductive system of female worms. In addition, the possibility that both subunits may co-assemble or compete for assembly with other subunits of the L-AChR can not be ignored despite the lack of confirmation from electrophysiology experiments.



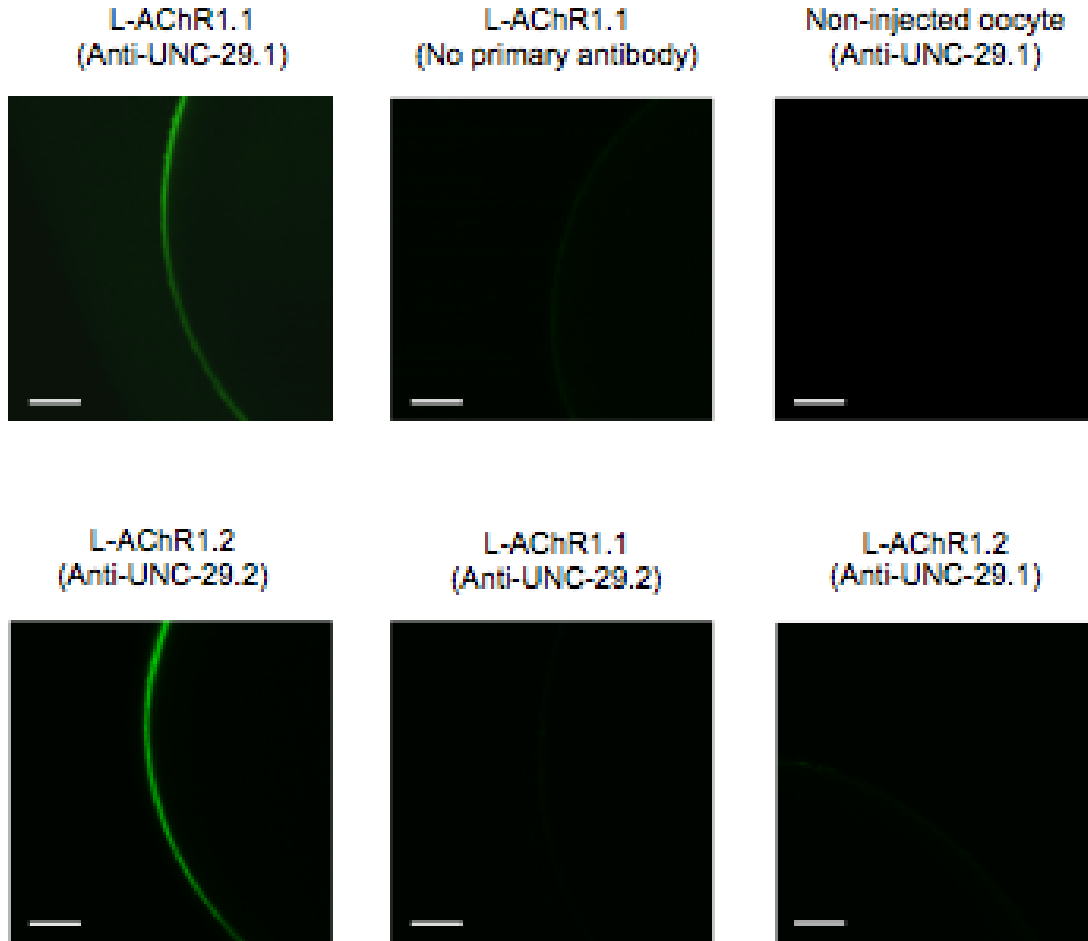


**Figure 2.6: Cross-reactivity assay between Anti-Hco-UNC-29.1 and anti-Hco-UNC-29.2 primary antibodies.**

cRNA mixtures corresponding to the L-AChR1.1 and L-AChR1.2 were prepared and injected in mature *Xenopus* oocytes. After 5 days, oocytes were checked for expression using the TEVC technique (when applicable). Oocytes were then fixed and incubated with affinity-purified antibodies raised against Hco-UNC-29.1 and Hco-UNC-29.2 specific peptides. Alexa 488-labeled secondary antibodies (green) were used to localize subunits. Controls consisted in un-injected oocytes incubated in anti-UNC-29.1 antibodies and L-AChR1-expressing oocytes incubated with the secondary antibodies only. Confocal microscopy was performed on the whole oocytes. All slides were observed under 20x magnification. Scale bars correspond to 100  $\mu\text{m}$ .

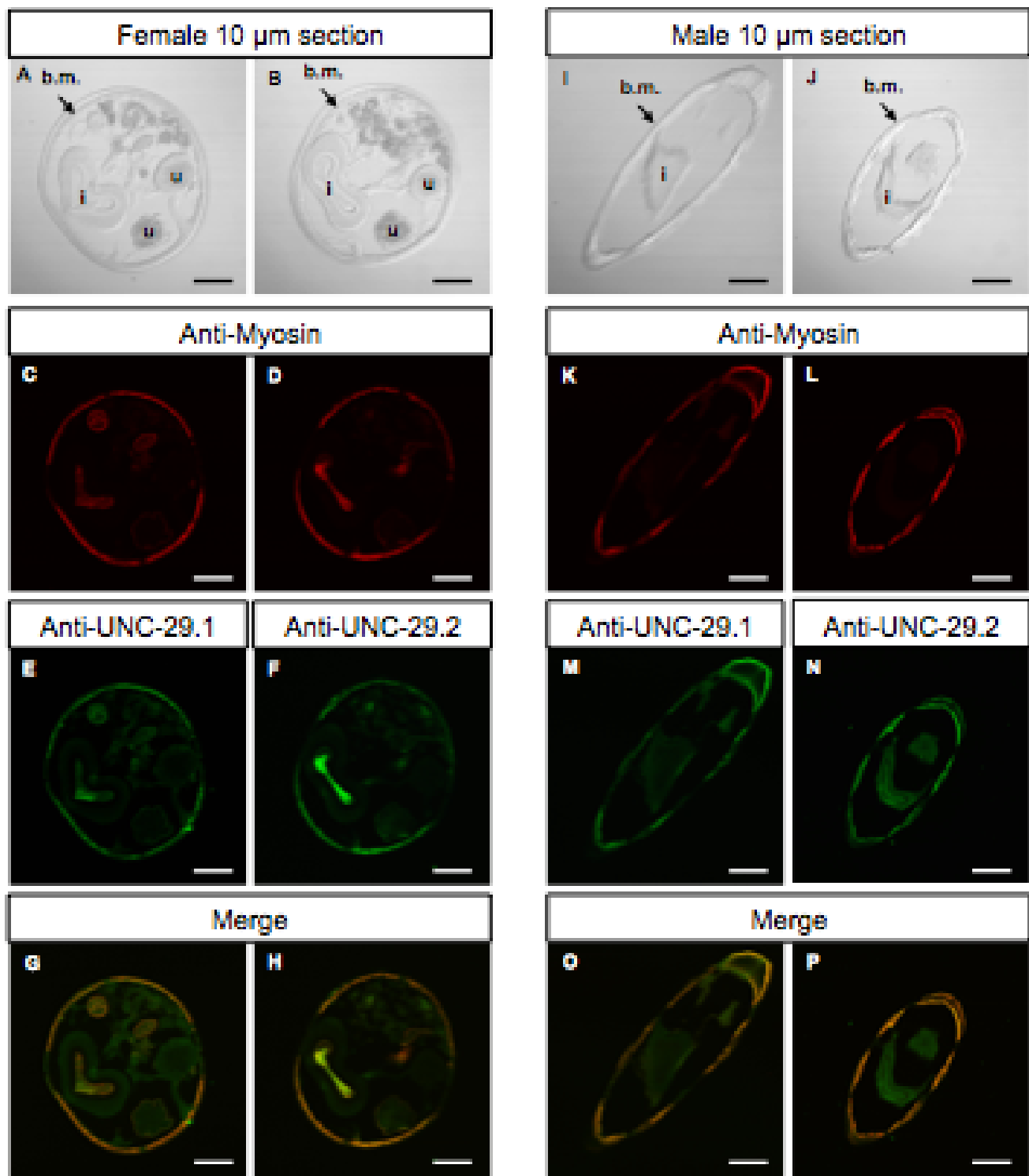


**Figure 2.7: Immunolocalization of UNC-29.1 and UNC-29.2 in adult *H. contortus***

Adults were fixed and incubated with affinity-purified antibodies raised against UNC-29.1 or UNC-29.2 specific peptides. The localization of both subunits were performed using Alexa 488-labeled secondary antibodies (green). **A–H)** Confocal microscopy performed on female 10 µm transversal cryosections. **A)** and **B)** Transmitted light imaging performed on two separate sections. Letters indicate body muscles (b.m.), uterus (u) and intestine lumen (i). **C)** and **D)** Localization of the muscles using

primary antibodies raised against myosin protein and stained with secondary, Alexa 594-labeled antibodies (red). **E)** Staining of UNC-29.1 showing expression in the body muscle as well as the uterus external muscular layer. **F)** Staining of UNC-29.2 revealing a similar localization to UNC-29.1. **G)** and **H)** Merge of green (UNC-29.1 or UNC-29.2) and red (myosin) signals. **I–P)** Confocal microscopy performed on male 10  $\mu$ m transversal cryosections. **I)** and **J)** Transmitted light imaging performed on two separate sections. **K)** and **L)** Localization of the muscles with Alexa 594 secondary antibody (red). **M)** Staining of UNC-29.1 showing exclusive expression in the body muscles. **N)** Staining of UNC-29.2 revealing a similar localization. **O)** and **P)** Merge of UNC-29 copy (green) and myosin (red) signals. All slices are representative of the middle of the worm body and scale bars correspond to 100  $\mu$ m.

## 2.3 Discussion

The *unc-29* group of AChR subunits, despite a variability in subunit composition, is represented in every nematode clade including clade V, in which a specific, ongoing gene expansion is observed. Bioinformatic analysis suggests that the *unc-29* gene is often duplicated within the strongylid parasitic nematodes. The four paralogs present in the trichostrongylids experienced positive selection pressure that suggests they may have diverged in function (Duguet et al., 2016). In this chapter, expression of the four *H. contortus* *unc-29* copies in transgenic *C. elegans* provided strong evidence that functional AChRs integrating the subunit copies can be assembled *in vivo* and confer LEV sensitivity, including the UNC-29.2 subunit.

Expression and reconstitution of different L-AChR subunit combinations in *Xenopus* oocytes provided evidence that the four *Hco-unc-29* paralogs have indeed diverged in function, each one possessing unique characteristics. The L-AChR1.1, 1.3 and 1.4 were characterized by distinct relative responses to LEV and 1.4 by a substantially lower maximal current overall. L-AChR1.3 was only partially antagonized by the non-competitive antagonist meca. It is possible to speculate that the very similar EC<sub>50</sub> values of each functional *H. contortus* L-AChR for ACh may be due to the fact that each paralog must produce receptors that respond correctly to ACh, *in vivo* and may reflect evolutionary pressure to preserve ACh response *in vivo*.

The most striking functional discrepancy was the failure to reconstitute a functional L-AChR1.2 in oocytes despite the successful rescue of LEV sensitivity in transgenic *C. elegans* and reconstitution of a functional admixture *C. elegans* L-AChR in oocytes. This chapter and the most recent bioinformatic data (Duguet et al., 2016) are consistent with a hypothesis that evolutionary pressure may have led to exclusion of UNC-29.2 from interfering with the other *H. contortus* L-AChR subunits. In other words, such a theory would indicate that the sequences of L-AChR subunits contain features that determine

compatibility between subunits in the receptor but that this may break down in the interaction between subunits from different species. The next chapter will focus on these subunit interactions between subunits from *C. elegans* and *H. contortus* in order to understand their effects on reconstitution of a functional receptor.

## Chapter III - Subunit interaction in the levamisole sensitive acetylcholine receptor from *H. contortus* and *C. elegans*.

### 3.1 Introduction

We have put forward duplication of the L-AChR non- $\alpha$  subunit *unc-29* in the trichostrongylid nematodes as a model of subunit diversification more generally. The previous chapter demonstrated that the selectively accelerated sequence changes determined from analysis of the sequences (Duguet et al., 2016) correspond to changes in function between the copies. Of particular interest was the difference between *unc-29.1* and *unc-29.2* in terms of their ability to produce a functional receptor, with other subunits, that depended on which other subunits were present. Both these genes were expressed in adult muscular tissue but no evidence was found that UNC-29.1 and UNC-29.2 could be present in the same receptor. It is possible to speculate that some mechanism may evolve to specialize individual subunits for their ability to take part in assembly of specific receptors. Such a mechanism would also require changes in the other subunits forming the receptor, leading to co-adaptation in a particular system. Combining subunits from different closely related species into admixture receptors might be expected to disrupt this and provide a means to define them.

Each of the five subunits present in the *C. elegans* L-AChR is required (Boulin et al., 2008). In other words, removal of any one subunit can not be compensated by another taking its place. The L-AChRs identified from parasitic nematodes exhibit more flexible subunit arrangements. For example, an *A. suum* L-AChR can be reconstituted from only subunits encoded by *unc-38* and *unc-29* (Williamson et al., 2009). Two different L-AChRs can be reconstituted from either three or four different subunit types from *H. contortus* and from *O. dentatum* a total of four different L-AChRs have been produced from either two, three or four different subunits (Boulin et al., 2011, Buxton et al., 2014). In each case, the receptor produced from the largest number of subunits produces the largest current in response to ligand activation and likely corresponds to a receptor present *in vivo* (Buxton et al., 2014). This flexibility coincides with two important evolutionary changes that occurred during the evolution of the parasitic species. First, according to recent phylogenetic analyses, the *lev-1* gene appeared before the divergence of clade III and clade V nematodes but has subsequently been lost from clade III, requiring a change in receptor composition (Beech et al., 2014). *H. contortus* encodes *lev-1* in its genome but it is

not required for the formation of the *H. contortus* L-AChR1.1 *in vitro*. In addition, the LEV-1 protein does not contain a signal peptide, which likely explains its lack of function in *Xenopus* oocytes (Neveu et al., 2010, Boulin et al., 2011). Second, the *acr-13* and *acr-8* genes correspond to a duplication event after divergence of the clade I nematodes but in the common ancestor of the other clades (Beech et al., 2014). The *acr-13* subunit, also known as *lev-8* (Jones et al., 2007), is absolutely required to produce the *C. elegans* L-AChR (Boulin et al., 2011) while *C. elegans* *acr-8* expression is only detected in L1 larvae and is not an essential component. In contrast, trichostrongylid nematodes appear to have lost *acr-13* and the most recent functional data shows that *acr-8* has been recruited in to the L-AChR (Boulin et al., 2011, Beech et al., 2015). It would appear that the loss of subunits is associated with the ability of others to occupy different positions within the pentameric receptor and a change in the compatibility of subunits to combine into functional receptors.

In the context of evaluating subunit compatibilities that have arisen, combining subunits from different species to create an admixture receptor is an approach that has already been used for a variety of applications (Millar 2009). The expression "admixture" here refers to combinations of subunits from different species as opposed to "chimera" that typically refers to a protein where regions have been exchanged with a related protein. The heterologous expression of insect and arthropod AChRs remains challenging, particularly in *Xenopus* oocytes. An alternative is their co-expression with vertebrate subunits to establish a functional hybrid receptor (Lansdell et al., 2012, Lees et al., 2014). In nematodes, the characterization of a GABA-gated chloride channel subunit from *H. contortus* was achieved in combination with a subunit from *C. elegans* (Feng et al., 2002). Similarly the identification of the morantel-sensitive AChR in *H. contortus* and *P. equorum* has been complemented by the co-expression of ACR-26 and ACR-27 subunits from both species. Only the receptor mixing Peq-ACR-26 and Hco-ACR-27 exhibited detectable currents and a reduced sensitivity to ACh and morantel (Courtot et al., personal communication).

In this chapter, admixtures of various combinations of *C. elegans* and *H. contortus* L-AChR subunits in *Xenopus* oocytes have been used to define which subunit combinations are able to reconstitute functional receptors. This will, in turn provide information on features of the mechanisms that determine this compatibility.

## 3.2 Results

### 3.2.1 Admixtures in a *C. elegans* L-AChR subunit background

In order to compare subunit admixtures and validate their function, the *C. elegans* L-AChR was used as a positive control and expressed in *Xenopus* oocytes. Thus, under exposure to 100  $\mu$ M ACh and LEV,  $\mu$ A range currents were successfully recorded (n=10) and corresponded to those observed by Boulin *et al.*, (Boulin *et al.*, 2008) (Figure 3.1A, 3.6).

As observed in Chapter II, the replacement of Cel-UNC-29 by the Hco-UNC-29 copies exhibited recordable signals for each, after activation by the same agonists (Figure 3.1B, 3.6). However, removal of Cel-LEV-1 from the same subunit mixtures produced an increase in response for Hco-UNC-29.1, 29.3 and 29.4 but in contrast, UNC-29.2 produced no significant response to 100 ACh or LEV in the absence of Cel-LEV-1 (n=8) (Figure 3.1E, 3.6). Similar admixtures with UNC-29.3 and UNC-29.4 produced functional receptors with responses to 100  $\mu$ M ACh of  $337.4 \pm 72.9$  nA (n=9) and  $346.9 \pm 206.0$  nA (n=6) for Hco-UNC-29.3 and Hco-UNC-29.4 respectively (Figure 3.1G, I, 3.6). The response to LEV produced  $38.3 \pm 2.9$  % and  $50.3 \pm 4.9$  % of the ACh responses, respectively (Figure 3.1G, I, 3.6). Only the UNC-29.2 appears to require the presence of LEV-1 to produce a functional receptor.

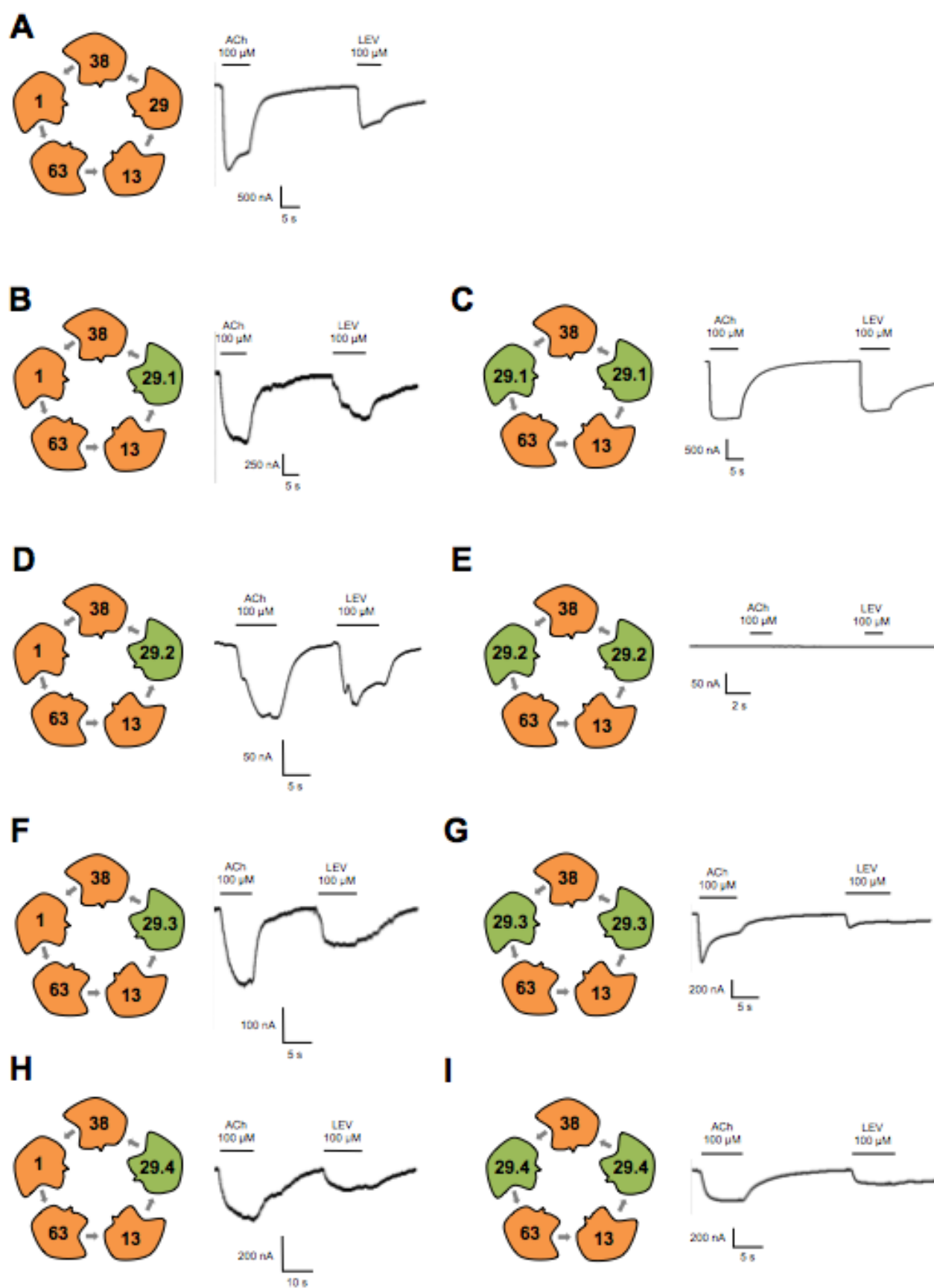




**Figure 3.1: Replacement of *Cel-LEV-1* and *Cel-UNC-29* with the *Hco-UNC-29* copies in a *C. elegans* L-AChR background.**

Two-electrodes voltage-clamp experiments were performed on *Xenopus* oocytes injected with *C. elegans* and *H. contortus* L-AChR subunit cRNA mixes combined with the *H. contortus* cRNAs: *ric-3*, *unc-50* and *unc-74* encoding accessory proteins. Diagrams represent L-AChR subunits from *C. elegans* (orange) and *H. contortus* (green). Traces are representative of single oocytes perfused with 100  $\mu$ M ACh and LEV. Black horizontal bars show the time period of agonist application.

The two  $\alpha$ -type subunit genes *acr-8* and *acr-13* derive from a duplication that occurred within the common ancestor of nematodes not found in clade I and *acr-13* has then been lost prior to the emergence of trichostrongylid nematodes (Blanchard-Letort *et al.*, 2017 submitted). Whereas replacement of ACR-13 by *Cel-ACR-8* produced hardly detectable currents (n=9) (Figure 3.2A, 3.6), the replacement of ACR-13 by *Hco-ACR-8* produced robust inward currents of  $955.5 \pm 108.4$  nA with oocytes perfused with 100  $\mu$ M ACh (n=9) (Figure 3.2B, 3.6). The same concentration of LEV produced responses corresponding to  $105.5 \pm 0.9$  % of ACh-evoked signals (Figure 3.2B, 3.6). It appears that *Hco-ACR-8*, unlike *Cel-ACR-8*, can functionally replace *Cel-ACR-13*.

The two non- $\alpha$  subunits of the *C. elegans* L-AChR are both required to produce a functional receptor and can not substitute for one another. This argues for some evolved mechanism conferring specificity that acts through interaction with other subunits in the receptor. To investigate whether loss of the *Cel-ACR-13* subunit plays a role in this mechanism, admixture combinations of the *C. elegans* L-AChR subunits, replacing ACR-13 with *Hco-ACR-8*, were evaluated. With this combination, *Cel-UNC-29* was able to function as the only non- $\alpha$  subunit, with ACh dependent average currents (n=14) were observed with an average of  $432.8 \pm 67.3$  nA and a LEV response corresponding to  $128.5 \pm 1.6$  % of the ACh-evoked currents (Figure 3.2C, 3.6). *Cel-LEV-1* was not able to serve as the only non- $\alpha$  subunit and no currents were observed (n=13) (Figure 3.2D, 3.6). The *H. contortus* UNC-29.1, UNC-29.3 and UNC-29.4 were each similar to the *C. elegans* UNC-29 in that they could each serve as the only non- $\alpha$  subunit. Interestingly, *Hco-UNC-29.2* was the only paralog that required the presence of *Cel-LEV-1* in order to produce a functional receptor, with induced ACh-sensitive inward currents of about  $156.1 \pm 39.8$  nA (n=7) and LEV responses corresponding to  $141.0 \pm 5.1$  % of the ACh signals (Figure 3.3B, 3.6). In summary and according to previous observations, the replacement of ACR-13 with *Hco-ACR-8* removes the requirement that the LEV-1 subunit be present for all *C. elegans* and *H. contortus* UNC-29 subunits with the exception of UNC-29.2.

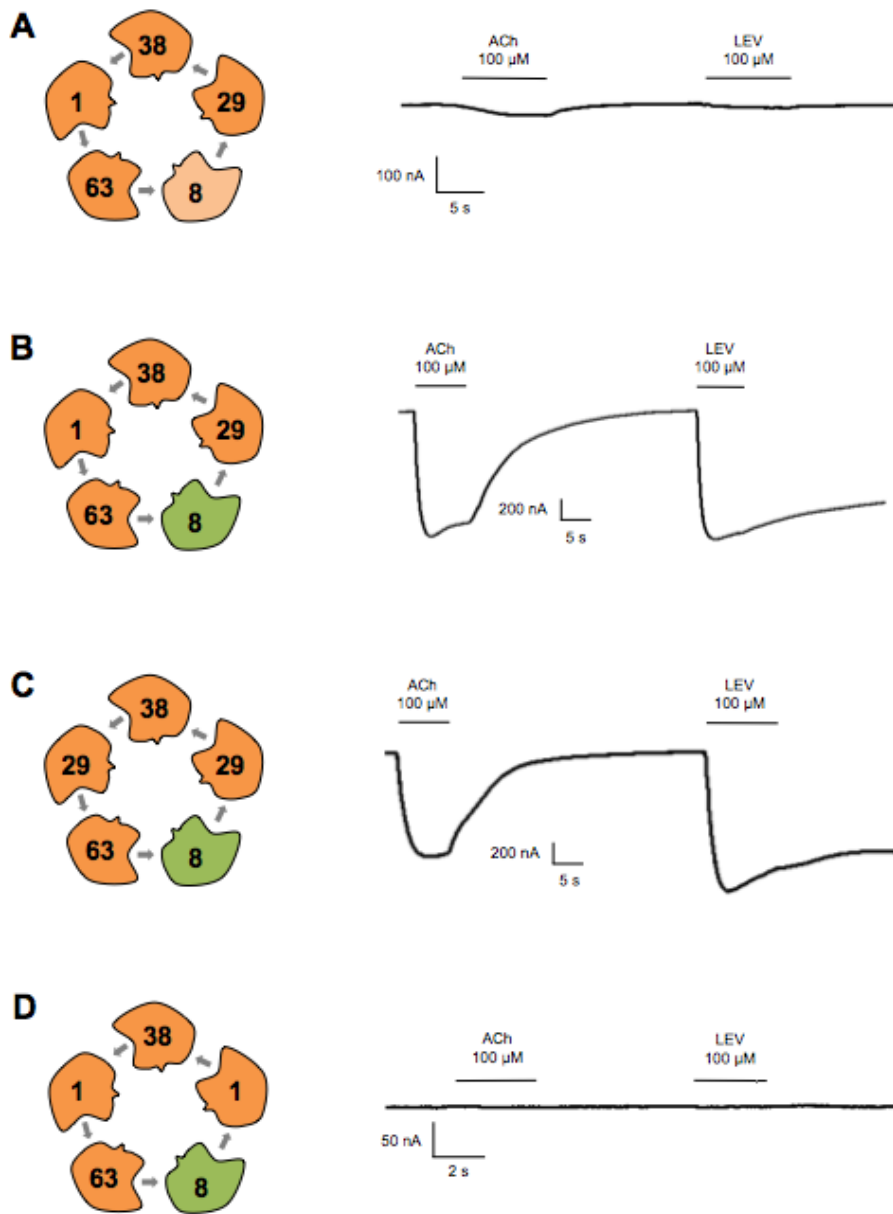


**Figure 3.2: Replacement of *Cel-ACR-13* with *Hco-ACR-8* in a *C. elegans* L-AChR background.**

Two-electrodes voltage-clamp experiments were performed on *Xenopus* oocytes injected with *C. elegans* and *H. contortus* L-AChR subunit cRNA mixes combined with the *H. contortus* cRNAs: *ric-3*, *unc-50* and *unc-74* encoding accessory proteins. Diagrams represent L-AChR subunits from *C. elegans* (orange) and *H. contortus* (green). Traces are representative of single oocytes perfused with 100  $\mu$ M ACh and LEV. Black horizontal bars show the time period of agonist application.

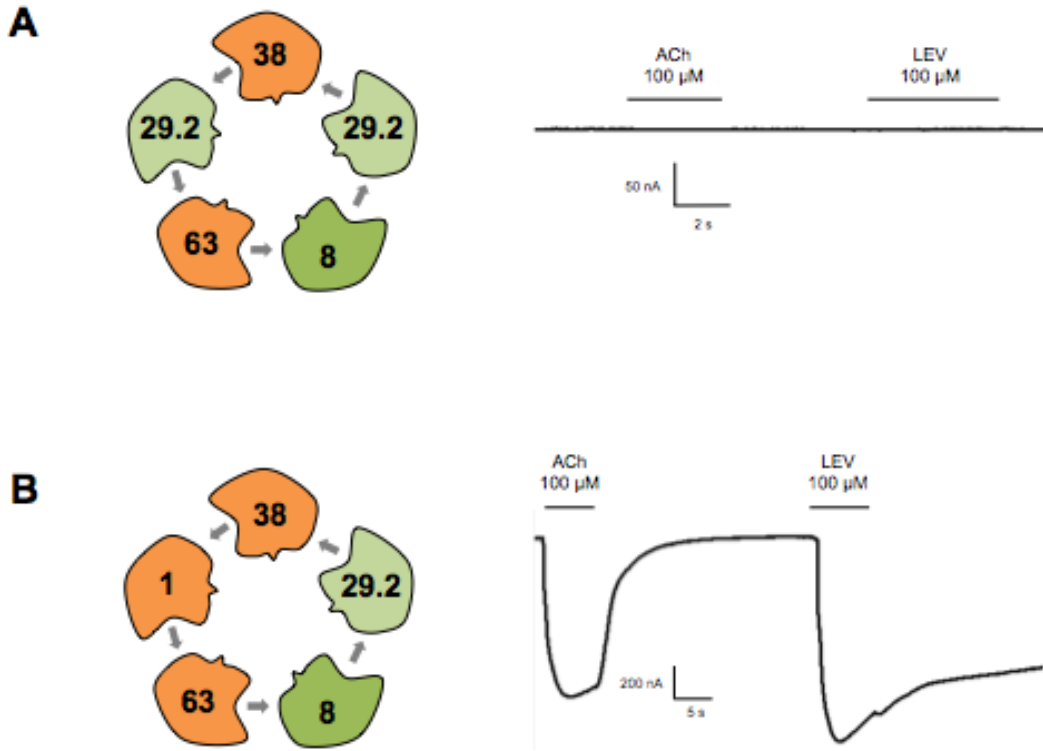


**Figure 3.3: Replacement of *Cel-ACR-13* and *Cel-UNC-29* with *Hco-ACR-8* and *Hco-UNC-29.2* in a *C. elegans* L-AChR background.**

Two-electrodes voltage-clamp experiments were performed on *Xenopus* oocytes injected with *C. elegans* and *H. contortus* L-AChR subunit cRNA mixes combined with the *H. contortus* cRNAs: *ric-3*, *unc-50* and *unc-74* encoding accessory proteins. Diagrams represent L-AChR subunits from *C. elegans* (orange) and *H. contortus* (green). Traces are representative of single oocytes perfused with 100  $\mu$ M ACh and LEV. Black horizontal bars show the time period of agonist application.

Subunit combination	ACh currents (nA $\pm$ S.E)	LEV response relative to ACh (% $\pm$ S.E)	n
<i>C. elegans</i> L-AChR (C63-C38-C13-C1-C29)	1016.8 $\pm$ 128.6	54.7 $\pm$ 2.4	10
C63-C38-C13-C1-H29.1	471.1 $\pm$ 51.5	64.2 $\pm$ 1.9	9
C63-C38-C13-H29.1	1766.1 $\pm$ 85.6	92.1 $\pm$ 1.7	10
C63-C38-C13-C1-H29.2	28.6 $\pm$ 5.2	46.2 $\pm$ 2.8	10
C63-C38-C13-H29.2	N/A	N/A	N/A
C63-C38-C13-C1-H29.3	109.6 $\pm$ 20.9	65.3 $\pm$ 2.3	9
C63-C38-C13-H29.3	337.4 $\pm$ 72.9	38.3 $\pm$ 2.9	9
C63-C38-C13-C1-H29.4	77.1 $\pm$ 34.2	60.4 $\pm$ 6.0	7
C63-C38-C13-H29.4	346.9 $\pm$ 84.1	50.3 $\pm$ 4.9	7
C63-C38-C8-C1-C29	50.9 $\pm$ 15.8	56.2 $\pm$ 17.6	9
C63-C38-H8-C1-C29	955.5 $\pm$ 108.4	105.5 $\pm$ 0.9	9
C63-C38-H8-C29	432.8 $\pm$ 67.3	128.5 $\pm$ 1.6	11
C63-C38-H8-C1	N/A	N/A	N/A
C63-C38-H8-C1-H29.2	156.1 $\pm$ 39.8	141.0 $\pm$ 5.1	7
C63-C38-H8-H29.2	N/A	N/A	N/A

**Table 3.1: ACh and LEV responses of *C. elegans* / *H. contortus* subunit admixtures in a *C. elegans* subunit background**

### 3.2.2 Admixtures in a *H. contortus* L-AChR subunit background

*H. contortus* L-AChRs that were reconstituted in chapter II contained a single type of non- $\alpha$  subunit. Replacing Hco-UNC-29.1 by Cel-UNC-29 in the L-AChR1.1 produced a maximum current of  $527.2 \pm 157.9$  nA (n=8) in response to 100  $\mu$ M ACh (Figure 3.4A, 3.6). The response to LEV was  $124.0 \pm 7.6$  % of the ACh-evoked current. Unlike with the *C. elegans* background, if Cel-LEV-1 was present alone, a functional receptor produced maximal currents of  $119.4 \pm 25.6$  nA in response to an identical concentration of ACh (n=8) (Figure 3.4B, 3.6). LEV induced  $26.7 \pm 2.4$  % of the ACh currents at equimolar concentrations (Figure 3.4B, 3.6).

In the *H. contortus* background, replacement of Hco-ACR-8 with Cel-ACR-13 produced functional receptors responding at an average of  $1223.8 \pm 185.1$  nA to 100  $\mu$ M ACh (n=7) whereas equimolar concentration of LEV induced  $80.1 \pm 2.3$  % of ACh-evoked currents (Figure 3.4C, 3.6).

Similar replacement of Hco-ACR-8 with Cel-ACR-13 into a L-AChR1.2 background did not allow the recording of any detectable current (n=6) (Figure 3.5A, 3.6). The same absence of functional receptor was also reported by successively swapping Hco-UNC-63 (n=5) and Hco-UNC-38 (n=5) with their *C. elegans* homologs (Figure 3.5B, C, 3.6). However, including Cel-LEV-1 as a supplementary non- $\alpha$  subunit into the L-AChR1.2 restored the functionality of the receptor as  $281.2 \pm 50.3$  nA (n=13) currents were observed under ACh exposure (Figure 3.5D, 3.6). These signals were significantly higher than *H. contortus* receptor containing Cel-LEV-1 as the sole non- $\alpha$  subunit (Figure 3.5A) (Student's t-test, p=0.011)

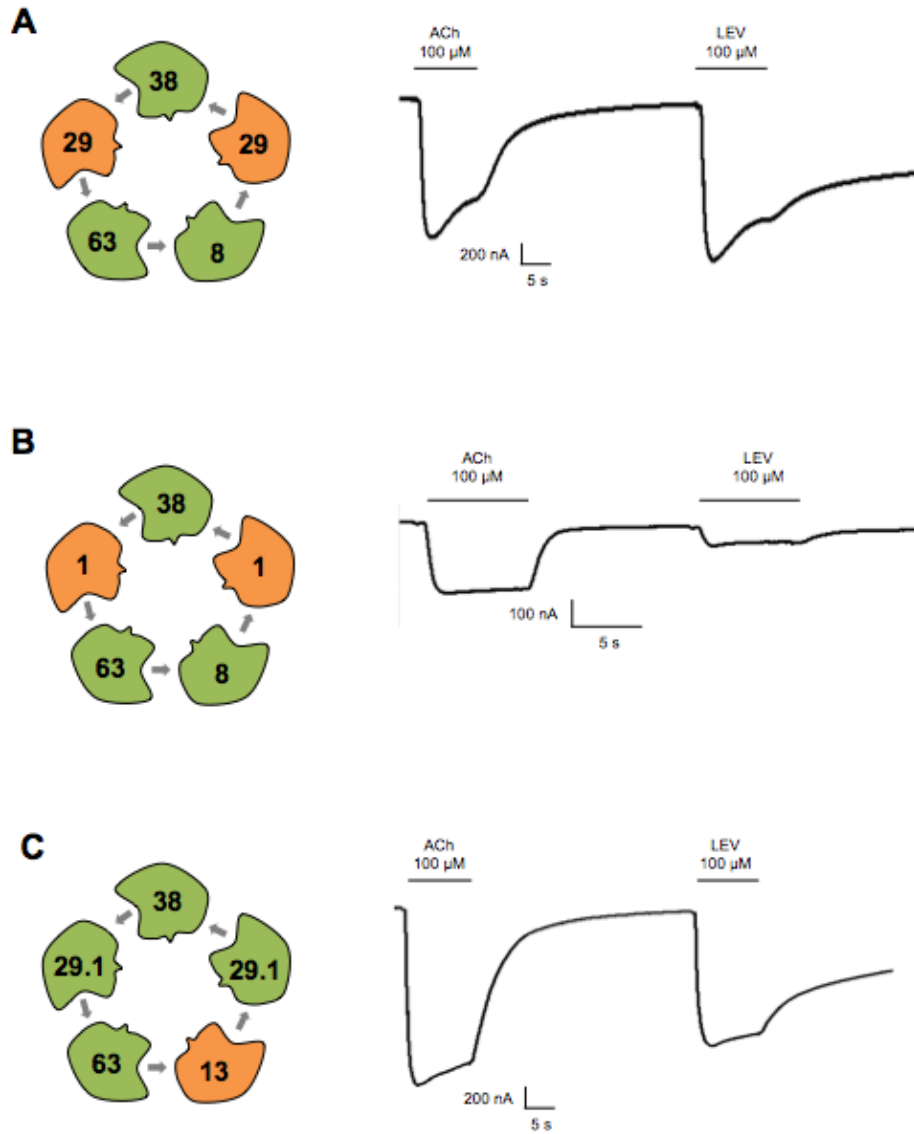


**Figure 3.4: Replacement of Hco-ACR-8 and Hco-UNC-29.1 in a L-AChR1.1 background.**

Two-electrodes voltage-clamp experiments were performed on *Xenopus* oocytes injected with *C. elegans* and *H. contortus* L-AChR subunit cRNA mixes combined with the *H. contortus* cRNAs: *ric-3*, *unc-50* and *unc-74* encoding accessory proteins. Diagrams represent L-AChR subunits from *C. elegans* (orange) and *H. contortus* (orange). Traces are representative of single oocytes perfused with 100  $\mu$ M ACh and LEV. Black horizontal bars show the time period of agonist application.

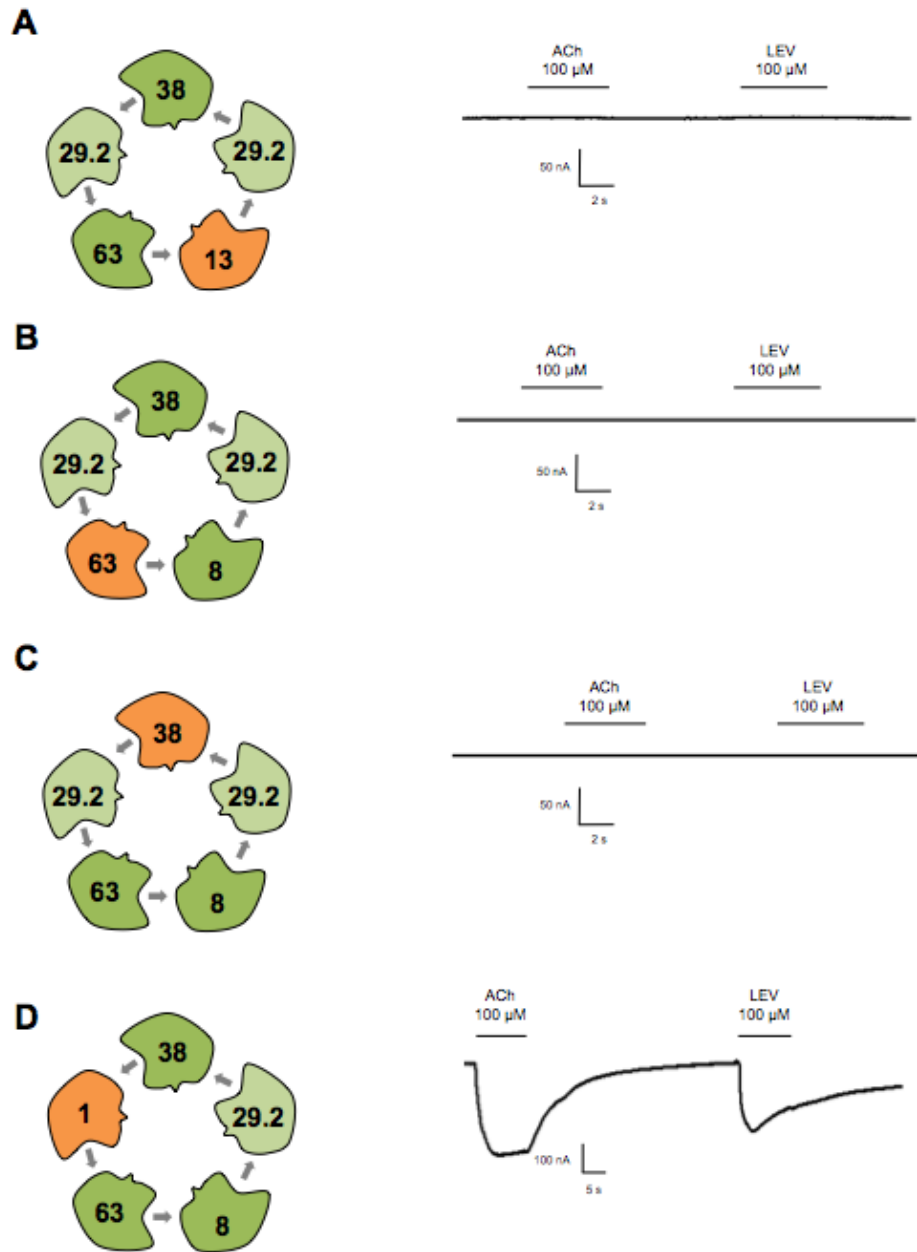


**Figure 3.5: Replacement of *H. contortus* subunits with *C. elegans* L-AChR subunit in a L-AChR1.2 background.**

Two-electrodes voltage-clamp experiments were performed on *Xenopus* oocytes injected with *C. elegans* and *H. contortus* L-AChR subunit cRNA mixes combined with the *H. contortus* cRNAs: ric-3, unc-50 and unc-74 encoding accessory proteins. Diagrams represent L-AChR subunits from *C. elegans* (green) and *H. contortus* (orange). Traces are representative of single oocytes perfused with 100  $\mu$ M ACh and LEV. Black horizontal bars show the time period of agonist application.

<b>Subunit combination</b>	<b>ACh currents (nA <math>\pm</math> S.E)</b>	<b>LEV response relative to ACh (% <math>\pm</math> S.E)</b>	<b>n</b>
<b>H63-H38-H8-C29</b>	527.2 $\pm$ 157.9	124.0 $\pm$ 7.6	7
<b>H63-H38-H8-C1</b>	119.4 $\pm$ 25.6	26.7 $\pm$ 2.4	8
<b>H63-H38-C13-H29.1</b>	1223.8 $\pm$ 185.1	80.1 $\pm$ 2.3	7
<b>H63-H38-C13-H29.2</b>	N/A	N/A	N/A
<b>C63-H38-H8-H29.2</b>	N/A	N/A	N/A
<b>H63-C38-H8-H29.2</b>	N/A	N/A	N/A
<b>H63-H38-H8-C1-H29.2</b>	281.2 $\pm$ 50.3	98.6 $\pm$ 5.7	13

***Table 3.2: ACh and LEV responses of C. elegans / H. contortus subunit admixtures in a H. contortus subunit background***





### 3.3 Discussion

The duplication of the *unc-29* L-AChR subunit gene in *H. contortus* shows potential as a model for understanding the mechanisms involved in the appearance of new types of subunits and novel receptor classes. Chapter II compared the effect of substituting each copy into a common subunit receptor combination and identified conservation of maximum response for the natural ligand, ACh (Table 2.1), and minor differences in response to the agonist LEV (Figure 2.1A-C) and the antagonist meca (Figure 2.1D-F). The most striking differences were in the greatly reduced maximal current of the L-AChR1.4 (Figure 2.1C) and the absence of a response for L-AChR1.2 (Figure 2.2). The fact that Hco-UNC-29.2 could function in combination with subunits from *C. elegans* suggested that compatibility among subunits to produce a functional receptor is a feature that may change rapidly following subunit duplication and may provide a means of identifying the mechanisms involved. In this chapter, various admixture combinations of *C. elegans* and *H. contortus* subunits were evaluated to establish these patterns of compatibility.

The non- $\alpha$  subunits, Cel-UNC-29 and Cel-LEV-1, in the *C. elegans* L-AChR are each required to produce a functional receptor. Each of the three paralogs, Hco-UNC-29.1, Hco-UNC-29.3 and Hco-UNC-29.4 can serve as the only non- $\alpha$  subunit in either an *H. contortus* (Figure 2.1) or *C. elegans* L-AChR (Figure Figure 3.1C, G, I). Since only four subunit types are present in these cases, two subunits in the pentameric receptor must be identical. We can not, as yet, know for certain which subunit is represented twice but all the data produced for this thesis and what is known about the vertebrate AChRs is consistent with there being at least two non- $\alpha$  subunits in any functional receptor. In fact, no evidence for a heteromeric receptor containing either one or four non- $\alpha$  subunits has been reported in any organism so far. Indeed, a 3:2 or 2:3  $\alpha$ :non- $\alpha$  stoichiometry is often observed and can lead to receptors involved in different functions (Millar et al., 2009). A possible explanation would be the essential role of  $\alpha$  type subunits required to form a sufficient number of functional ligand binding sites (Kao et al., 1984). However, even within homopentameric receptors the occupation of two to three binding sites seems to be an absolute requirement for a efficient gating (Rayes et al., 2009, Mowrey et al., 2013).

Based on this assumption we could interpret these observations as the ability of these three *H. contortus* UNC-29 paralogs to function as Cel-UNC-29 as well as Cel-LEV-1. The fact that Cel-UNC-29 and Cel-LEV-1 must both be present in the *C. elegans* L-AChR implies that they each fulfill

specific requirements for their structural role and that each is limited to that role by their interaction with other subunits of the receptor.

The paralogous  $\alpha$  subunits Cel-ACR-13 and Cel-ACR-8 in *C. elegans* are distinct, with Cel-ACR-13 contributing to a robust L-AChR (Figure 3.1A) while Cel-ACR-8 leads to a receptor with only a minimal response to ACh (Figure 3.2A). The Cel-ACR-13 subunit appears absent from the *H. contortus* genome and is replaced by Hco-ACR-8 in the Hco-L-AChR (Neveu et al., 2010, Beech et al., 2015). Replacing Cel-ACR-13 in the *C. elegans* L-AChR with Hco-ACR-8 produces a robust channel (Figure 3.2B). Interestingly, this new channel no longer requires Cel-LEV-1 (Figure 3.2C). The specificity of Cel-UNC-29 that normally prevents it from replacing Cel-LEV-1 appears dependent on an interaction with the Cel-ACR-13 subunit. No functional receptor is produced when Cel-LEV-1 is the only non- $\alpha$  subunit, which implies that the mechanism that confers specificity on the Cel-LEV-1 subunit remains intact in the presence of Hco-ACR-8. An admixture containing Hco-UNC-38, Hco-UNC-63 and Hco-ACR-8 does a functional receptor in combination with the Cel-LEV-1 subunit alone (Figure 3.4B). This suggests that the mechanism that confers specificity on Cel-LEV-1 is distinct from that of Cel-UNC-29 and involves an interaction with UNC-38, UNC-63 or both.

These results suggest that subunits within the L-AChR become specialized over time in their specific roles in the functional receptor. The L-AChR of *C. elegans* represents an extreme example of this, where each subunit is restricted to a single role (Boulin et al., 2008). Loss and duplication of subunits, likely involves a disruption of previously evolved inter-subunit specificity and may explain why different combinations of subunits from *H. contortus* and *O. dentatum* are able to produce functional receptors (Boulin et al., 2011, Buxton et al., 2014).

Duplication of subunits initially creates identical copies that, if co-expressed, will be indistinguishable and should combine equally into functional receptors. In the case of Hco-UNC-29.1 and Hco-UNC-29.2, both are expressed in the same muscular tissue (Figure 2.7) and could theoretically co-assemble into the same receptor complex. No evidence in support of this was observed in chapter II where the addition of excess *Hco-unc-29.2* cRNA had no effect on the expression or pharmacology of L-AChR1.1, suggesting that Hco-UNC-29.2 does not interact nor affect assembly of receptors containing Hco-UNC-29.1 (Figure 2.3, Table 2.2). This could be explained by a mechanism that has evolved to prevent interference between these duplicate subunits allowing them to diverge independently.

Hco-UNC-29.2 requires the presence of Cel-LEV-1 to form a functional receptor. The *lev-1* gene encoded in the *H. contortus* genome lacks the 5' sequence corresponding to a signal peptide, a typical

requirement for proteins embedded in the ER membrane during synthesis. Recently, the Hco-LEV-1 with an artificially added signal peptide has been shown to form a functional L-AChR with Hco-UNC-29.2 and the three *H. contortus*  $\alpha$  subunits (Charvet *et al.*, personal communication). Without eliminating the fact that Hco-LEV-1 may be assembled but not transported to the plasma membrane, we could also speculate that inclusion of Hco-LEV-1 in an *H. contortus* L-AChR occurs *via* an assembly pathway that is physically distinct from that normally followed by AChRs and that such a pathway may have a specific requirement for Hco-UNC-29.2.

It is not yet possible to know why no functional receptor is produced from certain admixture combinations. One possibility is that subunits are physically incompatible and simply do not assemble. A second is that the subunits do indeed co-assemble, but the complex produced is either incapable of conducting ions across the membrane or of binding an activating ligand. A third is that the complex formed during assembly is identified and targeted for degradation (Fu *et al.*, 2016). We can still conclude, however, that the ability to produce a functional receptor depends on interactions between different subunits within the receptor.

The restriction of Cel-UNC-29 and Hco-UNC-29.2 from acting as the sole non- $\alpha$  subunit is dependent on the Cel-ACR-13/Hco-ACR-8 subunit. Similarly, restriction of the Cel-LEV-1 subunit is dependent on the UNC-38/UNC-63 subunits. One obvious question is whether the Cel-UNC-29 subunit is physically adjacent to the Cel-ACR-13 subunit in the *C. elegans* L-AChR and similarly whether Cel-LEV-1 is physically adjacent to Cel-UNC-38 and/or Cel-UNC-63. If the precise order of subunits within the L-AChR were known it may be possible to say whether direct physical contact could explain these data. It would also be highly valuable to have an insight into the process by which individual subunits are assembled into a finished receptor to know if this could play a role. The next chapter focuses specifically on using subunits physically joined into concatamers specifically to determine the quaternary structure and assembly pathway of the *C. elegans* L-AChR..

## Chapter IV - Quaternary structure of the *C. elegans* levamisole receptor.

### 4.1 Introduction

The major premise of this thesis is that the four copies of the L-AChR non- $\alpha$  subunit *unc-29* in the trichostrongylid nematode parasite of sheep, *Haemonchus contortus*, represents a tractable model for the appearance of novel pLGIC subunits more generally. Chapter II was able to show that the copies of *unc-29* are functionally distinct, diverging in terms of the pharmacological response of reconstituted L-AChRs produced in *Xenopus* oocytes. A prominent feature was the different ability of the copies, with the exception of Hco-UNC-29.2 to combine with other subunits to produce a functional receptor. In chapter III, various admixture combinations of subunits from *C. elegans* and *H. contortus* demonstrated that interactions between  $\alpha$  and non- $\alpha$  type subunits were involved in determining whether a functional receptor could be produced. This highlights the need to understand the quaternary organization of the pentameric receptor and hence which subunits are in physical contact. This is the goal of the work presented in this chapter.

The muscular L-AChR of the nematode *C. elegans* is composed of five different subunits, encoded by different genes, each of which is required to produce a functional receptor (Boulin et al., 2008). The decision to focus on the structural organization of this receptor was based on the fact that with five distinct subunits, there would be no ambiguity regarding composition of the receptor and this would remove one complicating factor for this challenging project.

Assembly of pLGICs is a finely controlled process, beginning in the endoplasmic reticulum, that represents a critical step of receptor biosynthesis (Fu et al., 2016). For example, the most abundant form of vertebrate GABA<sub>A</sub> receptors are composed of  $\alpha$ ,  $\beta$  and  $\gamma$ -type subunits and their assembly consists of combining two heterodimers of  $\alpha$  and  $\beta$  subunits followed by the insertion of a  $\gamma$ -type subunit, completing the pentameric structure (Luscher et al., 2011). In contrast, assembly of vertebrate AChRs seems to proceed differently between muscular and neuronal receptor subtypes and between native and recombinant receptors (Fu et al., 2016). In skeletal muscle cells, the AChRs initially described in the electric ray *Torpedo californica* are composed of the  $\alpha$ -type subunit  $\alpha 1$ , and the non- $\alpha$  subunits called  $\beta 1$ ,  $\gamma$ , and  $\delta$  and are represented in a 2:1:1:1 ratio (Reynolds et al., 1978). Interestingly,

the 2 + 2 + 1 assembly model has also been described with an initial association of two  $\delta\alpha1:\gamma\alpha1$  dimers and completion with a  $\beta$ -type subunit (Saedi et al., 1991, Kreienkamp et al., 1995). Alternatively, the  $\alpha1\beta\gamma$  trimer can also be formed and combined subsequently with the  $\delta$  then the  $\alpha1$  monomer, which corresponds to the sequential model 3 + 1 + 1 (Green et al., 1993, Green et al., 1998). Interpretation of these results is complicated in that they depend on the measured molecular weight of protein complexes. A large group of chaperon proteins, including RIC-3, play a central role in subunit assembly of the L-AChR (Boulin et al., 2008, Boulin et al., 2011) and it has been shown that RIC-3 physically interacts with individual subunits of an AChR during assembly (Cohen Ben-Ami et al., 2009).

A variety of technical approaches exist to validate subunit position within pLGICs. For example, the assembly of the human  $\alpha4\beta2$  AChR was visualized by expression of fluorescently labeled subunits in cultured mammalian cells and midbrain neurones using fluorescence resonance energy transfer (Nashmi et al., 2003). This method is technically demanding and caution must be used with interpretation of the results (Day et al., 2012). Coupling subunits through artificial disulphide bonds, the so-called "disulphide trapping" method, has notably been used to characterize benzodiazepine modulation between the  $\alpha1$  and  $\gamma2$  subunits of the vertebrate GABA<sub>A</sub> receptor (Hanson et al., 2011).

The relative high number of cysteines within nematode AChR subunits and the fact that four of these per subunit, two in the cys-loop and two in the C-loop, are required for function of the channel, would make this technically difficult. The method chosen here involves concatenation of subunits into a single protein chain such that the distance between TM4 of the first subunit, anchored in the cell membrane, and the N-terminal of the second subunit is restricted and limits the subunits to one specific configuration. The stop codon of all but the final subunit and the signal peptide sequence of all but the first subunit were removed, fusing them into a single open reading frame. This method offers significant advantages including a developed literature establishing the technique (Minier et al., 2004, Ericksen et al., 2007, Millar 2009), straight forward manipulation of the subunits and more importantly, a way of testing single subunit arrangements among multiple possible combinations expressed in oocytes. This technique has potential in the future for examination of specific structural combinations and for evaluation of the effects of substituting subunits from different species at specific positions in the receptor.

## 4.2 Results

### 4.2.1 Construction and expression of dimers of L-AChR subunits

All subunits, with the exception of UNC-63 were determined to have a tail, post TM4, of the appropriate length to serve as the linker between concatameric subunits. This was based on a low resolution 3D model of the structure using the human  $\alpha 4/\beta 2$  AChR (PDB: 5KXI) as a template (Beech, personal communication). UNC-63 required the addition of an artificial linker of five copies of the sequence Thr-Ala-Ser fused to the C-terminal. This modified monomer of UNC-63 was expressed with other L-AChR subunits to verify that the linker addition did not affect the normal function of the subunit. Responses to 100  $\mu$ M ACh and LEV were similar to the native L-AChR (Figure 4.5), which suggests that addition of the linker to UNC-63 had no effect on its normal function.

The number of different possible subunit arrangements in the the *C. elegans* L-AChR totals 24 ( $4 * 3 * 2 * 1$ ). Given the complexity of producing any pentameric combination, an initial strategy beginning with two subunits combined into dimers was chosen. Even the number of possible dimers is large (20) and so only combinations (12) in which the first subunit was an  $\alpha$  subunit were evaluated in *Xenopus* oocytes, in combination with the remaining three subunits as monomers. Given these combinations, at least three dimers would contain subunits in the correct relative position, no matter the real organization of the receptor. Among the total of 12 dimers tested, only oocytes expressing the UNC-38:LEV-1 dimer responded to 100  $\mu$ M ACh and LEV (Figure 4.1). Indeed, an average of  $1148.8 \pm 121.3$  nA currents ( $n=9$ ) were recorded with ACh. LEV induced signals corresponding to  $52.5 \pm 1.9$  % of the ACh-evoked currents (Figure 4.1 and 4.5). The LEV response of the native L-AChR were about  $54.7 \pm 2.4$  % (Figure 4.5). A working hypothesis was formulated that UNC-38:LEV-1 is one of the initial steps of receptor assembly. Subunits present in dimers with the correct organization that were not functional may need to join the growing receptor complex as individual subunits.

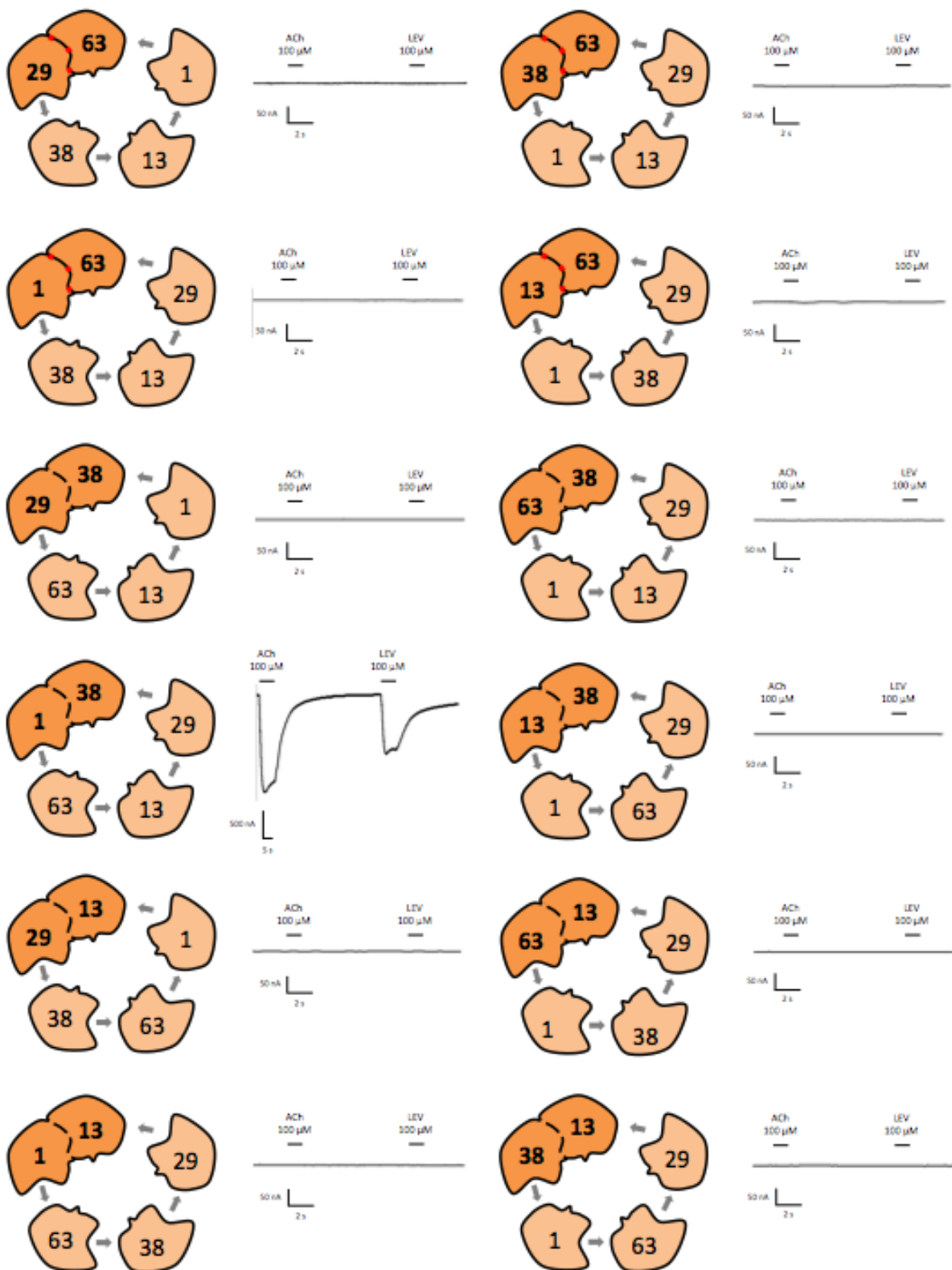


**Figure 4.1: Expression of *C. elegans* L-AChR subunit dimers in *Xenopus* oocytes.**



Mature *Xenopus* oocytes were injected with different *C. elegans* cRNA mixtures corresponding to dimers and monomers of subunits. The *H. contortus* UNC-50, UNC-74 and RIC-3.1 were used as accessory proteins for the heterologous expression. Concatenated subunits are represented in form of a diagram and visualized in dark orange. Dashed line represents the limit between the two subunits. The red dashed line corresponds to the artificial linker that was added to the C-terminal of Cel-UNC-63. Monomers are showed in light orange. The perfusion of 100  $\mu$ M ACh and LEV was applied to test the functionality of the concatamers. Electrophysiology traces are representative of a single oocyte. Black horizontal bars show the time period of agonist application.

#### 4.2.2 Construction and expression of trimers of L-AChR subunits

Subunits UNC-63 or ACR-13 were fused to the UNC-38:LEV-1 dimer at the first or third position in the trimer. UNC-29 was only fused at the first position since it seemed unlikely that the two non- $\alpha$  type subunits in a receptor would be adjacent. The five trimeric constructions were then expressed in *Xenopus* oocytes along with the remaining two subunits as monomers. As with the dimers, only one combination produced a response under the perfusion of 100  $\mu$ M ACh. Indeed, ACh produced  $655.4 \pm 43.2$  nA average currents with the UNC-38:LEV-1:UNC-63 trimer ( $n=10$ ) and LEV responses corresponded to  $44.7 \pm 2.1$  % of the ACh currents (Figure 4.2 and 4.5), which appeared not to be significantly different from the native L-AChR (unpaired Student's t-test,  $p>0.05$ ). The data so far were consistent with a 3 + 1 + 1 assembly model that would predict a functional receptor should be produced using the LEV-1:UNC-63 dimer that had not been tested in the original screen. In fact, the LEV-1:UNC-63 dimer produced measurable currents corresponding to an average of  $597.7 \pm 97.7$  nA on exposure to ACh at 100  $\mu$ M and the same concentration of LEV induced responses at about  $49.4 \pm 1.5$  % of the ACh-evoked signals ( $n=12$ ) (Figure 4.3 and 4.5). Comparatively, the native L-AChR exhibited  $1016.8 \pm 128.6$  nA ACh-currents that were significantly higher ( $p=0.018$ , unpaired Student's t-test).

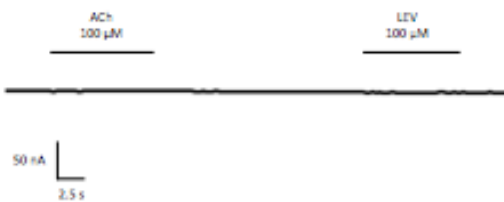
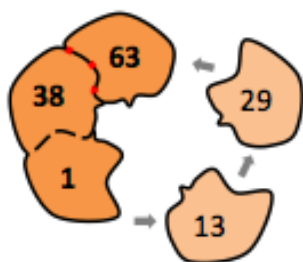
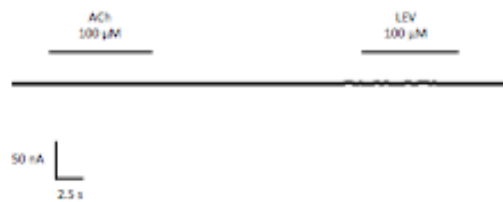
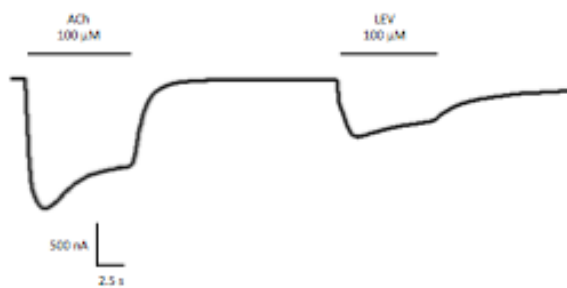


**Figure 4.2: Expression of *C. elegans* L-AChR subunit trimers in *Xenopus* oocytes**

Mature *Xenopus* oocytes were injected with different *C. elegans* cRNA mixtures corresponding to trimers and monomers of subunits. The *H. contortus* UNC-50, UNC-74 and RIC-3.1 were used as accessory proteins for the heterologous expression. Concatenated subunits are represented in form of a diagram and visualized in dark orange. Dashed line represents the limit between the two subunits. The red dashed line corresponds to the artificial linker that was added to the C-terminal of Cel-UNC-63. Monomers are showed in light orange. The perfusion of 100  $\mu$ M ACh and LEV was applied to test the functionality of the concatamers. Electrophysiology traces are representative of a single oocyte. Black horizontal bars show the time period of agonist application.

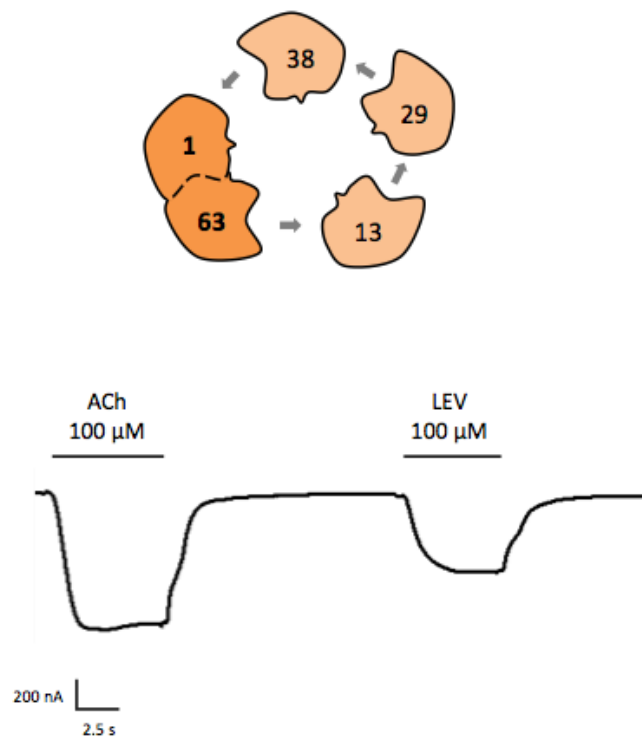


**Figure 4.3: Expression of the *LEV-1::UNC-63* dimer in *Xenopus* oocytes**

Mature *Xenopus* oocytes were injected with a *C. elegans* cRNA mixtures corresponding to the LEV-1:UNC-63 dimer and the ACR-13, UNC-29 and UNC-38 monomers. The *H. contortus* UNC-50, UNC-74 and RIC-3.1 were used as accessory proteins for the heterologous expression. Concatenated subunits are represented in form of a diagram and visualized in dark orange. Dashed line represents the limit between the two subunits. Monomers are showed in light orange. The perfusion of 100  $\mu$ M ACh and LEV was applied to test the functionality of the concatamers. Electrophysiology traces are representative of a single oocyte. Black horizontal bars show the time period of agonist application.

### 4.2.3 Identification of the pentameric structure of the *C. elegans* L-AChR

Successful reconstitution of the UNC-38:LEV-1:UNC-63 trimer offered the possibility to identify the complete quaternary structure of the L-AChR. Only two possible arrangement of the subunits remained with either ACR-13 followed by UNC-29 or *vice versa*. The dimers UNC-63:ACR-13, ACR-13:UNC-29, UNC-63:UNC-29 and ACR-13:UNC-38 were all found to be non-functional, which suggested that ACR-13 and UNC-29 must join the growing receptor complex as monomers but provided no clue to which was adjacent to UNC-63. Therefore, two tetramers based on the UNC-38:LEV-1:UNC-63 trimer, were constructed, with either ACR-13 or UNC-29 in the last position, and expressed in *Xenopus* oocytes with the fifth subunit included as a monomer and their functionality was tested as before.

Expression of the UNC-38:LEV-1:UNC-63:UNC-29 tetramer produced no detectable current (n=14) when ACh or LEV were applied on the oocytes (Figure 4.4B). The UNC-38:LEV-1:UNC-63:ACR-13 tetramer produced weak currents that did not exceed 20 to 30 nA under ACh and LEV perfusion (n=18) (Figure 4.4A and 4.5), which corresponded to a loss of  $96 \pm 0.6$  % of the ACh-evoked currents exhibited by the native L-AChR (Figure 1.5). Finally, expression of the two pentamers: UNC-38:LEV-1:UNC-63:ACR-13:UNC-29 or UNC-38:LEV-1:UNC-63:UNC-29:ACR-13, produced no detectable response (Figure 4.4C, D).

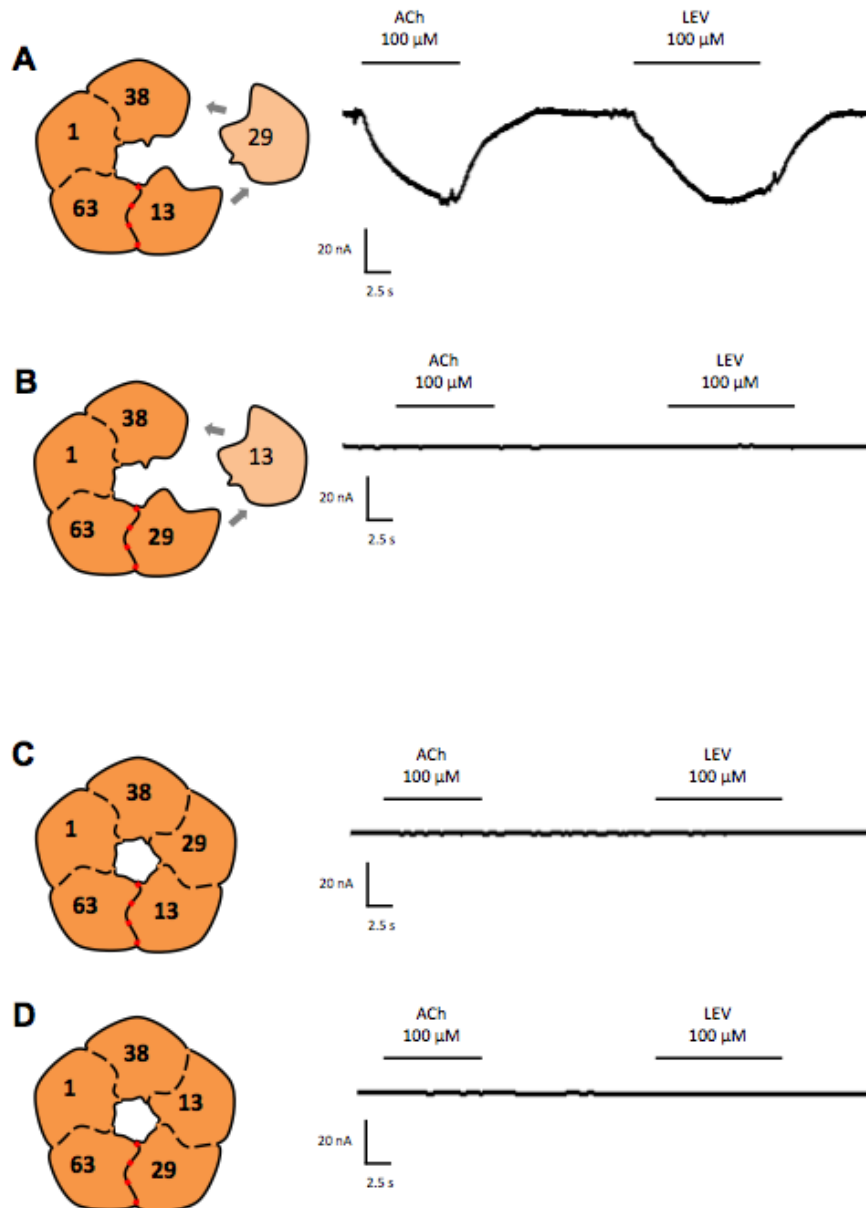


**Figure 4.4: Expression of *C. elegans* L-AChR subunit tetramers and pentamers in *Xenopus* oocytes**  
 Mature *Xenopus* oocytes were injected with different *C. elegans* cRNA mixtures corresponding to tetramers, pentamers and monomers of subunits. The *H. contortus* UNC-50, UNC-74 and RIC-3.1 were used as accessory proteins for the heterologous expression. Concatenated subunits are represented in form of a diagram and visualized in dark orange. Dashed line represents the limit between the two subunits. The red dashed line corresponds to the artificial linker that was added to the C-terminal of Cel-UNC-63. Monomers are showed in light orange. The perfusion of 100  $\mu$ M ACh and LEV was applied to test the functionality of the concatamers. Electrophysiology traces are representative of a single oocyte. Black horizontal bars show the time period of agonist application.

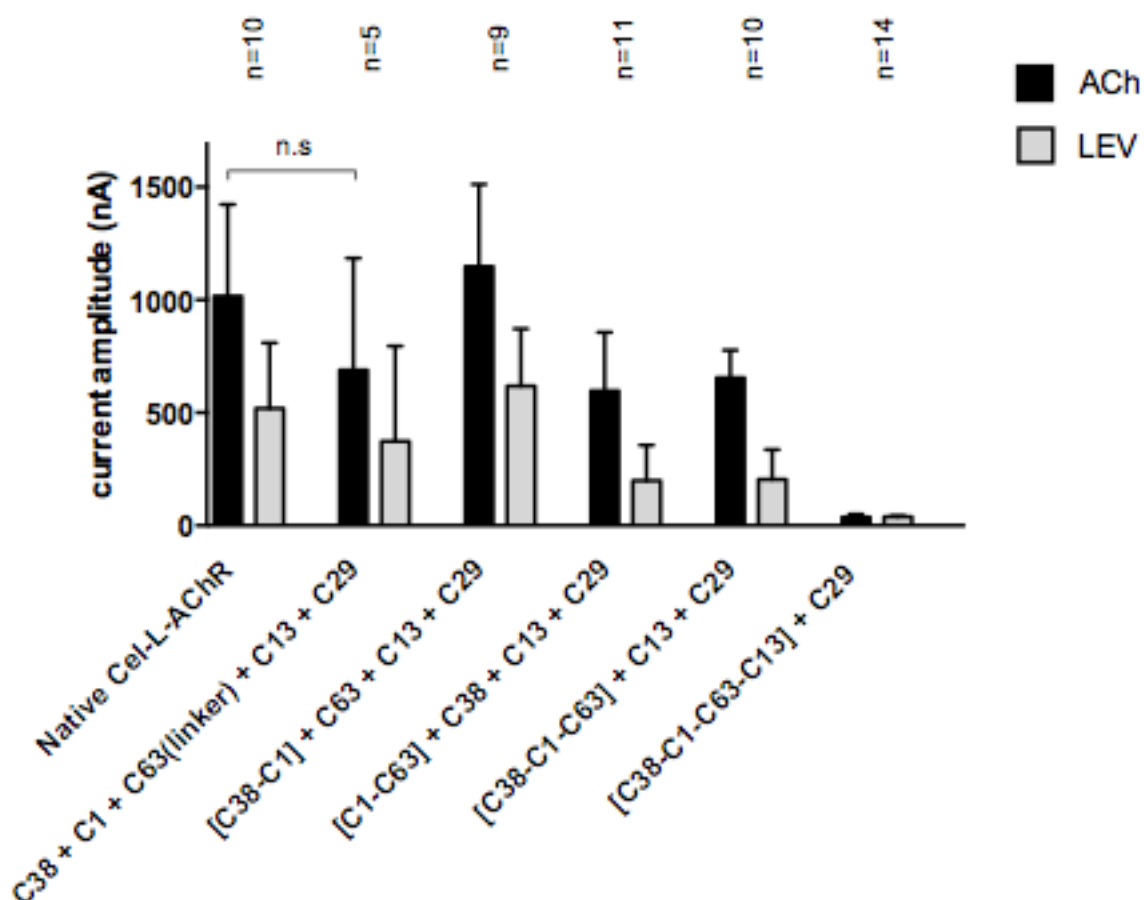


**Figure 4.5: Summary of L-AChR concatamer responses to 100  $\mu$ M ACh and LEV.**

Subunit concatamers were expressed in *Xenopus* oocytes in combination with monomers and co-expressed with the *H. contortus* accessory proteins UNC-50, UNC-74 and RIC-3.1. Two-electrode voltage clamp experiments were performed these oocytes in order to record electric signals produced under ACh or LEV perfusion at 100  $\mu$ M. Columns show current amplitude (nA) produced by ACh (black columns) and LEV (light grey columns) exposure. "C" and "H" correspond to the abbreviations of *C. elegans* and *H. contortus* respectively. Brackets represent subunit concatamers. Error bars indicate SE. N.S: non-significantly different according to a unpaired Student's t-test with a P-value > 0.05.

### 4.3 Discussion

The strict requirement for five different subunits to reconstitute the pentameric *C. elegans* L-AChR simplified the problem of determining subunit positions uniquely given that there is no ambiguity involved with any one subunit being present more than once. Given the high risk that this technique would work at all, a stepwise approach based on the *C. elegans* L-AChR was used.

Low resolution structural models of the various dimeric concatamers, produced by Dr Beech, were used to evaluate that the length of each C-terminal tail beyond TM4, anchored in the membrane was sufficient to fuse to the N-terminal of the second subunit without serious distortion of the structure but short enough to require the second subunit to be physically adjacent in the receptor. This assumed the presence of no significant secondary structure in this tail region (Minier et al., 2004). The lengths were consistent with physical distances verified for other receptors such as the human  $\alpha 4\beta 2$  AChR, which exhibits a distance of 70 to 80 Å (Morales-Perez et al., 2016). Only the UNC-63 C-terminal tail that was too short required the addition of five copies of the repeat, Ser-Ala-Thr, chosen as small, non-branched, hydrophylic amino acids. Addition of this linker had no effect on the function of the UNC-63 subunit (Figure 4.5).

An initial list of dimeric constructs was synthesized to establish if the technique had the potential to work at all. With twenty possible dimer permutations, an arbitrary decision was made to only use combinations where the first subunit was an  $\alpha$ -type. This limited the number of combinations to twelve and guaranteed that no matter which of the 24 permutations of five subunits in the final receptor, three of the dimers would have subunits in their correct relative positions. Surprisingly, only the dimer UNC-38:LEV-1 produced a strong response (Figure 4.1). This meant that two dimers with subunits in their correct relative positions failed to reconstitute any functional receptor. If this were due to some technical failure then it would not be possible to continue with this technique. Alternatively, the assembly pathways inferred for other receptors require addition of subunits in a specific order (Green et al., 1993, Green et al., 1998, Wanamaker et al., 2003). It may be that failed dimer combinations blocked the normal receptor assembly process.

Of the trimeric constructs that included the dimer UNC-38:LEV-1, only the combination UNC-38:LEV-1:UNC-63 produced a strong response (Figure 4.2). One of the other trimers, with either UNC-29 or ACR-13 before UNC-38 should be in the correct configuration and yet neither produced any response to ACh (Figure 4.2). This result confirmed that the concatamer strategy had potential and could provide valuable information. The "sequential model" (Green et al., 1993, Green et al., 1998,

Wanamaker et al., 2003) where an initial trimer of three subunits forms rapidly followed by sequential addition of single subunits to this complex would account for the fact that two dimers and one trimer failed to produce a functional receptor despite having subunits in the correct configuration. The prediction that the LEV-1:UNC-63 dimer, that was not tested initially, should produce a functional receptor was subsequently confirmed (Figure 4.3).

The only tetramer that produced any response to ACh was UNC-38:LEV-1:UNC-63:ACR-13 plus UNC-29 as a monomer (Figure 4.4A). The fact that this could produce a functional receptor supports the quaternary structure of the *C. elegans* L-AChR as UNC-38:LEV-1:UNC-63:ACR-13:UNC-29 (Figure 4.6). The small current observed with the tetramer was in contrast to the large ACh-specific currents ( $655.4 \pm 43.2$  nA) observed with the trimer (Figure 4.2) and is a cause for concern. Evaluation of the two pentameric constructs with ACR-13 and UNC-29 in either position produced no observable current (Figure 4.4C, D).

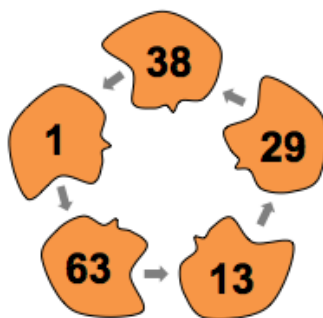


**Figure 4.6: Putative subunit arrangement of the *C. elegans* L-AChR**

The success of the two dimers, UNC-38:LEV-1 and LEV-1:UNC-63, and the trimer UNC-38:LEV-1:UNC-63 supports a model of assembly in *Xenopus* oocytes similar to that of the vertebrate muscular AChR where an initial trimer forms rapidly, followed by sequential addition of the final two subunits (Wanamaker et al., 2003). The fact that no current was observed for the dimers UNC-63:ACR-13 and ACR-13:UNC-29 (Figure 4.1) and trimer UNC-29:UNC-38:LEV-1 (Figure 4.2) is in agreement with this model that would require the ACR-13 and UNC-29 subunits to join the complex individually. In vertebrates, only 30 % of translated AChR subunits are properly assembled and exported in the form of functional pentamers (Wanamaker et al., 2003). The tetrameric and pentameric versions of the *C. elegans* L-AChR may pose particular problems for the assembly and processing machinery of the



*Xenopus* oocyte and result in redirection of mis-assembled complexes for breakdown. Examples exist of pentameric concatenated vertebrate pLGIC subunits exhibiting reduced response to ligands in oocytes despite the insertion of artificial linkers (Zhou et al., 2003, Groot-Kormelink et al., 2006, Carbone et al., 2009, Shu et al., 2012).

Another interesting possibility is a model in which assembly requires addition of UNC-29 to the initial trimer before addition of ACR-13 that would insert between the UNC-63 and UNC-29 subunits. Synthesis of a concatamer proceeds in the endoplasmic reticulum, in order, from the N-terminal subunit first to the C-terminal last. A tetramer with ACR-13 last plus monomeric UNC-29, leaves the possibility that before completion of the ACR-13 subunit there may be monomeric UNC-29 present that could join the growing complex in the ER during synthesis. Completion of ACR-13 would then allow insertion between UNC-63 and UNC-29. A tetramer with UNC-29 in the last position and monomeric ACR-13 would not function because UNC-29 would be forced adjacent to UNC-63 by the linker length, in the wrong configuration. In the case of a pentamer in the correct configuration, there would be no free UNC-29 able to join the growing complex and so would explain the lack of response. If true, it would imply that initial assembly of all five subunits occurs in the ER before transport away from the site of active protein synthesis. Further work is required to investigate this possibility. One testable prediction of this model is that addition of a long linker between the last two subunits could produce a functional receptor only for the pentamer in which UNC-29 comes before ACR-13. UNC-29 during synthesis would be available to join the growing complex before ACR-13. Synthesis of ACR-13 last in combination with the long linker may allow insertion of ACR-13 between the UNC-63 and UNC-29 subunits. In the other combination, the lack of UNC-29 to join the growing complex before production of ACR-13 would mean that even though a long linker would physically allow the subunits to occupy their correct physical positions, the required assembly pathway would be blocked.

Interestingly, the *in silico* study carried out by Hernando *et al.*, (Hernando et al., 2012) on different possible subunit arrangements of the *C. elegans* L-AChR revealed an optimal orientation and binding energy of ACh and LEV into the ACR-13(+)/UNC-29(-) and UNC-38(+)/LEV-1(-) interfaces. However, this study was only based on a few possible subunit arrangements, most of which are incorrect based on the data presented here.

The model proposed here is that UNC-38, LEV-1 and UNC-63 form an initial complex to which UNC-29 and ACR-13 are added individually. Of particular interest is the admixture of *C. elegans* UNC-38, UNC-63 and UNC-29 together with ACR-8 from *H. contortus* that produces a functional channel (Figure 3.2B). This implies that UNC-38, UNC-29 and UNC-63 can form an initial complex which

becomes functional if ACR-8 is ultimately included, but not if ACR-13 takes its place. This would imply either that inclusion of UNC-29 in the initial complex normally results in a large fraction of non-functional receptors that may be targeted for degradation, or that it is possible for the initial trimer to disassemble into its component subunits once more and subsequently reassemble.

Taken together, the use of admixtures of subunits from different species and the creation of concatenated subunits represent an informative and robust strategy to understand subunit evolution according to their position and functional interaction with adjacent subunits. A plethora of alternative techniques exist to decipher the subunit arrangement of pLGICs. Among these, subunit cross-linking approaches coupled with electron microscopy or atomic force microscopy have notably demonstrated their efficacy on the *T. californica* AChR (Karlin et al., 1983), the vertebrate GABA<sub>A</sub>  $\alpha 4\beta 3\delta$  (Barrera et al., 2008) and 5-HT<sub>3</sub> receptors (Barrera et al., 2005). Coupled with mass spectrometry, subunit cross-linking represents a new alternative as the technology becomes more adaptable to membrane multi-protein complexes (Barrera et al., 2011). Alternatively, anti-subunit antibodies may represent a suitable approach in identifying subunit position and pLGIC-interacting chaperons through tandem affinity purification of *in vivo* receptors (Gottschalk et al., 2005). Unfortunately, altogether these techniques remain technically difficult in terms of preparation, material or interpretation of data compared to concatenation of subunits. In contrast, the disulphide-trapping approach used on the GABA<sub>A</sub> receptor (Hanson et al., 2011) may represent a suitable technique for validating subunit position. It consists of inserting cysteines by mutagenesis on either side of the ligand-binding pocket. Therefore, adjacent subunits would expose cysteines to the formation of disulphide bonds that would theoretically induce a measurable change of channel gating properties only if the cysteine residues are sufficiently close.

Applied to native AChRs, the major interest of concatenated subunits will be to decipher the subunit position within the parasitic nematode L-AChRs. This will be able to determine, for example, if the ACR-8 from *H. contortus* is a simple physical substitution for the *C. elegans* ACR-13 or if it is associated with some rearrangement of the other subunits. Similarly, the same approach will confirm the position and the stoichiometry of the Hco-UNC-29 copies. Indeed, taking the *C. elegans* L-AChR as a model and according to the different functional subunit admixtures, a similar pattern of concatenation could also be transposed to parasitic nematode receptors and will represent a ideal way for addressing their mode of assembly.

Taken as a whole, the identification of the quaternary structure of the *C. elegans* L-AChR as UNC-38:LEV-1:UNC-63:ACR-13:UNC-29 represents the final step in the search for the structure of this

receptor since the initial screen for LEV resistant mutants of *C. elegans* in the early 1980's (Lewis et al., 1980).

## Chapter V: General Discussion.

The search for an explanation of how muscle movement is controlled in response to an electrical stimulus has driven research in this field since the original observation by Luigi Galvani in 1780 that direct application of electricity to a frog's leg caused movement. Dale and Loewi shared the Nobel prize in 1936 for the discovery of the first neurotransmitter, ACh, that it is released by activated nerve cells and that its application on heart muscle produces a slowing of contraction. The effects of ACh in the central nervous system and skeletal muscle are mediated by pLGICs present in the post-synaptic membrane that respond rapidly to the binding of ACh by opening a channel for  $\text{Na}^+$  and  $\text{Ca}^{2+}$  ions that depolarize the post-synaptic cell membrane and trigger a response. The search for different neurotransmitters and various compounds that target the pLGICs has revealed a large family of subunits that combine into homo- or heteropentameric receptors that regulate membrane potential in response to molecules including ACh, serotonin, dopamine, histamine, glycine, GABA, glutamate, biogenic amines and protons among others.

Phylogenetic reconstruction of the origin of pLGICs reveals that the major classes of subunit type arose during the early evolution of animal life some 700 MYr ago (Dent 2006). The specific mechanistic details of how these classes arose can reveal the underlying biology of their function but since these events occurred so long ago, the amino acid changes responsible for their functional differences are obscured by hundreds of millions of years of subsequent random sequence change. In order to study this process in any detail, much more recent events that produce novel pLGIC subunits must be found to minimize the degree of sequence change, allowing the use of bioinformatic and experimental techniques to reveal the pattern of functional adaptation. This approach has revealed an adaptive change of the human CHRNA10 AChR subunit that forms a heteromeric AChR in the cochlea, with CHRNA9, likely explains the acute sense of hearing in mammals *via* a specific increase in the conductance of  $\text{Ca}^{2+}$  (Franchini et al., 2006). In this case, re-adaptation of a specific gene is involved but events where recent gene duplications create novel subunits and thus mimic the origin of pLGIC diversity would ideal.

The nematodes characteristically encode many pLGIC subunit genes in their genomes and the ongoing Helminth Genome Initiative provides a rich data source that allows identification of pLGIC subunit genes in up to 70 different species. A search for recent duplication events identified an expansion of the *unc-29* AChR subunit gene in the trichostrongylid nematodes (Neveu et al., 2010). This thesis develops

these duplications as a model for pLGIC subunit duplication and diversification in general. One major advantage of investigating the L-AChR of nematodes is that an L-AChR has been reconstituted in *Xenopus* oocytes from *C. elegans* and a variety of related parasitic nematodes and so methods of experimental assessment of subunit function are available. It is particularly interesting that the L-AChR is expressed in the same synaptic junctions as the N-AChR encoded as a homopentamer of the ACR-16 subunit. It is not at all clear why the N-AChR should be homopentameric while the L-AChR of *C. elegans* should require five distinct subunits. It suggests that some aspect of the biological role the L-AChR plays, favours the retention and diversification of subunit duplications.

An evolutionary instability of the L-AChR is reflected in the fact that subunit composition is different among the nematode species for which the L-AChR has been reconstituted. The *C. elegans* L-AChR requires five different subunits UNC-38, UNC-63, ACR-13, UNC-29 and LEV-1 (Boulin et al., 2008). The L-AChR of the pig parasite *O. dentatum* does not require either the ACR-13 or LEV-1 subunit, but functional receptors can be produced using ACR-8 in various combinations of two, three or four different subunits (Buxton et al., 2014). The sheep parasite *H. contortus* does not appear to encode a copy of the *acr-13* gene, the *lev-1* gene lacks a signal peptide and in addition encodes four copies of the *unc-29* subunit gene. Functional L-AChRs with either three or four different subunits have been reconstituted in *Xenopus* oocytes (Boulin et al., 2011).

A successful model of subunit duplication and diversification should meet several criteria. First, the model should be representative of a more general phenomenon and so be useful in a broad context. Second, the degree of sequence divergence among duplicate copies should be sufficiently small that the effects of selective pressure acting on the sequence should be detectable and it should be feasible ultimately to match functional changes to specific amino acid replacements. Third, the different duplicate subunits should possess different functional characteristics that correlate with sequence change.

The first of these requirements is met by duplication of the *unc-29* L-AChR subunit gene. The filarial clade III nematodes and the *Caenorhabditis* group all retain a single copy of *unc-29*. The parasitic strongylid nematodes display at least nine different *unc-29* duplication events since divergence from the *Caenorhabditis* group. The duplications within *H. contortus* are clearly part of the same, more general, pattern of ongoing instability within the L-AChR of strongylid nematodes. The second requirement is also met since the sequence divergence among copies of *unc-29* is no more than 25 %, most of which lies within the intracellular loop of the receptor. Analysis of codon substitution rates among the different copies of *unc-29* reveals a signature of altered selection pressure and is able to

identify specific amino acids sites experiencing positive, directional selection (Duguet et al., 2016). The third requirement, for divergent function between the copies remained an open question and was addressed in Chapter II.

## 5.1 Hco-UNC-29 copies are functionally divergent

Expansion of the *unc-29* genes occurred through multiple, independent events within the Strongyloidea (Duguet et al., 2016) suggests that particular circumstances of the L-AChR in these nematodes favour this phenomenon. It is technically very challenging to identify the composition of and characterize native pLGICs *in vivo*. As a result it is not known what the composition of the native L-AChR of *H. contortus* might be *in vivo*. Faced with this technical challenge, the question of whether the normal function of the different UNC-29 paralogs had changed was restricted to whether any observable difference between them could be identified at all. Substituting each paralog in turn, in the different experimental systems, while holding everything else constant, would mean that any differences must be due only to differences in the amino acid sequence of the different proteins.

Reconstituting functional receptors with *H. contortus* UNC-29.1, UNC-29.3 and UNC-29.4 in turn revealed very similar EC<sub>50</sub> values for ACh (Figure 2.1G-I). This may result from the fact that any receptor produced *in vivo* would have to respond to the same ACh signal and therefore we might expect purifying selection to maintain the response to the natural neurotransmitter among subunit copies. The response to a variety of other agonists and antagonists, relative to the ACh response, was largely similar. The response to levamisole was slightly different between the three successfully reconstituted receptors (Figures 2.1A-C) and the response of L-AChR1.3 to mecamylamine was also different (Figure 2.1E). The great majority of anthelmintic compounds and other modulators of AChR function are not normally encountered by nematodes in their natural environment leaving no opportunity for functional adaptation of their principal target receptors. The anthelmintic ivermectin may be a rare exception to this (Ghosh et al., 2012). Random substitutions within the amino acid sequence may therefore account for the few functional differences observed for channel response.

The more striking difference among the four copies of UNC-29 was their ability to produce a functional receptor. UNC-29.1 and UNC-29.3 both produced receptors in *Xenopus* oocytes with a robust response to ACh. UNC-29.4 produced smaller currents (Figure 2.1C) and no currents were observed for UNC-29.2 at all (Figure 2.2). UNC-29.1 and UNC-29.2 co-localize in adult muscle tissue

(Figure 2.7) and it would seem reasonable that this has persisted since the original duplication event. Immediately following duplication, both proteins would be identical and would almost certainly take part in assembly of functional L-AChRs along with the same pool of other subunit proteins. Any functional adaptation by one or other of the subunits would lead to an uncertain mix of L-AChRs with different functional properties unless assembly of the two subunits into the L-AChR complex were regulated differently. For both subunit copies to persist, it makes sense for such assembly regulation to evolve. Functional adaptation in response to selection pressure could therefore explain why differences in production of a functional receptor were more marked than differences in response to a variety of artificial ligands.

It is not clear why the UNC-29.2 subunit failed to produce a functional receptor in combination with the remaining *H. contortus* subunits. Immunolocalization of UNC-29.2 at the oocyte surface suggests that the protein is exported to the surface (Figure 2.6) but given the sensitivity of antibody detection, only a fraction of the total protein synthesized may explain this signal. Another possibility is that UNC-29.2 requires another non- $\alpha$  subunit as is the case for UNC-29 and LEV-1 in *C. elegans*. No evidence was found to suggest that in the presence of UNC-29.1 that UNC-29.2 altered the reconstituted receptor in any way (Figure 2.3). Either UNC-29.2 was not incorporated, or it did not change the properties of the final receptor in any detectable way. The fact that all four copies of *H. contortus* UNC-29 could rescue a *C. elegans* knock-out of UNC-29 and could replace UNC-29 in the *C. elegans* L-AChR shows that UNC-29.2 is indeed functional (Figure 2.5).

One remaining possibility is that UNC-29.2 requires the presence of LEV-1. In the *C. elegans* L-AChR, a functional receptor is produced by UNC-29.2 only if the *C. elegans* LEV-1 is also present. *H. contortus* encodes *lev-1* in its genome but lacks a signal peptide. Addition of an artificial signal peptide to the Hco-LEV-1 produces a subunit that successfully combines with other subunits into a functional L-AChR in *Xenopus* oocytes. Mechanisms do exist to install proteins into the cell membrane independent of the pathway followed by proteins with a signal peptide sequence (Kuchler et al., 1992). It is interesting to speculate that UNC-29.1 lost the requirement for LEV-1 to produce a functional receptor at around the time that the *lev-1* gene lost the signal peptide sequence. If some alternative mechanism were available to import LEV-1 into the membrane, UNC-29.2 may have co-adapted with this to avoid competition for assembly with the UNC-29.1 subunit. This hypothesis raises many technical questions that will require future research to answer.

The four paralogous copies of *unc-29* in *H. contortus* met the three requirements set out for a good model of pLGIC duplication and diversification. The next step was therefore to investigate aspects of

functional divergence among copies, define their characteristics and interpret these observations in the context of evolutionary changes in the composition of the L-AChR. This was achieved in Chapter III using admixture combinations of subunits from different species.

## 5.2 Sequence dependent mechanisms determine production of a functional L-AChRs

The subunits UNC-29.1 and UNC-29.2 differ in their ability to produce a functional L-AChR in combination with the other L-AChR subunits evaluated from *H. contortus*. In contrast, both were able to produce functional L-AChRs in combination with the other L-AChR subunits from *C. elegans* in *Xenopus* oocytes, although UNC-29.2 produced smaller maximal currents (Figure 2.4). Both subunits were also able to rescue a defective *unc-29* gene *in vivo* in transgenic *C. elegans*. This difference highlights the fact that amino acid changes between UNC-29.1 and UNC-29.2 are responsible for the difference in compatibility, and that interactions with other subunits in the receptor also play a critical role.

In combination with other *C. elegans* subunits, UNC-29.1 did not require the presence of *C. elegans* LEV-1 to produce a functional receptor while UNC-29.2 did. If the receptor requires two non- $\alpha$  subunits, which seems likely, then this difference could be explained by an ability of UNC-29.1 to occupy both non- $\alpha$  positions of the receptor, while UNC-29.2 was limited only to one of these. A similar mechanism can explain the requirement for both UNC-29 and LEV-1 in the *C. elegans* L-AChR. Sequence specific difference prevent either one from fulfilling the role of the other. The most obvious difference in the gene complement of *C. elegans* and *H. contortus* is the lack of any *acr-13* in the *H. contortus* genome. ACR-8 from *H. contortus* could replace ACR-13 in the *C. elegans* L-AChR and *vice versa*, (Figure 3.2B) the subunits appearing in many ways to be functionally equivalent. In the presence of ACR-8, however, the *C. elegans* UNC-29 now no longer required the presence of LEV-1, much like the UNC-29.1 of *H. contortus* (Figure 3.2C). UNC-29 was able to fill the role of the second non- $\alpha$  subunit, something that was not true for LEV-1 (Figure 3.2D), which could not produce a functional receptor without UNC-29. The specificity of UNC-29 therefore depended on some form of interaction with ACR-13, a mechanism that was disrupted when ACR-8 from *H. contortus* was present. Replacing UNC-38 and UNC-63 with their orthologs from *H. contortus* allowed LEV-1 to function as the only non- $\alpha$  subunit (Figure 3.4B). This implies that the mechanism to limit the role of LEV-1 depended on an interaction with UNC-38 or UNC-63.



Analysis of admixture receptors from the two model nematode species proved to be a valuable technique in deciphering the functional specialization of different subunit and their evolution between two closely related species. The interaction between subunits to determine compatibility appears to be a major feature of the diversification of subunits following duplication. The *C. elegans* L-AChR represents an extreme example where each subunit is limited to one specific role in the receptor. Changes in subunit availability due to gene loss (*acr-13*) or modification (*lev-1*) appear to lead to a disruption of the mechanisms determining specificity and allow subunits the ability to serve multiple roles in a functional receptor. This could explain the observation that several different combination of subunits can produce a functional AChR in *O. dentatum* (Buxton et al., 2014) and *H. contortus* (Boulin et al., 2011).

These admixture combinations led to a speculation that compatibility between subunits may involve physical contact, particularly between UNC-29 and ACR-13 and between LEV-1 and UNC-38 and UNC-63. This hypothesis is consistent with the fact that a majority of positively selected residues of the *H. contortus unc-29* paralogs were principally located in regions involved in contact with adjacent subunits (Duguet et al., 2016). Whether these subunits are in physical contact in the L-AChR was not known and this was addressed in Chapter IV.

### 5.3 Assembly of the *C. elegans* L-AChR subunits form a unique quaternary structure

Contact between pLGIC subunits is a structural feature that is essential for the formation of a channel-shaped protein but also for ensuring ligand specificity and receptor activation. The L-AChRs, as heteromeric receptors, exhibit complex subunit organizations that directly affect channel function and pharmacology. The observations made throughout this thesis brought consistent evidence that subunit interaction is an important feature of the L-AChR that responds to evolutionary pressure and that such a phenomenon likely depends on physical contact and therefore the precise order of subunits within the L-AChR.

The identification of the quaternary structure of the *C. elegans* L-AChR was an ambitious project that integrated scientific knowledge collected during the past decades of research on L-AChRs in general. Many years of research, following the initial screen for LEV resistance mutations (Lewis et al., 1980) were needed to identify the various individual genes that play a role in producing the L-AChR of *C.*

*elegans*. Successful reconstitution of the *C. elegans* L-AChR in *Xenopus* oocytes (Boulin et al., 2008) confirmed the minimal set of *C. elegans* required proteins to produce the receptor and defined its functional properties. Establishing the relative position of the five subunits within the L-AChR represented a final and essential step in determining the structure of this important receptor.

The synthesis and expression of concatenated subunits represented a suitable methodological approach that is based on an rich literature establishing all the aspects and interpretations of results (Groot-Kormelink et al., 2004, Ericksen et al., 2007, Carbone et al., 2009, Steinbach et al., 2011). The stepwise approach, beginning with dimers followed by systematic testing of trimers, then tetramers and finally pentamers reduced the complexity of this work to make it manageable. This approach also revealed important results that allowed a model of receptor assembly to be put forward.

The success of only one dimeric construction, UNC-38:LEV-1 (Figure 4.1), implied two things. First, that the successful dimer likely represented one of the first steps in the assembly process and second that dimerization of other pairs of subunits in their correct physical organization prevented their successful integration into the growing receptor complex. The 3+1+1 assembly model from vertebrates (Green et al., 1993) suggested that extending the successful dimer by an additional subunit had the potential to produce a functional trimer. This indeed proved to be the case. A trimer of UNC-38:LEV-1:UNC-63 was able to produce efficiently a functional receptor when ACR-13 and UNC-29 were provided as monomers (Figure 4.2). Interpretation of this result in terms of the 3+1+1 model predicted that a dimer of LEV-1:UNC-63 should also be functional, as was indeed the case (Figure 4.3). The final addition of subunits one by one to the growing receptor complex predicted by the model could explain why dimers involving these subunits did not produce any functional receptor.

Only two possible configurations remained for the final two subunits. Either ACR-13 followed by UNC-29 or the reverse. While the initial trimer is believed to form so rapidly that it may not matter which dimer forms first (Green et al., 1993), the final subunits are believed to join the complex in a specific order. If the subunits join the complex in the same order in which they appear in the physical organization of the receptor, then production of the subunits during protein synthesis in the ER would follow the required assembly sequence. Otherwise, production of the subunits from the ribosome would be in the wrong order for assembly. The small maximal currents observed for oocytes injected with UNC-38:LEV-1:UNC-63:ACR-13 and monomeric UNC-29 (Figure 4.4A) suggest a problem with production of a robust L-AChR. It may be the case that production of such a complex protein aggregate in the form of a single polypeptide chain leads to many failed receptors that are never expressed on the cell surface. On the other hand, the suggestion that the physical order of the final two subunits was

ACR-13:UNC-29 but that the subunits join the growing complex in the reverse order is compelling. This would also explain why the tetramer plus monomeric UNC-29 could produce a few functional receptors but the pentamer could not. In this last case, there would never be any free UNC-29 available to join the growing complex at the appropriate point.

UNC-38:LEV-1:UNC-63:ACR-13:UNC-29 appears to be the quaternary structure of the *C. elegans* L-AChR (Figure 4.6) with the first three subunits forming a trimeric complex to which UNC-29 followed by ACR-13 may be added. This will require further experimentation to establish beyond doubt. This structure is consistent with the idea the ACR-13 and UNC-29 interact physically in a way suggested by the admixture combinations from Chapter III. LEV-1 also interacts physically with both UNC-38 and UNC-63.

## 5.4 Remaining questions and prospects

Expansion of subunit diversity in trichostrongylid nematodes compared to the rhabditid group poses legitimate questions about the reasons for such a complex number of AChR subunits. The homomeric ACR-16 (N-type) receptor and the heteromeric L-AChR both contribute in transmitting excitatory signals to the muscle cells at the *C. elegans* neuromuscular junction (Richmond et al., 1999, Touroutine et al., 2005, Boulin et al., 2008). The reasons for such a contrast between a structurally conserved and a diversified receptor remain obscure. The N-AChR produces a rapid inward flux of cations in response to ACh when the receptor rapidly desensitizes and the ion flow is terminated even in the presence of ACh. The L-AChR on the other hand, responds rapidly but does not desensitize in the same way, remaining open as long as ACh is present (Boulin et al., 2008). It is tempting to speculate that the N-AChR is responsible for an "all or nothing" response at the synapse whereas the L-AChRs and its diversified subunit composition allow specific fine tuning of the response that is transmitted to the muscles. Adaptation to a parasitic lifestyle may require a finer degree of control over muscular movement and may go some way to explain the increased complexity of the L-AChR in strongylid parasitic nematodes. The work presented in this thesis provides initial groundwork for a means to investigate this question.

*Xenopus* oocytes represent an invaluable system for the heterologous expression of pLGICs and ion-channels in general. It allows a better understanding of subunit interactions and a precise functional characterization of new receptors. However, this thesis highlights the crucial need for *in vivo* research

that could validate our knowledge obtained over the past decades on nematode L-AChRs. Indeed, the reconstitution of receptors remains an artificial method that may reflect the reality of the worm muscle in only a limited way. Moreover, the oocyte machinery and the AChR biosynthesis pathway are not necessarily identical to the situation in the worm *in vivo* and may lead to misinterpretation (Krashia et al., 2010). Subpopulations of receptors that have been produced in oocytes may not faithfully represent those in nematodes, for example, only one of the possible combinations for the L-AChR of *O. dentatum* appears to correspond to the receptor found *in vivo* (Buxton et al., 2014). More extensive investigation of L-AChRs in parasitic nematodes directly, *in vivo*, would avoid these issues. Alternative approaches that will have to be considered include genetic manipulation such as transgenesis, RNAi or the recently developed CRISPR-Cas9 system that has been used extensively in *C. elegans* (Dickinson et al., 2013, Waaijers et al., 2013, Dickinson et al., 2016) but remains poorly developed in parasitic nematodes. One interesting approach is that of extracting, purifying and transferring nematode receptors or membrane extracts directly at the protein level into *Xenopus* oocytes (Morales et al., 1995, Miledi et al., 2006, Crespin et al., 2016).

Analysis of admixtures presented in Chapter III highlighted changes in compatibility between units as a principal result of diversification of subunits following duplication. The restriction of the non- $\alpha$  subunits to one specific role in the L-AChR is a result of interactions with specific  $\alpha$  subunits and depends on the specific sequence of those subunits. The next step will be to determine precisely those amino acid residues responsible. This could be achieved by mutually exchanging sections of the UNC-29.1 and UNC-29.2 sequences, for example, and determining which part of the sequence determines their behaviour. Progressively shorter segments of the protein could be exchanged, leading ultimately to site directed mutagenesis and a demonstration of a causal relationship between the specific sequence and its effects.

Establishing the quaternary structure of the *C. elegans* L-AChR represents a major advance in this field and represents a reference for similar studies regarding the structure of the L-AChR from parasitic nematodes including *H. contortus*. The failure to produce a functional fully pentameric receptor is a concern. Further work is required to establish the cause and hopefully achieve a means of more robust expression. Manipulation of the length of the linker between the last two subunits of the pentamer may indicate if the order of subunit addition to the trimer is reversed from the order of subunits in the quaternary structure. If this is the case, there is a clear prediction that a sufficiently long linker before the last subunit should produce a functional receptor with UNC-38:LEV-1:UNC-63:UNC-29:ACR-13 but not for UNC-38:LEV-1:UNC-63:ACR-13:UNC-29. Concatamers may provide additional

information for observations made with the admixtures in Chapter III. For example, Hco-UNC-29.2 can functionally replace Cel-UNC-29 but not LEV-1, ACR-8 can functionally replace ACR-13, Hco-UNC-29.1 can replace both UNC-29 and LEV-1. Concatamers may help to reveal if this functional replacement is achieved by direct physical substitution of the subunit in the quaternary structure or if a more extensive rearrangement of the structure is involved.

In conclusion, this PhD project has established the duplicate copies of *unc-29* in *H. contortus* as a model of the process by which novel pLGIC subunits appear, persist and acquire new characteristics. Using this model it was possible to show that interactions between subunits within the receptor were responsible for their ability to produce functional receptors and that this is a characteristic that evolves rapidly following subunit duplication. Establishing the order and physical interactions of the subunits within the L-AChR using concatamers provides a powerful technique that will accelerate our ability to decipher those evolutionary changes critical for the origin of novel neurotransmitter signalling and understand the origin and implications of the differences in receptor composition between parasitic species of nematode and the *C. elegans* model.

## Chapter VI: Material and methods.

### 6.1 Animals

Animals (sheep and frogs) used in the present study were maintained and manipulated by certified personnel under conditions laid out in the Animal Use Protocols (AUP), which had been preliminarily validated and approved by the Macdonald Campus Facility Animal Care Committee of McGill University. Every accepted protocols strictly respected the rules and guidelines set out by the Canadian Council on Animal Care in Science.

#### 6.1.1 *Caenorhabditis elegans*

The different strains used throughout the study were obtained from the *Caenorhabditis* Genetics Center (CGC), funded by the National Institute of Health National Center for Research Resources. The Bristol N2 and the CB1072:e1072 animals were respectively used as wild-type and mutant strains. Worms were maintained on NGM (Nematode Growth Medium) plates at 20°C seeded with *Escherichia coli* OP50 according to standard culture methods (Brenner 1974).

#### 6.1.2 *Haemonchus contortus*

Approximately 5,000 L3 stage larvae of the laboratory anthelmintic sensitive isolate PF23, were administered to sheep by oral gavage. Sheep were maintained, infected and treated under the Animal Use Protocol #AUP3845. During the maintenance of sheep, eggs were regularly collected from faeces and cultured into L2 and L3 larvae at 18°C.

30 days after infection, the abomasal mucosa of sheep was dissected at necropsy to collect adult male and female nematodes.

#### 6.1.3 *Xenopus laevis*

All procedures regarding housing, handling, surgery and recovery were applied regarding the Animal Use Protocol #AUP2584.

## 6.2 AChR cDNA/cRNA library

The *C. elegans* and *H. contortus* cDNA clones used in this study were obtained as integrated in the bacterial expression vector pTB207 (Boulin et al., 2008, Boulin et al., 2011) The *C. elegans* cDNA were initially cloned and kindly provided by Dr. Thomas Boulin (Institut NeuroMyoGène - INMG CNRS UMR 5310 - INSERM U1217 - Université Claude Bernard Lyon1, Villeurbanne, France). The *H. contortus* cDNAs encoding subunits and ancillary proteins were cloned and also kindly provided by Dr. Cédric Neveu , Dr. Claude Charvet and Dr. Aymeric Fauvin (INRA, UMR1282, Infectiologie Santé Publique, Tours, France).

### 6.2.1 Accession numbers

Every cDNA clone sequences are identifiable with the following accession numbers: *Cel-unc-63* (NP491533), *Cel-unc-38* (NP491472), *Cel-acr-13* (or *Cel-lev-8*) (NP509932), *Cel-lev-1* (NP502534), *Cel-unc-29* (NP492399), *Hco-unc-63a* (GU060985), *Hco-unc-38* (GU060984), *Hco-acr-8* (EU006785), *Hco-unc-29.1* (GU060980), *Hco-unc-29.2* (GU060981), *Hco-unc-29.3* (GU060982), *Hco-unc-29.4* (GU060983), *Hco-unc-50* (HQ116822), *Hco-unc-74* (HQ116821), *Hco-ric-3.1* (HQ116823).

### 6.2.2 Linearization

Plasmids containing subunit and chaperon sequences were linearized prior to *in vitro* transcription. A minimum of 6 µg of plasmid were digested with the FastDigest *NheI* (ThermoFisher Scientific, Waltham MA) restriction enzyme at 37°C for at least two hours. The digestion product was then purified using a GeneJET gel extraction kit (ThermoFisher Scientific, Waltham MA).

### 6.2.3 In vitro RNA transcription

The *NheI*-linearized plasmids were used as template for *in vitro* transcription, which was carried out with the mMESSAGE mMACHINE T7 kit (Ambion). Newly synthesized cRNA were then precipitated with lithium chloride according to the manufacturer's instructions and dissolved in RNase-free distilled water. The concentration of the purified cRNAs was measured using a Nanodrop spectrophotometer (ThermoFisher Scientific, Waltham MA) and the integrity and quality was verified by electrophoresis through a 0.8 % nuclease-free agarose gel mixed with the nucleic acid dye GreenGlo (Denville Inc.).

Individual cRNA types were initially diluted at a concentration of 500 ng/ $\mu$ L in nuclease-free water. Then, the desired subunit combinations were prepared by mixing cRNAs encoding AChR subunits and ancillary proteins. Nuclease-free water was added to adjust the final concentration to 50 ng/ $\mu$ L for each cRNA.

## 6.3 *Xenopus laevis* oocytes - electrophysiology

### 6.3.1 Oocyte extraction

Mature female *Xenopus laevis* were anesthetized according to the AUP2584 procedure and an incision on one side of the abdomen was performed in order to collect lobes of ovaries containing oocytes. The lobes were then placed into a solution of  $\text{Ca}^{2+}$ -free OR2 (Goldin 1991) and manually divided in smaller pieces with thin tweezers. A final incubation of the oocytes was carried out for 75 min in 40 mg/mL collagenase 1A (Sigma-Aldrich Co.) in order to separate the oocytes and eliminate their follicular envelop. A final control of the digestion was visually confirmed under a dissecting scope. The oocytes were then washed at least five times in  $\text{Ca}^{2+}$ -free OR2 and finally placed into a ND96 solution (NaCl 96 mM, KCl 2 mM,  $\text{CaCl}_2$  1.8 mM,  $\text{MgCl}_2$  1 mM and HEPES 5 mM, pH 7.3) supplemented with sodium pyruvate 2.5 mM (Forrester et al., 2003) and incubated at 19°C until injection.

### 6.3.2 Oocyte injection

After the collagenase treatment, oocytes were injected in the animal pole (dark side) with approximately 36 nL of a designated cRNA mix prepared beforehand. Oocytes were placed on a suitable plastic support immersed in ND96 and injected with a Nanoject system (Drummond Scientific, Broomall, PA). Immediately after injection, oocytes were incubated at 19°C for at least three days before measurements were recorded, the ND96 buffer being changed once or twice a day.

### 6.3.3 Pharmacological compounds

The electrophysiological experiments required the use of different cholinergic agonists: acetylcholine chloride (ACh), bephenium hydroxynaphthoate (BEPH), 1,1-dimethyl-4-phenylpiperazinium iodide



(DMPP), (-)-tetramisole hydrochloride (LEV), (-)-nicotine hydrogen tartrate (NIC), pyrantel citrate (PYR).

Cholinergic antagonists were also tested: (+)-tubocurarine chloride hydrate (dTC), mecamylamine hydrochloride (Meca) and dihydro- $\alpha$ -erythroidine hydrobromide (DH $\alpha$ E).

All compounds were purchased from Sigma-Aldrich and DH $\alpha$ E was obtained from Tocris Bioscience.

#### *6.3.4 Two-electrode voltage clamp*

Oocytes were preliminary incubated into ND96 supplemented with 100  $\mu$ M of the calcium chelator BAPTA-AM four hours before the recording process. This treatment prevents the activation of endogenous calcium-activated chloride channels as noticed by Boulin et al. (2008).

Single oocytes were placed in a RC3Z chamber (Harvard Apparatus) filled with a recording solution (NaCl 100 mM, KCl 2.5 mM, CaCl<sub>2</sub> 1 mM, HEPES 5 mM, pH 7.3). This chamber was connected to a perfusion system supplying both recording buffer and drug solutions by gravity. The perfusion chamber was grounded through a 3 M KCl 1% agar bridge.

B150F-4 borosilicate glass capillaries (World Precision Instruments, Sarasota, FL) were pulled to make electrodes. Then, the tips were broken with a pair of thin tweezers and the electrodes were filled with 3 M KCl before being installed into their respective holders. The electrode were checked for a resistance between 0.5 and 3 M $\Omega$ .

Measurements were carried out using a Geneclamp 500B amplifier and Digidata 1322M (Axon Instruments, Sunnyvale, CA) and the voltage was clamped at -60 mV. Recording and analysis of the data were respectively performed with Clampex 9.2 and Clampfit 9.2 softwares (Axon Instruments, Sunnyvale, CA). The final traces were filtered at 10 Hz and the intensity of the peak currents corresponding to responses to the different drugs were measured and collected through Excel (Microsoft, USA) software. The GraphPad Prism 5.0 (GraphPad Software, San Diego, CA, USA) was used to make final graphs and calculate the mean  $\pm$  SE of the different drug responses. The same software was ran to establish concentration-response relationships by applying the Hill equation as previously described (Boulin et al., 2008).

## 6.4 *Caenorhabditis elegans* - Transgenesis

### 6.4.1 Molecular biology

The expression of *H. contortus* or *C. elegans* genes into *C. elegans* specific tissues required to make suitable expression vectors that would be directly injected in mature hermaphrodite *C. elegans*.

The backbone of the bacterial pPD96.52 plasmid (Addgene L2534) containing the *myo-3* promoter was used as a template for the insertion of the five following genes: *Cel-unc-29*, *Hco-unc-29.1*, *Hco-unc-29.2*, *Hco-unc-29.3* and *Hco-unc-29.4*.

In order position the genes correctly into the vector, every subunit sequence in pTB207 were re-amplified by PCR with primers containing restriction sites (Table 6.1).

The PCR products were digested with the corresponding FastDigest (ThermoFisher Scientific, Waltham MA) restriction enzymes (Table 5.1) for two hours at 37°C. In parallel, the pPD96.52 vector was digested with the same enzymes. All the digestion products were purified (GeneJET gel extraction kit - ThermoFisher Scientific, Waltham MA) and the T4 DNA Ligase (New England Biolabs) was used to ligate the vector and the inserts (1:3 ratio) for one hour at room temperature. The quality of the insertion was checked by sequencing the new plasmid constructs at the McGill University and Génome Québec Innovation Centre.

### 6.4.2 Microinjection

The pPD96.52 plasmids containing both the *C. elegans* and *H. contortus* genes were diluted at a concentration of 30 ng/μL in water and mixed with the *ttx-3::GFP*-expressing plasmids (Hobert et al., 1997) that was used as a transformation marker at identical concentration. This marker drives the expression of GFP in the two AIY head neurons (Hobert et al., 1997).

The mixed plasmids were microinjected into the gonad syncytium of young hermaphrodite adults, as described by Mello et al., (Mello et al., 1991). Two days later, the F1 transgenic fluorescent progeny were selected and maintained as two separated worm lines for each injected construct.

### 6.4.3 Paralysis assay

This experiment was performed to assess the paralyzing action of LEV on the transgenic and wild-type worms. 12 young fluorescent adults were picked and transferred on unseeded NGM plates containing

200  $\mu$ M LEV. Every worm were prodded with a hair type as described by Hernando et al., (Hernando et al., 2012) in order to observe movement. This procedure was carried out every 15 min for at least two hours and the whole paralysis assay was repeated three times. Non fluorescent worms such as wild-type and mutant strains were randomly picked at the young adult stage.

## 6.5 Immunohistochemistry

### 6.5.1 Antibodies

Synthetic peptides were selected from the two *H. contortus* subunits UNC-29.1 and UNC-29.2 and corresponded to parts of the intracellular loop between the third and the fourth transmembrane domains of the subunits. For UNC-29.1, the peptide sequences were: "EKTASPKTLNCAMELTTRDPQL" and "PIPEPAPPEITQLP" whereas the UNC-29.2 peptide sequences were "VSIKVLNCGDDIPKDP" and "MTKKKRGATVAKLP". The UNC-29.1

The UNC-29.1 peptides were used to immunized rabbits and the UNC-29.2 peptides were injected in rats (21<sup>st</sup> Century Biochemicals - Marlborough, MA).

The specificity of the peptide-derived polyclonal antibodies was verified by enzyme-linked immunosorbent assay (ELISA) and antibodies were titrated against both peptides.

### 6.5.2 *Xenopus* oocytes - whole cell immunochemistry

Oocyte collection, treatment, injection and current recordings was performed according to the previous description to reconstitute receptors (§6.3). TEVC was applied in identical conditions to verify the electrophysiological responses of the receptors to 100  $\mu$ M ACh.

Overnight incubation of the oocytes in 4% paraformaldehyde (PFA) diluted in 1X phosphate buffered saline (PBS) at 4°C was initiated and followed by five min washes with 1X PBS (repeated three times). Unspecific sites were blocked overnight in a antibody diluent solution (AbD) containing 1X PBS, 0.2 % gelatin from the skin of cold water fish, 2 % Triton X-100 and 0.1 % sodium azide. Oocytes were then incubated overnight at 4°C with the primary polyclonal antibodies diluted in AbD at a 1:100 ratio and washed three times, five min each, with the AbD solution. Corresponding secondary antibodies conjugated with the Alexa Fluor 488 (Invitrogen, USA) were applied overnight at 4°C on the oocytes and diluted in the AbD at a 1:500 ratio. The oocytes were finally washed two times with the AbD and two times with a mix of 1X PBS and 0.1 % (v/v) Triton X-100. Water-injected oocytes as well as AChR expressing-oocytes without the primary antibodies were considered as negative controls.

The oocytes were placed on microscope slides designated for the observation of thick material (Hanging Drop Slides - ThermoFisher Scientific, Waltham MA). Two drops of a mounting media (Sigma Aldrich) was applied and a coverslip slide was added on the observation field.

A Zeiss LSM710 confocal microscope (Carl Zeiss Inc., Canada) was used to observe the membrane of the oocytes and the Zeiss Zen 2010 software was run to analyze and control the imaging process.

### 6.5.3 *H. contortus* - cryosection immunochemistry

Freshly extracted adult male and female *H. contortus* from the PF23 strains were immediately fixed overnight at 4°C in a solution of 4 % paraformaldehyde diluted in 1X PBS. Then, three washes with 1X PBS were applied before incubating overnight at 4°C on a rocking platform in a solution of 1X PBS mixed with 30 % of sucrose. The nematodes were placed in a metal mold filled with an optimal cutting temperature compound (OCT) (ThermoFisher Scientific, Waltham MA). The whole mold was immediately frozen on dry ice and 10 µm cryosections were obtained using a Thermo Shandon cryotome (ThermoFisher Scientific, Waltham MA) and assembled on cold microscope slides. The transversal sections were blocked overnight at 4°C using the same AbD solution previously used on *Xenopus* oocytes. The same dilution of primary antibodies were applied on the slides and left for incubation overnight at 4°C. The sections were then washed 5 times with the AbD before being incubated in identical conditions with the corresponding secondary antibodies conjugated with the Alexa 488 fluorophore (Invitrogen, USA) at a dilution ration of 1:500. The final washing step was similar as previously described and the same mounting media was applied on the worm slices.

Confocal microscopy was performed using the same material and software. Negative controls consisted in using pre-adsorbed primary antibodies with 0.25 mg/mL of the corresponding peptide. Also, some sections were observed without incubating the primary antibodies.

## 6.6 AChR subunit concatenation

The *C. elegans* L-AChR subunit sequences initially inserted into pTB207 were used as templates for the construction of subunit dimers, trimers, tetramers and pentamers. In this configuration, the method consists in fusing the C-terminal extracellular tail of a subunit to the extracellular N-terminal of a second one. UNC-63 remained an exception as the C-terminal tail of this subunit was considered too

short to be properly joined to the second subunit without affecting the structure of the receptor. In consequence, an artificial linker made of five repeats of Threonine-Serine-Alanine was added at the C-terminal of UNC-63 when this subunit was used.

This synthesis process required to amplify every subunits by PCR in order to add unique restriction sites at both 5' and 3' ends of the subunit sequences for an optimal assembly by ligation and to either delete the signal peptide or the stop codon depending on the desired combinations. Figure 6.1 and Table 6.2 respectively show the strategy designed to assemble subunit concatamers and a list of primers used to generate compatible combinations.

Finally, cRNA corresponding to every concatamer *in vitro* synthesized and injected into *Xenopus* oocytes along with the corresponding monomer cRNAs. The TEVC electrophysiological technique was applied as previously described and the functionality of the constructions were tested with 100  $\mu$ M of both ACh and LEV.

#### 6.6.1 Dimers

A total of 13 combinations were made in order to create two different subunit associations: the  $\alpha$  type subunits in first position (principal) with the non- $\alpha$  in second (complementary) and all the six possible  $\alpha/\alpha$  combinations. The LEV-1:UNC-63 dimer was the only subunit combination consisting of a non- $\alpha/\alpha$  pair. PCRs were run using primer listed in Table 5.2. 20  $\mu$ L PCR reactions were prepared by mixing 1  $\mu$ L of each primer at a concentration of 10  $\mu$ M, 10 to 20 ng of plasmid template, 0.5  $\mu$ L of 10 mM dNTPs, 2  $\mu$ L of 10X Buffer, nuclease-free water adjusted to 19.8  $\mu$ L and 0.2  $\mu$ L of Taq polymerase (DreamTaq DNA polymerase - ThermoFisher Scientific, Waltham MA). The PCR program was: 30 sec at 95°C, 30 sec at 56°C, 2 min at 72°C repeated 35 to 38 times. The PCR products were run through electrophoresis in a 0.8 % agarose gel and the bands were cut under UV light. A gel extraction column-based protocol was used to purify the DNA according to the instructions of the manufacturer (GeneJET gel extraction kit - ThermoFisher Scientific, Waltham MA). Purified PCR products were immediately ligated into the pGEM-T bacterial cloning vector (pGEM-T Easy Vector Systems - Promega, Fitchburg WI) and incubated overnight at 4°C. Thermocompetent DH5- $\alpha$  *Escherichia coli* (Subcloning Efficiency™ DH5 $\alpha$ ™ Competent Cells - ThermoFisher Scientific, Waltham, MA) were then transformed with these ligation products.

The transfer of the PCR into a cloning vector allowed a better conservation of the subunit sequence in bacteria and a better template for further digestion.

pGEM-T plasmids containing the subunit sequences of interest were grown in bacterial liquid culture and purified using the GeneJET gel extraction kit (ThermoFisher Scientific, Waltham MA).

For every dimer, the FastDigest *NotI*, *XbaI* and *ApaI* restrictions enzymes (ThermoFisher Scientific, Waltham MA) were the six base cutters used to assemble subunits without changing the codon reading frame. The whole amount of plasmid was digested at 37°C for minimum two hours with 2 µL of each enzyme mixed to 5 µL of the 10X FastDigest buffer and water adjusted to a total volume of 50 µL. In parallel, the empty pTB207 plasmid was digested under the same conditions with the *NotI* and *ApaI* enzymes and was considered as the plasmid backbone receiving the ligated subunits. The digested products were then run through a 0.8 % agarose gel by electrophoresis and the bands corresponding to the subunit monomers (~1500 bp in size) or the linearized pTB207 (~3500 bp) were extracted and purified using the gel extraction kit previously described.

A sticky end ligation of the pTB207 and the two subunits was immediately carried out for one hour at room temperature using the T4 DNA Ligase (New England Biolabs, Ipswich MA) and its related protocol. Then, DH5- $\alpha$  were transformed with the purified digestion products while the remaining material was stored at -80°C.

Few colonies were screened by PCR and checked for the presence of the dimers into pTB207 by using different sets of primers such as T7 and SP6 universal primers which bind to the pTB207 vector on either side of the insertion region. Subunit specific primers were also used to check the orientation and the integrity of the newly constructed dimer. Positive clones were grown and their respective plasmids were purified and sequenced as previously described.

cRNAs of the dimer were finally synthesized following the protocol detailed in §6.2.4.

### 6.6.2 Trimers

The reconstitution of the different dimers coupled with monomers in *Xenopus* oocytes opened the way towards the synthesis of trimers of subunits. According to the electrophysiology results, the UNC-38:LEV-1 dimer served as a backbone for the construction of 5 trimers by either inserting a subunit at the third or the first position (version #1 and #2 respectively, Figure 6.1).

The version #1 trimer required to create a unique six base restriction site (*AflIII*) in order to insert the third subunit in the right position. Primers listed in Table 6.2 were used to amplify *unc-63*, *acr-13* and *unc-29* in order to insert changes required to form a complete trimer of subunits. The same methods used in the "dimer" section were applied to amplify monomers, digest and ligate PCR products with the

pTB207 and synthesize cRNAs. The version #2 consisted in creating the *PteI* site at the 5' end of *unc-38* and other sets of primers (Table 6.2) were used to amplify *unc-63* and *acr-13* in order to generate compatible sticky end PCR products.

### 6.6.3 Tetramers

The UNC-38:LEV-1:UNC-63 trimer is the unique construction being functional in *Xenopus* oocytes when co-expressed with corresponding monomers (*acr-13* and *unc-29*). Consequently, two tetramers were synthesized from this construct (Figure 6.1) by adding a fourth subunit (*acr-13* or *unc-29*) at the 3' end of *unc-63*.

The approach consisted in digesting a version #1 trimer with the *AflIII* and *ApaI* restriction enzymes. Then, *unc-63*, *acr-13* and *unc-29* were re-amplified by PCR with primers listed in Table 6.2 containing specific restriction sites represented in Figure 6.1. A new six base restriction site (*AvrII*) was created at the interface between *unc-63* and the fourth subunit sequence. A final ligation was carried out to fuse the pTB207 (containing *unc-38:lev-1*), *unc-63* and *acr-13* or *unc-29*.

### 5.6.4 Pentamers

Two pentamers UNC-38:LEV-1:UNC-63:ACR-13:UNC-29 and UNC-38:LEV-1:UNC-63:UNC-29:ACR-13 were constructed from a tetramer that was digested with *AvrII* and *ApaI* (Figure 6.1). *acr-13* and *unc-29* PCR products were generated in order to adjust their respective position within the final constructs (Figure 6.1 and Table 6.2). The final ligation consisted in assembling the UNC-38:LEV-1:UNC-63 trimer already in pTB207 with a fourth and fifth subunit as described in Figure 6.1.





Subunit	Primer	Primer sequence (5'-3')	Restriction enzyme
<i>Hco-unc-29.1</i>	Td-112 (forward)	AAGCTAGCATGCGTTTCGAACTCCTGATT	<i>NheI</i>
	Td-113 (reverse)	TGGCGGAAATCGTGATTAAACCGGTAA	<i>AgeI</i>
<i>Hco-unc-29.2</i>	Td-114 (forward)	AAAGCTAGCATGCGCCTACATCCACTTCT	<i>NheI</i>
	Td-115 (reverse)	TGGTGGTATCCGTGATTAACTCGAGAAA	<i>XhoI</i>
<i>Hco-unc-29.3</i>	Td-116 (forward)	AAGCTAGCATGCAAATCGGACATCTTG	<i>NheI</i>
	Td-117 (reverse)	AATCTGGAGATAACAGTTAACTCGAGAAA	<i>XhoI</i>
<i>Hco-unc-29.4</i>	Td-118 (forward)	AAAGCTAGCATGCTTTTCTATCAGCTTCTT	<i>NheI</i>
	Td-119 (reverse)	GACACGAGGCAGTAGCTAGCTCGAGAAA	<i>XhoI</i>
<i>Cel-unc-29</i>	Td-120 (forward)	AAGCTAGCATGAGGACCAACCGACTAT	<i>NheI</i>
	Td-121 (reverse)	CAGCATCCAATATTCCCTGACTCGAGAA	<i>XhoI</i>

**Table 6.1: Primers used for the insertion of L-AChR subunits in the *C. elegans* expression vector pPD96.52**

Concatamer	Subunit combination	Primer	Primer sequence (5'-3')	Restriction site	Signal peptide	Stop codon
Dimers	<i>unc-38</i> (1st position)	Cel-011 (forward)	GCGGCCGCATGCGCTCTTTTGGTTATTCCT	<i>NotI</i>	Yes	-
		Cel-012 (forward)	TCTAGAGAACTAATTGGATTAGCAGATAA	<i>XbaI</i>	-	No
	<i>unc-38</i> (2nd position)	Cel-021 (forward)	TCTAGAGGAAATGAAGATGCTAAACGGCTT	<i>XbaI</i>	No	-
		Cel-022 (reverse)	GGGCCCTCAGAACTAATTGGATTAGCAGAT	<i>ApaI</i>	-	Yes
	<i>unc-63</i> (1st position)	Cel-007 (forward)	GCGGCCGCATGGGACCAAATGACCACGG	<i>NotI</i>	Yes	-
		Cel-008 (reverse)	TCTAGAAGCCGTAGATGCGGTACTAGCGTTGAAG CAGTAGATGCAGTGCTAGCAAGAGCCGGCGTGTTA T	<i>XbaI</i>	-	No (+linker)
	<i>unc-63</i> (2nd position)	Cel-025 (forward)	TCTAGAGCGAACAGAGATGCGAATCG	<i>XbaI</i>	No	-
		Cel-026 (reverse)	GGGCCCTAAGCAAGAGCCGGCGTG	<i>ApaI</i>	-	Yes
	<i>acr-13</i> (1st position)	Cel-015 (forward)	GCGGCCGCATGTGGATACCTCAACGGATAAG	<i>NotI</i>	Yes	-
		Cel-016 (reverse)	TCTAGAGGTGTTAAGAACGTTGATGGTTC	<i>XbaI</i>	-	No

Concatamer	Subunit combination	Primer	Primer sequence (5'-3')	Restriction site
Dimers	<i>acr-13</i> (2nd position)	Cel-023 (forward)	TCTAGAGCCAACAAACATGTTTCGCAA	<i>XbaI</i>
		Cel-024 (reverse)	GGGCCCTCAGGTGTTAAGAACGTTGATGG	<i>ApaI</i>
	<i>lev-1</i> (1st position)	Cel-051 (forward)	GCGGCCGCATGATGTTAGGAGGTGGTGGAGG	<i>NotI</i>
		Cel-053 (reverse)	TCTAGAGAAAATACCAAGAACTGTGTCGT	<i>XbaI</i>
	<i>lev-1</i> (2nd position)	Cel-013 (forward)	TCTAGAGACATAGATGCCGAGGATCGC	<i>XbaI</i>
		Cel-014 (reverse)	GGGCCCTCAGAAAATACCAAGAACTGTGTC	<i>ApaI</i>
	<i>unc-29</i> (2nd position)	Cel-009 (forward)	TCTAGATCGGATGATGAAGAACGATTGA	<i>XbaI</i>
		Cel-010 (reverse)	GGGCCCTCAGGGAATATTGGATGCTGTATC	<i>ApaI</i>

Concatamer	Subunit combination	Primer	Primer sequence (5'-3')	Restriction site
Trimers	<i>unc-63</i> (1st position)	Cel-007 (forward)	<b>GCGGCCGCATGGGACCAAATGACCACGG</b>	<i>NotI</i>
		Cel-031 (reverse)	<b>GCGCGCAGCCGTAGATGCGGTACTAGCGTTGAAGCAGTAGATGCA GTGCTAGCAAGAGCCGGCGTGTAT</b>	<i>PteI</i>
	<i>unc-63</i> (3rd position)	Cel-035 (forward)	<b>CTTAAGGCGAACAGAGATGCGAATCG</b>	<i>AflIII</i>
		Cel-026 (reverse)	<b>GGGCCCCCTAAGCAAGAGCCGGCGTG</b>	<i>ApaI</i>
	<i>acr-13</i> (1st position)	Cel-015 (forward)	<b>GCGGCCGCATGTGGATACCTCAACGGATAAG</b>	<i>NotI</i>
		Cel-032 (reverse)	<b>GCGCGCGGTGTTAAGAACGTTGATGGTTC</b>	<i>PteI</i>
	<i>acr-13</i> (3rd position)	Cel-036 (forward)	<b>CTTAAGGCCAACAAACATGTTTCGCAA</b>	<i>AflIII</i>
		Cel-024 (reverse)	<b>GGGCCCTCAGGTGTTAAGAACGTTGATGG</b>	<i>ApaI</i>
	<i>unc-29</i> (1st position)	Cel-033 (forward)	<b>GCGGCCGCATGAGGACCAACCGACTATC</b>	<i>NotI</i>
		Cel-034 (reverse)	<b>GCGCGCTCGGGGAATATTGGATGCTG</b>	<i>PteI</i>

Concatamer	Subunit combination	Primer	Primer sequence (5'-3')	Restriction site
Tetramers	<i>unc-63</i> (3rd position)	Cel-035 (forward)	<b>CTTAAGGCGAACAGAGATGCGAATCG</b>	<i>AflIII</i>
		Cel-046 (reverse)	<b>CCTAGGAGCCGTAGATGCGGTACTAGCG</b>	<i>AvrII</i>
	<i>acr-13</i> (4th position)	Cel-047 (forward)	<b>CCTAGGGCCAACAAACATGTTTCGCAA</b>	<i>AvrII</i>
		Cel-024 (reverse)	<b>GGGCCCTCAGGTGTTAAGAACGTTGATGG</b>	<i>ApaI</i>
	<i>unc-29</i> (4th position)	Cel-048 (forward)	<b>CCTAGGTCGGATGATGAAGAACGATTGA</b>	<i>AvrII</i>
		Cel-010 (reverse)	<b>GGGCCCTCAGGGAATATTGGATGCTGTATC</b>	<i>ApaI</i>

Concatamer	Subunit combination	Primer	Primer sequence (5'-3')	Restriction site
Pentamers	<i>acr-13</i> (4th position)	Cel-047 (forward)	CCTAGGGCCAACAAACATGTTTCGCAA	<i>AvrII</i>
		Cel-016 (reverse)	TCTAGAGGTGTTAAGAACGTTGATGGTTC	<i>XbaI</i>
	<i>acr-13</i> (5th position)	Cel-023 (forward)	TCTAGAGCCAACAAACATGTTTCGCAA	<i>XbaI</i>
		Cel-024 (reverse)	GGGCCCTCAGGTGTTAAGAACGTTGATGG	<i>ApaI</i>
	<i>unc-29</i> (4th position)	Cel-048 (forward)	CCTAGGTCGGATGATGAAGAACGATTGA	<i>AvrII</i>
		Cel-052 (reverse)	TCTAGAGGGAATATTGGATGCTGTATCGT	<i>XbaI</i>
	<i>unc-29</i> (5th position)	Cel-009 (forward)	TCTAGATCGGATGATGAAGAACGATTGA	<i>XbaI</i>
		Cel-010 (reverse)	GGGCCCTCAGGGAATATTGGATGCTGTATC	<i>ApaI</i>

**Table 6.2: Primers used for the concatenation of *C. elegans* L-AChR subunits.**

## References

- Abad, P., J. Gouzy, J. M. Aury, P. Castagnone-Sereno, E. G. Danchin, E. Deleury, . . . P. Wincker** (2008). "Genome sequence of the metazoan plant-parasitic nematode *Meloidogyne incognita*." *Nature Biotechnology* 26(8): 909-915.
- Abongwa, M., S. K. Buxton, E. Courtot, C. L. Charvet, C. Neveu, C. J. McCoy, . . . R. J. Martin** (2016). "Pharmacological profile of *Ascaris suum* ACR-16, a new homomeric nicotinic acetylcholine receptor widely distributed in *Ascaris* tissues." *British Journal of Pharmacology* 173(16): 2463-2477.
- Aceves, J., D. Erlij and R. Martinez-Maranon** (1970). "The mechanism of the paralysing action of tetramisole on *Ascaris* somatic muscle." *British Journal of Pharmacology* 38(3): 602-607.
- Aguinaldo, A. M., J. M. Turbeville, L. S. Linford, M. C. Rivera, J. R. Garey, R. A. Raff and J. A. Lake** (1997). "Evidence for a clade of nematodes, arthropods and other moulting animals." *Nature* 387(6632): 489-493.
- Akabas, M. H.** (2011). "Ion channels: Manipulating the munchies in mice." *Nature Chemical Biology* 7(11): 759-760.
- Albertson, D. G. and J. N. Thomson** (1976). "The pharynx of *Caenorhabditis elegans*." Philosophical transactions of the Royal Society of London. *Series B, Biological Sciences* 275(938): 299-325.
- Alexander, J. K., A. P. Govind, R. C. Drisdell, M. P. Blanton, Y. Vallejo, T. T. Lam and W. N. Green** (2010). "Palmitoylation of nicotinic acetylcholine receptors." *Journal of Molecular Neuroscience* : MN 40(1-2): 12-20.
- Alexander, J. K., D. Sagher, A. V. Krivoshein, M. Criado, G. Jefford and W. N. Green** (2010). "Ric-3 promotes  $\alpha 7$  nicotinic receptor assembly and trafficking through the ER subcompartment of

dendrites." *The Journal of Neuroscience : the official journal of the Society for Neuroscience* 30(30): 10112-10126.

**Almedom, R. B., J. F. Liewald, G. Hernando, C. Schultheis, D. Rayes, J. Pan, . . . A. Gottschalk** (2009). "An ER-resident membrane protein complex regulates nicotinic acetylcholine receptor subunit composition at the synapse." *The EMBO Journal* 28(17): 2636-2649.

**Almeida, F. A., K. C. O. D. Garcia, P. R. Torgerson and A. F. T. Amarante** (2010). "Multiple resistance to anthelmintics by *Haemonchus contortus* and *Trichostrongylus colubriformis* in sheep in Brazil." *Parasitology International* 59(4): 622-625.

**Amiri, S., K. Tai, O. Beckstein, P. C. Biggin and M. S. Sansom** (2005). "The  $\alpha 7$  nicotinic acetylcholine receptor: molecular modelling, electrostatics, and energetics." *Molecular Membrane Biology* 22(3): 151-162.

**Aubry, M. L., P. Cowell, M. J. Davey and S. Shevde** (1970). "Aspects of the pharmacology of a new anthelmintic: pyrantel." *British Journal of Pharmacology* 38(2): 332-344.

**Avramopoulou, V., A. Mamalaki and S. J. Tzartos** (2004). "Soluble, oligomeric, and ligand-binding extracellular domain of the human  $\alpha 7$  acetylcholine receptor expressed in yeast: replacement of the hydrophobic cysteine loop by the hydrophilic loop of the ACh-binding protein enhances protein solubility." *The Journal of Biological Chemistry* 279(37): 38287-38293.

**Barrera, N. P., J. Betts, H. You, R. M. Henderson, I. L. Martin, S. M. Dunn and J. M. Edwardson** (2008). "Atomic force microscopy reveals the stoichiometry and subunit arrangement of the  $\alpha 4\beta 3\delta$  GABA(A) receptor." *Molecular pharmacology* 73(3): 960-967.

**Barrera, N. P., P. Herbert, R. M. Henderson, I. L. Martin and J. M. Edwardson** (2005). "Atomic force microscopy reveals the stoichiometry and subunit arrangement of 5-HT<sub>3</sub> receptors." *Proceedings of the National Academy of Sciences of the United States of America* 102(35): 12595-12600.

**Barrera, N. P. and C. V. Robinson** (2011). "Advances in the mass spectrometry of membrane proteins: from individual proteins to intact complexes." *Annu Rev Biochem* 80: 247-271.

- Barry, P. H. and J. W. Lynch** (2005). "Ligand-gated channels." *IEEE transactions on nanobioscience* 4(1): 70-80.
- Basyoni, M. M. and E. M. Rizk** (2016). "Nematodes ultrastructure: complex systems and processes." *J Parasit Dis* 40(4): 1130-1140.
- Baur, R., R. N. Beech, E. Sigel and L. Rufener** (2015). "Monepantel irreversibly binds to and opens *Haemonchus contortus* MPTL-1 and *Caenorhabditis elegans* ACR-20 receptors." *Molecular Pharmacology* 87(1): 96-102.
- Beech, R. N. and C. Neveu** (2014). "The evolution of pentameric ligand-gated ion-channels and the changing family of anthelmintic drug targets." *Parasitology*: 1-15.
- Beech, R. N. and C. Neveu** (2015). "The evolution of pentameric ligand-gated ion-channels and the changing family of anthelmintic drug targets." *Parasitology* 142(2): 303-317.
- Beg, A. A. and E. M. Jorgensen** (2003). "EXP-1 is an excitatory GABA-gated cation channel." *Nature Neuroscience* 6(11): 1145-1152.
- Bennett, H. M., K. Lees, K. M. Harper, A. K. Jones, D. B. Sattelle, S. Wonnacott and A. J. Wolstenholme** (2012). "*Xenopus laevis* RIC-3 enhances the functional expression of the *C. elegans* homomeric nicotinic receptor, ACR-16, in *Xenopus* oocytes." *Journal of Neurochemistry*.
- Bennett, H. M., S. M. Williamson, T. K. Walsh, D. J. Woods and A. J. Wolstenholme** (2012). "ACR-26: A novel nicotinic receptor subunit of parasitic nematodes." *Molecular and Biochemical Parasitology*.
- Bianchi, L. and M. Driscoll** (2006). "Heterologous expression of *C. elegans* ion channels in *Xenopus* oocytes." *WormBook : the online review of C. elegans biology*: 1-16.
- Blaxter, M. and G. Koutsovoulos** (2015). "The evolution of parasitism in *Nematoda*." *Parasitology* 142 Suppl 1: S26-39.

- Blaxter, M. L., P. De Ley, J. R. Garey, L. X. Liu, P. Scheldeman, A. Vierstraete, . . . W. K. Thomas** (1998). "A molecular evolutionary framework for the phylum *Nematoda*." *Nature* 392(6671): 71-75.
- Bocquet, N., H. Nury, M. Baaden, C. Le Poupon, J. P. Changeux, M. Delarue and P. J. Corringer** (2009). "X-ray structure of a pentameric ligand-gated ion channel in an apparently open conformation." *Nature* 457(7225): 111-114.
- Boulin, T., A. Fauvin, C. Charvet, J. Cortet, J. Cabaret, J. L. Bessereau and C. Neveu** (2011). "Functional reconstitution of *Haemonchus contortus* acetylcholine receptors in *Xenopus* oocytes provides mechanistic insights into levamisole resistance." *British Journal of Pharmacology* 164(5): 1421-1432.
- Boulin, T., A. Fauvin, C. L. Charvet, J. Cortet, J. Cabaret, J. L. Bessereau and C. Neveu** (2011). "Functional reconstitution of *Haemonchus contortus* acetylcholine receptors in *Xenopus* oocytes provides mechanistic insights into levamisole resistance." *British Journal of Pharmacology* 164(5): 1421-1432.
- Boulin, T., M. Gielen, J. E. Richmond, D. C. Williams, P. Paoletti and J. L. Bessereau** (2008). "Eight genes are required for functional reconstitution of the *Caenorhabditis elegans* levamisole-sensitive acetylcholine receptor." *Proceedings of the National Academy of Sciences of the United States of America* 105(47): 18590-18595.
- Boulin, T., G. Rapti, L. Briseno-Roa, C. Stigloher, J. E. Richmond, P. Paoletti and J. L. Bessereau** (2012). "Positive modulation of a Cys-loop acetylcholine receptor by an auxiliary transmembrane subunit." *Nature Neuroscience*.
- Brejč, K., W. J. van Dijk, R. V. Klaassen, M. Schuurmans, J. van Der Oost, A. B. Smit and T. K. Sixma** (2001). "Crystal structure of an ACh-binding protein reveals the ligand-binding domain of nicotinic receptors." *Nature* 411(6835): 269-276.
- Brenner, S.** (1974). "The genetics of *Caenorhabditis elegans*." *Genetics* 77(1): 71-94.



- Brenner, S.** (1988). The Nematode *Caenorhabditis elegans*.
- Butler, A. S., S. A. Lindesay, T. J. Dover, M. D. Kennedy, V. B. Patchell, B. A. Levine, . . . N. M. Barnes** (2009). "Importance of the C-terminus of the human 5-HT<sub>3A</sub> receptor subunit." *Neuropharmacology* 56(1): 292-302.
- Buxton, S. K., C. L. Charvet, C. Neveu, J. Cabaret, J. Cortet, N. Peineau, . . . R. J. Martin** (2014). "Investigation of acetylcholine receptor diversity in a nematode parasite leads to characterization of tribendimidine- and derquantel-sensitive nAChRs." *PLoS Pathogens* 10(1): e1003870.
- Carbone, A. L., M. Moroni, P. J. Groot-Kormelink and I. Bermudez** (2009). "Pentameric concatenated ( $\alpha$ 4)<sub>2</sub>( $\beta$ 2)<sub>3</sub> and ( $\alpha$ 4)<sub>3</sub>( $\beta$ 2)<sub>2</sub> nicotinic acetylcholine receptors: subunit arrangement determines functional expression." *British Journal of Pharmacology* 156(6): 970-981.
- Castillo, M., J. Mulet, L. M. Gutierrez, J. A. Ortiz, F. Castelan, S. Gerber, . . . M. Criado** (2005). "Dual role of the RIC-3 protein in trafficking of serotonin and nicotinic acetylcholine receptors." *The Journal of Biological Chemistry* 280(29): 27062-27068.
- Changeux, J. P.** (2012). "The nicotinic acetylcholine receptor: the founding father of the pentameric ligand-gated ion channel superfamily." *The Journal of Biological Chemistry* 287(48): 40207-40215.
- Charvet, C. L., A. P. Robertson, J. Cabaret, R. J. Martin and C. Neveu** (2012). "Selective effect of the anthelmintic buphenium on *Haemonchus contortus* levamisole-sensitive acetylcholine receptors." *Invertebrate Neuroscience* 12(1): 43-51.
- Clark, C. H., G. K. Kiesel and C. H. Goby** (1962). "Measurements of blood loss caused by *Haemonchus contortus* infection in sheep." *American Journal of Veterinary Research* 23: 977-980.
- Cohen Ben-Ami, H., Y. Biala, H. Farah, E. Elishevitz, E. Battat and M. Treinin** (2009). "Receptor and subunit specific interactions of RIC-3 with nicotinic acetylcholine receptors." *Biochemistry* 48(51): 12329-12336.
- Connolly, C. N. and K. A. Wafford** (2004). "The Cys-loop superfamily of ligand-gated ion channels: the impact of receptor structure on function." *Biochemical Society Transactions* 32(Pt3): 529-534.

- Consortium, C. e. S.** (1998). "Genome sequence of the nematode *C. elegans*: a platform for investigating biology." *Science* 282(5396): 2012-2018.
- Corringer, P. J., N. Le-Novre and J. P. Changeux** (2000). "Nicotinic receptors at the amino acid level." *Annual Review of Pharmacology and Toxicology* 40: 431-458.
- Corsi, A. K., B. Wightman and M. Chalfie** (2015). "A Transparent Window into Biology: A Primer on *Caenorhabditis elegans*." *Genetics* 200(2): 387-407.
- Cottrell, G. A.** (1997). "The first peptide-gated ion channel." *The Journal of Experimental Biology* 200(Pt 18): 2377-2386.
- Courtot, E., C. Charvet, R. N. Beech, A. Harmache, A. Wolstenholme, L. Holden-Dye, . . . C. Neveu** (2015). "Functional characterization of a novel class of morantel-sensitive acetylcholine receptors in nematodes." *PLoS Pathogens* Submitted.
- Coyne, M. J., G. Smith and C. Johnstone** (1991). "A study of the mortality and fecundity of *Haemonchus contortus* in sheep following experimental infections." *International Journal for Parasitology* 21(7): 847-853.
- Crespin, L., C. Legros, O. List, H. Tricoire-Leignel and C. Mattei** (2016). "Injection of insect membrane in *Xenopus* oocyte: An original method for the pharmacological characterization of neonicotinoid insecticides." *Journal of Pharmacological and Toxicological Methods* 77: 10-16.
- Culetto, E., H. A. Baylis, J. E. Richmond, A. K. Jones, J. T. Fleming, M. D. Squire, . . . D. B. Sattelle** (2004). "The *Caenorhabditis elegans unc-63* gene encodes a levamisole-sensitive nicotinic acetylcholine receptor alpha subunit." *The Journal of Biological Chemistry* 279(41): 42476-42483.
- Cully, D. F., P. S. Paress, K. K. Liu, J. M. Schaeffer and J. P. Arena** (1996). "Identification of a *Drosophila melanogaster* glutamate-gated chloride channel sensitive to the antiparasitic agent avermectin." *The Journal of Biological Chemistry* 271(33): 20187-20191.

**Cully, D. F., D. K. Vassilatis, K. K. Liu, P. S. Paress, L. H. Van der Ploeg, J. M. Schaeffer and J. P. Arena** (1994). "Cloning of an avermectin-sensitive glutamate-gated chloride channel from *Caenorhabditis elegans*." *Nature* 371(6499): 707-711.

**Day, R. N. and M. W. Davidson** (2012). "Fluorescent proteins for FRET microscopy: monitoring protein interactions in living cells." *BioEssays : News and Reviews in Molecular, Cellular and Developmental Biology* 34(5): 341-350.

**De Planque, M. R., D. T. Rijkers, R. M. Liskamp and F. Separovic** (2004). "The  $\alpha$ M1 transmembrane segment of the nicotinic acetylcholine receptor interacts strongly with model membranes." *Magnetic Resonance Chemistry* 42(2): 148-154.

**Del Castillo, J., W. C. De Mello and T. Morales** (1967). "The initiation of action potentials in the somatic musculature of *Ascaris lumbricoides*." *The Journal of Experimental Biology* 46(2): 263-279.

**Delcastillo, J., W. C. Demello and T. Morales** (1963). "The Physiological Role of Acetylcholine in the Neuromuscular System of *Ascaris lumbricoides*." *Arch Int Physiol Biochim* 71: 741-757.

**Dent, J. A.** (2006). "Evidence for a diverse Cys-loop ligand-gated ion channel superfamily in early bilateria." *Journal of Molecular Evolution* 62(5): 523-535.

**Dent, J. A.** (2010). "The evolution of pentameric ligand-gated ion channels." *Advances in Experimental Medicine and Biology* 683: 11-23.

**Dent, J. A., M. W. Davis and L. Avery** (1997). "*avr-15* encodes a chloride channel subunit that mediates inhibitory glutamatergic neurotransmission and ivermectin sensitivity in *Caenorhabditis elegans*." *The EMBO Journal* 16(19): 5867-5879.

**Dent, J. A., M. M. Smith, D. K. Vassilatis and L. Avery** (2000). "The genetics of ivermectin resistance in *Caenorhabditis elegans*." *Proceedings of the National Academy of Sciences of the United States of America* 97(6): 2674-2679.

- Di, X. J., D. Y. Han, Y. J. Wang, M. R. Chance and T. W. Mu** (2013). "SAHA enhances Proteostasis of epilepsy-associated  $\alpha 1(A322D)\beta 2\gamma 2$  GABA(A) receptors." *Chemical Biology* 20(12): 1456-1468.
- Dickinson, D. J. and B. Goldstein** (2016). "CRISPR-Based Methods for *Caenorhabditis elegans* Genome Engineering." *Genetics* 202(3): 885-901.
- Dickinson, D. J., J. D. Ward, D. J. Reiner and B. Goldstein** (2013). "Engineering the *Caenorhabditis elegans* genome using *Cas9*-triggered homologous recombination." *Nature Methods* 10(10): 1028-1034.
- Du, J., W. Lu, S. Wu, Y. Cheng and E. Gouaux** (2015). "Glycine receptor mechanism elucidated by electron cryo-microscopy." *Nature* 526(7572): 224-229.
- Dufour, V., R. N. Beech, C. Wever, J. A. Dent and T. G. Geary** (2013). "Molecular Cloning and Characterization of Novel Glutamate-Gated Chloride Channel Subunits from *Schistosoma mansoni*." *PLoS Pathogens* 9(8): e1003586.
- Duguet, T. B., C. L. Charvet, S. G. Forrester, C. M. Wever, J. A. Dent, C. Neveu and R. N. Beech** (2016). "Recent Duplication and Functional Divergence in Parasitic Nematode Levamisole-Sensitive Acetylcholine Receptors." *PLoS Neglected Tropical Diseases* 10(7): e0004826.
- Durette-Desset, M. C., J. P. Hugot, P. Darlu and A. G. Chabaud** (1999). "A cladistic analysis of the *Trichostrongyloidea* (Nematoda)." *International Journal for Parasitology* 29(7): 1065-1086.
- Ealing, J., R. Webster, S. Brownlow, A. Abdelgany, H. Oosterhuis, F. Muntoni, . . . D. Beeson** (2002). "Mutations in congenital myasthenic syndromes reveal an epsilon subunit C-terminal cysteine, C470, crucial for maturation and surface expression of adult AChR." *Human Molecular Genetics* 11(24): 3087-3096.

- Eimer, S., A. Gottschalk, M. Hengartner, H. R. Horvitz, J. Richmond, W. R. Schafer and J. L. Bessereau** (2007). "Regulation of nicotinic receptor trafficking by the transmembrane Golgi protein UNC-50." *The EMBO Journal* 26(20): 4313-4323.
- Emery, D. L., P. W. Hunt and L. F. Le Jambre** (2016). "*Haemonchus contortus*: the then and now, and where to from here?" *International Journal for Parasitology* 46(12): 755-769.
- Ericksen, S. S. and A. J. Boileau** (2007). "Tandem couture: Cys-loop receptor concatamer insights and caveats." *Molecular Neurobiology* 35(1): 113-128.
- Fauvin, A., C. Charvet, M. Issouf, J. Cortet, J. Cabaret and C. Neveu** (2010). "cDNA-AFLP analysis in levamisole-resistant *Haemonchus contortus* reveals alternative splicing in a nicotinic acetylcholine receptor subunit." *Molecular and Biochemical Parasitology* 170(2): 105-107.
- Feng, X. P., J. Hayashi, R. N. Beech and R. K. Prichard** (2002). "Study of the nematode putative GABA type A receptor subunits: evidence for modulation by ivermectin." *Journal of Neurochemistry* 83(4): 870-878.
- Fleming, J. T., M. D. Squire, T. M. Barnes, C. Tornoe, K. Matsuda, J. Ahnn, . . . J. A. Lewis** (1997). "*Caenorhabditis elegans* levamisole resistance genes *lev-1*, *unc-29*, and *unc-38* encode functional nicotinic acetylcholine receptor subunits." *The Journal of Neuroscience : the Official Journal of the Society for Neuroscience* 17(15): 5843-5857.
- Floyd, R., E. Abebe, A. Papert and M. Blaxter** (2002). "Molecular barcodes for soil nematode identification." *Molecular Ecology* 11(4): 839-850.
- Forrester, S. G., R. K. Prichard, J. A. Dent and R. N. Beech** (2003). "*Haemonchus contortus*: HcGluCl $\alpha$  expressed in *Xenopus* oocytes forms a glutamate-gated ion channel that is activated by ibotenate and the antiparasitic drug ivermectin." *Molecular and Biochemical Parasitology* 129(1): 115-121.
- Franchini, L. F. and A. B. Elgoyhen** (2006). "Adaptive evolution in mammalian proteins involved in cochlear outer hair cell electromotility." *Molecular Phylogenetic Evolution* 41(3): 622-635.

**Francis, M. M., S. P. Evans, M. Jensen, D. M. Madsen, J. Mancuso, K. R. Norman and A. V. Maricq** (2005). "The Ror receptor tyrosine kinase CAM-1 is required for ACR-16-mediated synaptic transmission at the *C. elegans* neuromuscular junction." *Neuron* 46(4): 581-594.

**Fu, Y. L., Y. J. Wang and T. W. Mu** (2016). "Proteostasis Maintenance of Cys-Loop Receptors." *Advances Protein Chemistry and Structural Biology* 103: 1-23.

**Gally, C., S. Eimer, J. E. Richmond and J. L. Bessereau** (2004). "A transmembrane protein required for acetylcholine receptor clustering in *Caenorhabditis elegans*." *Nature* 431(7008): 578-582.

**B. Gasser** (2013). "The genome and developmental transcriptome of the strongylid nematode *Haemonchus contortus*." *Genome biology* 14(8): R89.

**Gelman, M. S., W. Chang, D. Y. Thomas, J. J. Bergeron and J. M. Prives** (1995). "Role of the endoplasmic reticulum chaperone calnexin in subunit folding and assembly of nicotinic acetylcholine receptors." *The Journal of Biological Chemistry* 270(25): 15085-15092.

**Gendrel, M., G. Rapti, J. E. Richmond and J. L. Bessereau** (2009). "A secreted complement-control-related protein ensures acetylcholine receptor clustering." *Nature* 461(7266): 992-996.

**Ghosh, R., E. C. Andersen, J. A. Shapiro, J. P. Gerke and L. Kruglyak** (2012). "Natural variation in a chloride channel subunit confers avermectin resistance in *C. elegans*." *Science* 335(6068): 574-578.

**Gilleard, J. S.** (2013). "*Haemonchus contortus* as a paradigm and model to study anthelmintic drug resistance." *Parasitology* 140(12): 1506-1522.

**Girod, R., G. Crabtree, G. Ernstom, J. Ramirez-Latorre, D. McGehee, J. Turner and L. Role** (1999). "Heteromeric complexes of  $\alpha 5$  and/or  $\alpha 7$  subunits. Effects of calcium and potential role in nicotine-induced presynaptic facilitation." *Annual New York Academy of Sciences* 868: 578-590.

**Goldin, A. L.** (1991). "Expression of ion channels by injection of mRNA into *Xenopus* oocytes." *Methods in Cell Biology* 36: 487-509.

- Gottschalk, A., R. B. Almedom, T. Schedletzky, S. D. Anderson, J. R. Yates, 3rd and W. R. Schafer** (2005). "Identification and characterization of novel nicotinic receptor-associated proteins in *Caenorhabditis elegans*." *The EMBO Journal* 24(14): 2566-2578.
- Gray, J. and H. W. Lissmann** (1964). "The Locomotion of Nematodes." *The Journal of Experimental Biology* 41: 135-154.
- Green, K. A., S. W. Falconer and G. A. Cottrell** (1994). "The neuropeptide Phe-Met-Arg-Phe-NH<sub>2</sub> (FMRFamide) directly gates two ion channels in an identified Helix neurone." *Pflugers Archiv : European Journal of Physiology* 428(3-4): 232-240.
- Green, W. N. and T. Claudio** (1993). "Acetylcholine receptor assembly: subunit folding and oligomerization occur sequentially." *Cell* 74(1): 57-69.
- Green, W. N. and C. P. Wanamaker** (1997). "The role of the cystine loop in acetylcholine receptor assembly." *The Journal of Biological Chemistry* 272(33): 20945-20953.
- Green, W. N. and C. P. Wanamaker** (1998). "Formation of the nicotinic acetylcholine receptor binding sites." *The Journal of neuroscience : the Official Journal of the Society for Neuroscience* 18(15): 5555-5564.
- Groot-Kormelink, P. J., S. Broadbent, M. Beato and L. G. Sivilotti** (2006). "Constraining the expression of nicotinic acetylcholine receptors by using pentameric constructs." *Molecular Pharmacology* 69(2): 558-563.
- Groot-Kormelink, P. J., S. D. Broadbent, J. P. Boorman and L. G. Sivilotti** (2004). "Incomplete incorporation of tandem subunits in recombinant neuronal nicotinic receptors." *Journal of General Physiology* 123(6): 697-708.
- Hahn, M. W.** (2009). "Distinguishing among evolutionary models for the maintenance of gene duplicates." *The Journal of Heredity* 100(5): 605-617.
- Hales, T. G., J. I. Dunlop, T. Z. Deeb, J. E. Carland, S. P. Kelley, J. J. Lambert and J. A. Peters** (2006). "Common determinants of single channel conductance within the large cytoplasmic loop of 5-

hydroxytryptamine type 3 and  $\alpha 4\beta 2$  nicotinic acetylcholine receptors." *The Journal of Biological Chemistry* 281(12): 8062-8071.

**Halevi, S., J. McKay, M. Palfreyman, L. Yassin, M. Eshel, E. Jorgensen and M. Treinin** (2002).

"The *C. elegans ric-3* gene is required for maturation of nicotinic acetylcholine receptors." *The EMBO Journal* 21(5): 1012-1020.

**Han, D. Y., B. J. Guan, Y. J. Wang, M. Hatzoglou and T. W. Mu** (2015). "L-type Calcium Channel Blockers Enhance Trafficking and Function of Epilepsy-associated  $\alpha 1$ (D219N) Subunits of GABA(A) Receptors." *ACS Chemical Biology* 10(9): 2135-2148.

**Hanna, M. C., P. A. Davies, T. G. Hales and E. F. Kirkness** (2000). "Evidence for expression of heteromeric serotonin 5-HT(3) receptors in rodents." *Journal of Neurochemistry* 75(1): 240-247.

**Hanson, S. M. and C. Czajkowski** (2011). "Disulphide trapping of the GABA(A) receptor reveals the importance of the coupling interface in the action of benzodiazepines." *British Journal of Pharmacology* 162(3): 673-687.

**Hassaine, G., C. Deluz, L. Grasso, R. Wyss, M. B. Tol, R. Hovius, . . . H. Nury** (2014). "X-ray structure of the mouse serotonin 5-HT3 receptor." *Nature* 512(7514): 276-281.

**Haugstetter, J., T. Blicher and L. Ellgaard** (2005). "Identification and characterization of a novel thioredoxin-related transmembrane protein of the endoplasmic reticulum." *The Journal of Biological Chemistry* 280(9): 8371-8380.

**Herd, R. P.** (1986). "Epidemiology and control of nematodes and cestodes in small ruminants. Northern United States." *The Veterinary Clinics of North America. Food Animal Practice* 2(2): 355-362.

**Hernando, G., I. Berge, D. Rayes and C. Bouzat** (2012). "Contribution of Subunits to *C. elegans* Levamisole-Sensitive Nicotinic Receptor Function." *Molecular Pharmacology*.

**Hernando, G., I. Berge, D. Rayes and C. Bouzat** (2012). "Contribution of subunits to *Caenorhabditis elegans* levamisole-sensitive nicotinic receptor function." *Molecular Pharmacology* 82(3): 550-560.



- Hibbs, R. E. and E. Gouaux** (2011). "Principles of activation and permeation in an anion-selective Cys-loop receptor." *Nature* 474(7349): 54-60.
- Hilf, R. J. and R. Dutzler** (2008). "X-ray structure of a prokaryotic pentameric ligand-gated ion channel." *Nature* 452(7185): 375-379.
- Hobert, O.** (2013). "The neuronal genome of *Caenorhabditis elegans*." *WormBook*: 1-106.
- Hobert, O., I. Mori, Y. Yamashita, H. Honda, Y. Ohshima, Y. Liu and G. Ruvkun** (1997). "Regulation of interneuron function in the *C. elegans* thermoregulatory pathway by the *ttx-3* LIM homeobox gene." *Neuron* 19(2): 345-357.
- Holden Dye, L. and R. Walker** (2007). "Anthelmintic drugs." *WormBook*: 1-13.
- Holden-Dye, L., M. Joyner, V. O'Connor and R. J. Walker** (2013). "Nicotinic acetylcholine receptors: A comparison of the nAChRs of *Caenorhabditis elegans* and parasitic nematodes." *Parasitology International*.
- Holland, P. W.** (2015). "Did homeobox gene duplications contribute to the Cambrian explosion?" *Zoological Lett* 1: 1.
- Holterman, M., A. van der Wurff, S. van den Elsen, H. van Megen, T. Bongers, O.**
- Holovachov, . . . J. Helder** (2006). "Phylum-wide analysis of SSU rDNA reveals deep phylogenetic relationships among nematodes and accelerated evolution toward crown Clades." *Molecular and Biological Evolution* 23(9): 1792-1800.
- Hoste, H., C. Chartier and Y. Le Frileux** (2002). "Control of gastrointestinal parasitism with nematodes in dairy goats by treating the host category at risk." *Veterinary Research* 33(5): 531-545.
- James, C. E., A. L. Hudson and M. W. Davey** (2009). "Drug resistance mechanisms in helminths: is it survival of the fittest?" *Trends in Parasitology* 25(7): 328-335.
- Jensen, M. L., A. Schousboe and P. K. Ahring** (2005). "Charge selectivity of the Cys-loop family of ligand-gated ion channels." *Journal of Neurochemistry* 92(2): 217-225.

- Jones, A. and D. Sattelle** (2010). "Diversity of insect nicotinic acetylcholine receptor subunits." *Advances in Experimental Medicine and Biology* 683: 25-43.
- Jones, A. K., A. N. Bera, K. Lees and D. B. Sattelle** (2010). "The cys-loop ligand-gated ion channel gene superfamily of the parasitoid wasp, *Nasonia vitripennis*." *Heredity* 104(3): 247-259.
- Jones, A. K., P. Davis, J. Hodgkin and D. B. Sattelle** (2007). "The nicotinic acetylcholine receptor gene family of the nematode *Caenorhabditis elegans*: an update on nomenclature." *Invertebrate Neuroscience : IN* 7(2): 129-131.
- Jones, A. K. and D. B. Sattelle** (2004). "Functional genomics of the nicotinic acetylcholine receptor gene family of the nematode, *Caenorhabditis elegans*." *BioEssays : News and Reviews in Molecular, Cellular and Developmental Biology* 26(1): 39-49.
- Jones, A. K. and D. B. Sattelle** (2006). "The cys-loop ligand-gated ion channel superfamily of the honeybee, *Apis mellifera*." *Invertebrate Neuroscience : IN* 6(3): 123-132.
- Jones, A. K. and D. B. Sattelle** (2008). "The cys-loop ligand-gated ion channel gene superfamily of the nematode, *Caenorhabditis elegans*." *Invertebrate Neuroscience : IN* 8(1): 41-47.
- Jorgensen, E. M. N., M.L.** (1995). "Neuromuscular junctions in the nematode *C. elegans*." *Seminars in Developmental Biology*.
- Jospin, M., Y. B. Qi, T. M. Stawicki, T. Boulin, K. R. Schuske, H. R. Horvitz, . . . Y. Jin** (2009). "A neuronal acetylcholine receptor regulates the balance of muscle excitation and inhibition in *Caenorhabditis elegans*." *PLoS Biology* 7(12): e1000265.
- Kandel, E. R., J. H. Schwartz and T. M. Jessell** (2000). *Principles of Neural Science*. New York, McGraw-Hill, Health Professions Division.
- Kao, P. N., A. J. Dwork, R. R. Kaldany, M. L. Silver, J. Wideman, S. Stein and A. Karlin** (1984). "Identification of the alpha subunit half-cystine specifically labeled by an affinity reagent for the acetylcholine receptor binding site." *The Journal of Biological Chemistry* 259(19): 11662-11665.

- Karlin, A., E. Holtzman, N. Yodh, P. Lobel, J. Wall and J. Hainfeld** (1983). "The arrangement of the subunits of the acetylcholine receptor of *Torpedo californica*." *The Journal of Biological Chemistry* 258(11): 6678-6681.
- Kehoe, J., S. Buldakova, F. Acher, J. Dent, P. Bregestovski and J. Bradley** (2009). "Aplysia cys-loop glutamate-gated chloride channels reveal convergent evolution of ligand specificity." *Journal of Molecular Evolution* 69(2): 125-141.
- Keller, S. H., J. Lindstrom and P. Taylor** (1996). "Involvement of the chaperone protein calnexin and the acetylcholine receptor beta-subunit in the assembly and cell surface expression of the receptor." *The Journal of Biological Chemistry* 271(37): 22871-22877.
- Keramidas, A., A. J. Moorhouse, P. R. Schofield and P. H. Barry** (2004). "Ligand-gated ion channels: mechanisms underlying ion selectivity." *Progress in Biophysics and Molecular Biology* 86(2): 161-204.
- Kesters, D., A. J. Thompson, M. Brams, R. van Elk, R. Spurny, M. Geitmann, . . . C. Ulens** (2013). "Structural basis of ligand recognition in 5-HT<sub>3</sub> receptors." *EMBO Reports* 14(1): 49-56.
- Krashia, P., M. Moroni, S. Broadbent, G. Hofmann, S. Kracun, M. Beato, . . . L. G. Sivilotti** (2010). "Human  $\alpha 3\beta 4$  neuronal nicotinic receptors show different stoichiometry if they are expressed in *Xenopus* oocytes or mammalian HEK293 cells." *PloS One* 5(10): e13611.
- Kreienkamp, H. J., R. K. Maeda, S. M. Sine and P. Taylor** (1995). "Intersubunit contacts governing assembly of the mammalian nicotinic acetylcholine receptor." *Neuron* 14(3): 635-644.
- Kuchler, K. and J. Thorner** (1992). "Secretion of peptides and proteins lacking hydrophobic signal sequences: the role of adenosine triphosphate-driven membrane translocators." *Endocrine Reviews* 13(3): 499-514.
- Laing, R., T. Kikuchi, A. Martinelli, I. J. Tsai, R. N. Beech, E. Redman, . . . J. A. Cotton** (2013). "The genome and transcriptome of *Haemonchus contortus*, a key model parasite for drug and vaccine discovery." *Genome Biology* 14(8): R88.

- Laing, R., A. Martinelli, A. Tracey, N. Holroyd, J. S. Gilleard and J. A. Cotton** (2016). "*Haemonchus contortus*: Genome Structure, Organization and Comparative Genomics." *Advances in Parasitology* 93: 569-598.
- Lansdell, S., V. Gee, P. Harkness, A. Doward, E. Baker, A. Gibb and N. Millar** (2005). "RIC-3 enhances functional expression of multiple nicotinic acetylcholine receptor subtypes in mammalian cells." *Molecular Pharmacology* 68(5): 1431-1438.
- Lansdell, S. J., T. Collins, J. Goodchild and N. S. Millar** (2012). "The *Drosophila* nicotinic acetylcholine receptor subunits D $\alpha$ 5 and D $\alpha$ 7 form functional homomeric and heteromeric ion channels." *BMC Neuroscience* 13: 73.
- Lee, D. L.** (2002). *The Biology of Nematodes*. London, Taylor & Francis.
- Lees, K., A. K. Jones, K. Matsuda, M. Akamatsu, D. B. Sattelle, D. J. Woods and A. S. Bowman** (2014). "Functional characterization of a nicotinic acetylcholine receptor alpha subunit from the brown dog tick, *Rhipicephalus sanguineus*." *International Journal of Parasitology* 44(1): 75-81.
- Lester, H. A., M. I. Dibas, D. S. Dahan, J. F. Leite and D. A. Dougherty** (2004). "Cys-loop receptors: new twists and turns." *Trends in Neurosciences* 27(6): 329-336.
- Lewis, J. A., C. H. Wu, H. Berg and J. H. Levine** (1980). "The genetics of levamisole resistance in the nematode *Caenorhabditis elegans*." *Genetics* 95(4): 905-928.
- Li, B. W., A. C. Rush and G. J. Weil** (2015). "Expression of five acetylcholine receptor subunit genes in *Brugia malayi* adult worms." *International Journal for Parasitology, Drugs and Drug Resistance* 5(3): 100-109.
- Littleton, J. T. and B. Ganetzky** (2000). "Ion channels and synaptic organization: analysis of the *Drosophila* genome." *Neuron* 26(1): 35-43.
- Loewi, O. and E. Navratil** (1926). "Über humorale Übertragbarkeit der Herznervenwirkung." *Pflüger's Archiv für die gesamte Physiologie des Menschen und der Tiere* 214(1): 678-688.

**Luscher, B., T. Fuchs and C. L. Kilpatrick** (2011). "GABA<sub>A</sub> receptor trafficking-mediated plasticity of inhibitory synapses." *Neuron* 70(3): 385-409.

**Lustigman, S., R. K. Prichard, A. Gazzinelli, W. N. Grant, B. A. Boatin, J. S. McCarthy and M. G. Basanez** (2012). "A research agenda for helminth diseases of humans: the problem of helminthiasis." *PLoS Neglected Tropical Diseases* 6(4): e1582.

**Lynagh, T., R. N. Beech, M. J. Lalande, K. Keller, B. A. Cromer, A. J. Wolstenholme and B. Laube** (2015). "Molecular basis for convergent evolution of glutamate recognition by pentameric ligand-gated ion channels." *Science Reports* 5: 8558.

**Martin, R. J., A. P. Robertson, H. Bjorn and N. C. Sangster** (1997). "Heterogeneous levamisole receptors: a single-channel study of nicotinic acetylcholine receptors from *Oesophagostomum dentatum*." *European Journal of Pharmacology* 322(2-3): 249-257.

**Martin, R. J., A. P. Robertson, S. K. Buxton, R. N. Beech, C. L. Charvet and C. Neveu** (2012). "Levamisole receptors: a second awakening." *Trends in Parasitology*.

**Mathew, M. D., N. D. Mathew, A. Miller, M. Simpson, V. Au, S. Garland, . . . D. Moerman** (2016). "Using *C. elegans* Forward and Reverse Genetics to Identify New Compounds with Anthelmintic Activity." *PLoS Neglected Tropical Diseases* 10(10): e0005058.

**McKay, J. P., D. M. Raizen, A. Gottschalk, W. R. Schafer and L. Avery** (2004). "*eat-2* and *eat-18* are required for nicotinic neurotransmission in the *Caenorhabditis elegans* pharynx." *Genetics* 166(1): 161-169.

**McLane, K. E., X. D. Wu, B. Diethelm and B. M. Conti-Tronconi** (1991). "Structural determinants of  $\alpha$ -bungarotoxin binding to the sequence segment 181-200 of the muscle nicotinic acetylcholine receptor  $\alpha$  subunit: effects of cysteine/cystine modification and species-specific amino acid substitutions." *Biochemistry* 30(20): 4925-4934.

- Meldal, B. H., N. J. Debenham, P. De Ley, I. T. De Ley, J. R. Vanfleteren, A. R. Vierstraete, . . . P. J. Lambhead** (2007). "An improved molecular phylogeny of the *Nematoda* with special emphasis on marine taxa." *Molecular Phylogenetic Evolution* 42(3): 622-636.
- Mellem, J. E., P. J. Brockie, D. M. Madsen and A. V. Maricq** (2008). "Action Potentials Contribute to Neuronal Signalling in *C. elegans*." *Nature Neuroscience* 11(8): 865-867.
- Mello, C. and A. Fire** (1995). "DNA transformation." *Methods in Cell Biology* 48: 451-482.
- Mello, C. C., J. M. Kramer, D. Stinchcomb and V. Ambros** (1991). "Efficient gene transfer in *C. elegans*: extrachromosomal maintenance and integration of transforming sequences." *The EMBO Journal* 10(12): 3959-3970.
- Miledi, R., E. Palma and F. Eusebi** (2006). "Microtransplantation of neurotransmitter receptors from cells to *Xenopus* oocyte membranes: new procedure for ion channel studies." *Methods in Molecular Biology* 322: 347-355.
- Millar, N. S.** (2003). "Assembly and subunit diversity of nicotinic acetylcholine receptors." *Biochemical Society Transactions* 31(Pt 4): 869-874.
- Millar, N. S.** (2009). "A review of experimental techniques used for the heterologous expression of nicotinic acetylcholine receptors." *Biochemical Pharmacology* 78(7): 766-776.
- Millar, N. S. and C. Gotti** (2009). "Diversity of vertebrate nicotinic acetylcholine receptors." *Neuropharmacology* 56(1): 237-246.
- Millar, N. S. and P. C. Harkness** (2008). "Assembly and trafficking of nicotinic acetylcholine receptors (Review)." *Molecular Membrane Biology* 25(4): 279-292.
- Miller, P. S. and A. R. Aricescu** (2014). "Crystal structure of a human GABA<sub>A</sub> receptor." *Nature* 512(7514): 270-275.
- Minier, F. and E. Sigel** (2004). "Techniques: Use of concatenated subunits for the study of ligand-gated ion channels." *Trends in Pharmacological Sciences* 25(9): 499-503.

- Mitreva, M., M. L. Blaxter, D. M. Bird and J. P. McCarter (2005).** "Comparative genomics of nematodes." *Trends in Genetics : TIG* 21(10): 573-581.
- Miyazawa, A., Y. Fujiyoshi, M. Stowell and N. Unwin (1999).** "Nicotinic acetylcholine receptor at 4.6Å resolution: transverse tunnels in the channel wall." *Journal of Molecular Biology* 288(4): 765-786.
- Miyazawa, A., Y. Fujiyoshi and N. Unwin (2003).** "Structure and gating mechanism of the acetylcholine receptor pore." *Nature* 423(6943): 949-955.
- Mongan, N. P., H. A. Baylis, C. Adcock, G. R. Smith, M. S. Sansom and D. B. Sattelle (1998).** "An extensive and diverse gene family of nicotinic acetylcholine receptor  $\alpha$  subunits in *Caenorhabditis elegans*." *Receptors Channels* 6(3): 213-228.
- Morales, A., J. Aleu, I. Ivorra, J. A. Ferragut, J. M. Gonzalez-Ros and R. Miledi (1995).** "Incorporation of reconstituted acetylcholine receptors from *Torpedo* into the *Xenopus* oocyte membrane." *Proceedings of the National Academy of Sciences of the United States of America* 92(18): 8468-8472.
- Morales-Perez, C. L., C. M. Noviello and R. E. Hibbs (2016).** "X-ray structure of the human  $\alpha 4\beta 2$  nicotinic receptor." *Nature* 538(7625): 411-415.
- Mowrey, D. D., M. H. Cheng, L. T. Liu, D. Willenbring, X. Lu, T. Wymore, . . . P. Tang (2013).** "Asymmetric Ligand Binding Facilitates Conformational Transitions in Pentameric Ligand-Gated Ion Channels." *Journal of the American Chemical Society*.
- Nashmi, R., M. E. Dickinson, S. McKinney, M. Jareb, C. Labarca, S. E. Fraser and H. A. Lester (2003).** "Assembly of  $\alpha 4\beta 2$  nicotinic acetylcholine receptors assessed with functional fluorescently labeled subunits: effects of localization, trafficking, and nicotine-induced upregulation in clonal mammalian cells and in cultured midbrain neurons." *The Journal of Neuroscience : the Official Journal of the Society for Neuroscience* 23(37): 11554-11567.

- Nelson, M. E., A. Kuryatov, C. H. Choi, Y. Zhou and J. Lindstrom** (2003). "Alternate stoichiometries of  $\alpha 4\beta 2$  nicotinic acetylcholine receptors." *Molecular Pharmacology* 63(2): 332-341.
- Neveu, C., C. L. Charvet, A. Fauvin, J. Cortet, R. N. Beech and J. Cabaret** (2010). "Genetic diversity of levamisole receptor subunits in parasitic nematode species and abbreviated transcripts associated with resistance." *Pharmacogenetics and Genomics* 20(7): 414-425.
- O'Connor, L. J., S. W. Walkden-Brown and L. P. Kahn** (2006). "Ecology of the free-living stages of major trichostrongylid parasites of sheep." *Veterinary Parasitology* 142(1-2): 1-15.
- Ohno, S.** (1970). Evolution by gene duplication. Berlin; New York, Springer-Verlag.
- Ortells, M. O. and G. G. Lunt** (1995). "Evolutionary history of the ligand-gated ion-channel superfamily of receptors." *Trends in Neurosciences* 18(3): 121-127.
- Parkinson, J., M. Mitreva, C. Whitton, M. Thomson, J. Daub, J. Martin, . . . M. L. Blaxter** (2004). "A transcriptomic analysis of the phylum *Nematoda*." *Nature Genetics* 36(12): 1259-1267.
- Pereira, L., P. Kratsios, E. Serrano-Saiz, H. Sheftel, A. E. Mayo, D. H. Hall, . . . O. Hobert** (2015). "A cellular and regulatory map of the cholinergic nervous system of *C. elegans*." *Elife* 4.
- Peron, S., M. A. Zordan, A. Magnabosco, C. Reggiani and A. Megighian** (2009). "From action potential to contraction: neural control and excitation-contraction coupling in larval muscles of *Drosophila*." *Comparative Biochemistry and Physiology part A: Molecular Integrative Physiology* 154(2): 173-183.
- Poppi, D. P., A. R. Sykes and R. A. Dynes** (1990). "The Effect of Endoparasitism on Host Nutrition - the Implications for Nutrient Manipulation." *Proceedings of the New Zealand Society of Animal Production, Vol 50* 1990 50: 237-243.
- Putrenko, I., M. Zakikhani and J. A. Dent** (2005). "A family of acetylcholine-gated chloride channel subunits in *Caenorhabditis elegans*." *The Journal of Biological Chemistry* 280(8): 6392-6398.



**Qian, H., R. J. Martin and A. P. Robertson** (2006). "Pharmacology of N-, L-, and B-subtypes of nematode nAChR resolved at the single-channel level in *Ascaris suum*." *The FASEB journal : official publication of the Federation of American Societies for Experimental Biology* 20(14): 2606-2608.

**Rand, J. B.** (2007). "Acetylcholine." *WormBook*: 1-21.

**Rapti, G., J. Richmond and J. L. Bessereau** (2011). "A single immunoglobulin-domain protein required for clustering acetylcholine receptors in *C. elegans*." *The EMBO Journal* 30(4): 706-718.

**Rayes, D., M. J. De Rosa, S. M. Sine and C. Bouzat** (2009). "Number and locations of agonist binding sites required to activate homomeric Cys-loop receptors." *The Journal of neuroscience : the official journal of the Society for Neuroscience* 29(18): 6022-6032.

**Renard, E., J. Vacelet, E. Gazave, P. Lapebie, C. Borchellini and A. V. Ereskovsky** (2009). "Origin of the neuro-sensory system: new and expected insights from sponges." *Integrative Zoology* 4(3): 294-308.

**Reynolds, J. A. and A. Karlin** (1978). "Molecular weight in detergent solution of acetylcholine receptor from *Torpedo californica*." *Biochemistry* 17(11): 2035-2038.

**Richmond, J.** (2005). "Synaptic function." *WormBook*: 1-14.

**Richmond, J. E. and E. M. Jorgensen** (1999). "One GABA and two acetylcholine receptors function at the *C. elegans* neuromuscular junction." *Nature Neuroscience* 2(9): 791-797.

**Robertson, A. P., H. E. Bjorn and R. J. Martin** (1999). "Resistance to levamisole resolved at the single-channel level." *The FASEB journal : official publication of the Federation of American Societies for Experimental Biology* 13(6): 749-760.

**Roeber, F., A. R. Jex and R. B. Gasser** (2013). "Impact of gastrointestinal parasitic nematodes of sheep, and the role of advanced molecular tools for exploring epidemiology and drug resistance - an Australian perspective." *Parasites & Vectors* 6: 153.

- Rufener, L., R. Baur, R. Kaminsky, P. Maser and E. Sigel** (2010). "Monepantel allosterically activates DEG-3/DES-2 channels of the gastrointestinal nematode *Haemonchus contortus*." *Molecular Pharmacology* 78(5): 895-902.
- Rufener, L., N. Bedoni, R. Baur, S. Rey, D. A. Glauser, J. Bouvier, . . . A. Puoti** (2013). "*acr-23* Encodes a Monepantel-Sensitive Channel in *Caenorhabditis elegans*." *PLoS Pathogens* 9(8): e1003524.
- Rufener, L., P. Maser, I. Roditi and R. Kaminsky** (2009). "*Haemonchus contortus* acetylcholine receptors of the DEG-3 subfamily and their role in sensitivity to monepantel." *PLoS Pathogens* 5(4): e1000380.
- Saedi, M. S., W. G. Conroy and J. Lindstrom** (1991). "Assembly of *Torpedo* acetylcholine receptors in *Xenopus* oocytes." *The Journal of Cell Biology* 112(5): 1007-1015.
- Safdie, G., J. F. Liewald, S. Kagan, E. Battat, A. Gottschalk and M. Treinin** (2016). "RIC-3 phosphorylation enables dual regulation of excitation and inhibition of *Caenorhabditis elegans* muscle." *Molecular Biology of the Cell* 27(19): 2994-3003.
- Schuske, K., A. A. Beg and E. M. Jorgensen** (2004). "The GABA nervous system in *C. elegans*." *Trends in Neurosciences* 27(7): 407-414.
- Schwarz, E. M., P. K. Korhonen, B. E. Campbell, N. D. Young, A. R. Jex, A. Jabbar, . . . R. B. Gasser** (2013). "The genome and developmental transcriptome of the strongylid nematode *Haemonchus contortus*." *Genome biology* 14(8): R89.
- Schwarz, E. M., Y. Hu, I. Antoshechkin, M. M. Miller, P. W. Sternberg and R. V. Aroian** (2015). "The genome and transcriptome of the zoonotic hookworm *Ancylostoma ceylanicum* identify infection-specific gene families." *Nature Genetics* 47(4): 416-422.

**Shu, H. J., J. Bracamontes, A. Taylor, K. Wu, M. M. Eaton, G. Akk, . . . S. Mennerick** (2012).

"Characteristics of concatemeric GABA(A) receptors containing  $\alpha 4/\delta$  subunits expressed in *Xenopus* oocytes." *British Journal of Pharmacology* 165(7): 2228-2243.

**Sloan, M. A., B. J. Reaves, M. J. Maclean, B. E. Storey and A. J. Wolstenholme** (2015).

"Expression of nicotinic acetylcholine receptor subunits from parasitic nematodes in *Caenorhabditis elegans*." *Molecular and Biochemical Parasitology* 204(1): 44-50.

**Smith, M. P. and D. A. Harper** (2013). "Earth science. Causes of the Cambrian explosion." *Science* 341(6152): 1355-1356.

**Steinbach, J. H. and G. Akk** (2011). "Use of concatemers of ligand-gated ion channel subunits to study mechanisms of steroid potentiation." *Anesthesiology* 115(6): 1328-1337.

**Stock, J. B., B. Rauch and S. Roseman** (1977). "Periplasmic space in *Salmonella typhimurium* and *Escherichia coli*." *The Journal of Biological Chemistry* 252(21): 7850-7861.

**Suarez, V. H., S. L. Cristel and M. R. Buseti** (2009). "Epidemiology and effects of gastrointestinal nematode infection on milk productions of dairy ewes." *Parasite* 16(2): 141-147.

**Sumikawa, K. and T. Nishizaki** (1994). "The amino acid residues 1-128 in the  $\alpha$  subunit of the nicotinic acetylcholine receptor contain assembly signals." *Brain Research. Molecular Brain Research* 25(3-4): 257-264.

**Talwar, S. and J. W. Lynch** (2014). "Phosphorylation mediated structural and functional changes in pentameric ligand-gated ion channels: implications for drug discovery." *International Journal of Biochemistry and Cell Biology* 53: 218-223.

**Tang, Y. T., X. Gao, B. A. Rosa, S. Abubucker, K. Hallsworth-Pepin, J. Martin, . . . M. Mitreva** (2014). "Genome of the human hookworm *Necator americanus*." *Nature Genetics* 46(3): 261-269.

**Tasneem, A., L. M. Iyer, E. Jakobsson and L. Aravind** (2005). "Identification of the prokaryotic ligand-gated ion channels and their implications for the mechanisms and origins of animal Cys-loop ion channels." *Genome Biology* 6(1): R4.

**Thienpont, D., O. F. Vanparijs, A. H. Raeymaekers, J. Vandenberg, J. A. Demoen, F. T. Allewijn, . . . P. A. Janssen** (1966). "Tetramisole (R 8299), a new, potent broad spectrum anthelmintic." *Nature* 209(5028): 1084-1086.

**Thompson, A. J., H. A. Lester and S. C. Lummis** (2010). "The structural basis of function in Cys-loop receptors." *Quarterly Reviews of Biophysics* 43(4): 449-499.

**Touroutine, D., R. M. Fox, S. E. Von Stetina, A. Burdina, D. M. Miller, 3rd and J. E. Richmond** (2005). "*acr-16* encodes an essential subunit of the levamisole-resistant nicotinic receptor at the *Caenorhabditis elegans* neuromuscular junction." *The Journal of Biological Chemistry* 280(29): 27013-27021.

**Towers, P. R., B. Edwards, J. E. Richmond and D. B. Sattelle** (2005). "The *Caenorhabditis elegans* *lev-8* gene encodes a novel type of nicotinic acetylcholine receptor  $\alpha$  subunit." *Journal of Neurochemistry* 93(1): 1-9.

**Tsetlin, V., D. Kuzmin and I. Kasheverov** (2011). "Assembly of nicotinic and other Cys-loop receptors." *Journal of Neurochemistry* 116(5): 734-741.

**Tyagi, R., A. Joachim, B. Ruttkowski, B. A. Rosa, J. C. Martin, K. Hallsworth-Pepin, . . . M. Mitreva** (2015). "Cracking the nodule worm code advances knowledge of parasite biology and biotechnology to tackle major diseases of livestock." *Biotechnology Advances* 33(6 Pt 1): 980-991.

**Unwin, N.** (1993). "Nicotinic acetylcholine receptor at 9Å resolution." *Journal of Molecular Biology* 229(4): 1101-1124.

**Unwin, N.** (2005). "Refined structure of the nicotinic acetylcholine receptor at 4Å resolution." *Journal of Molecular Biology* 346(4): 967-989.

**van Wyk, J. A., F. S. Malan and J. L. Randles** (1997). "How long before resistance makes it impossible to control some field strains of *Haemonchus contortus* in South Africa with any of the modern anthelmintics?" *Veterinary Parasitology* 70(1-3): 111-122.

- Vembar, S. S. and J. L. Brodsky** (2008). "One step at a time: endoplasmic reticulum-associated degradation." *Nat Rev Mol Cell Biol* 9(12): 944-957.
- Voglis, G. and N. Tavernarakis** (2006). "The role of synaptic ion channels in synaptic plasticity." *EMBO Reports* 7(11): 1104-1110.
- Waijers, S., V. Portegijs, J. Kerver, B. B. Lemmens, M. Tijsterman, S. van den Heuvel and M. Boxem** (2013). "CRISPR/Cas9-targeted mutagenesis in *Caenorhabditis elegans*." *Genetics* 195(3): 1187-1191.
- Waller, P. J., L. Rudby-Martin, B. L. Ljungstrom and A. Rydzik** (2004). "The epidemiology of abomasal nematodes of sheep in Sweden, with particular reference to over-winter survival strategies." *Veterinary Parasitology* 122(3): 207-220.
- Walley, J. K.** (1966). "Tetramisole (dl 2,3,5,6-tetrahydro-6-phenyl-imidazo (2,1-b) thiazole hydrochloride--Nilverm) in the treatment of gastro-intestinal worms and lungworms in domestic animals. 1. Sheep and goats." *The Veterinary Record* 78(12): 406-414.
- Walstab, J., C. Hammer, F. Lasitschka, D. Moller, C. N. Connolly, G. Rappold, . . . B. Niesler** (2010). "RIC-3 exclusively enhances the surface expression of human homomeric 5-hydroxytryptamine type 3A (5-HT3A) receptors despite direct interactions with 5-HT3A, -C, -D, and -E subunits." *The Journal of Biological Chemistry* 285(35): 26956-26965.
- Wanamaker, C. P., J. C. Christianson and W. N. Green** (2003). "Regulation of nicotinic acetylcholine receptor assembly." *Annual New York Academy of Sciences* 998: 66-80.
- White, J. G., E. Southgate, J. N. Thomson and S. Brenner** (1976). "The structure of the ventral nerve cord of *Caenorhabditis elegans*." *Philosophical transactions of the Royal Society of London. Series B, Biological sciences* 275(938): 327-348.
- White, J. G., E. Southgate, J. N. Thomson and S. Brenner** (1986). "The structure of the nervous system of the nematode *Caenorhabditis elegans*." *Philosophical Transactions of the Royal Society of London. Series B, Biological Sciences* 314(1165): 1-340.

- White, J. G., E. Southgate, J. N. Thomson and S. Brenner** (1986). "The structure of the nervous system of the nematode *Caenorhabditis elegans*." *Philosophical transactions of the Royal Society of London. Series B, Biological sciences* 314(1165): 1-340.
- Williamson, S., A. Robertson, L. Brown, T. Williams, D. Woods, R. Martin, . . . A. Wolstenholme** (2009). "The nicotinic acetylcholine receptors of the parasitic nematode *Ascaris suum*: formation of two distinct drug targets by varying the relative expression levels of two subunits." *PLoS Pathogens* 5(7): e1000517-e1000517.
- Williamson, S. M., T. K. Walsh and A. J. Wolstenholme** (2007). "The cys-loop ligand-gated ion channel gene family of *Brugia malayi* and *Trichinella spiralis*: a comparison with *Caenorhabditis elegans*." *Invertebrate Neuroscience : IN* 7(4): 219-226.
- Wolstenholme, A. J.** (2012). "Glutamate-gated Chloride Channels." *The Journal of Biological Chemistry*.
- Wolstenholme, A. J. and A. T. Rogers** (2005). "Glutamate-gated chloride channels and the mode of action of the avermectin/milbemycin anthelmintics." *Parasitology* 131 Suppl: S85-95.
- Yifrach, O.** (2004). "Hill coefficient for estimating the magnitude of cooperativity in gating transitions of voltage-dependent ion channels." *Biophysical Journal* 87(2): 822-830.
- Zajac, A. M.** (2006). "Gastrointestinal nematodes of small ruminants: life cycle, anthelmintics, and diagnosis." *The Veterinary Clinics of North America. Food Animal Practice* 22(3): 529-541.
- Zhou, Y., M. E. Nelson, A. Kuryatov, C. Choi, J. Cooper and J. Lindstrom** (2003). "Human alpha4beta2 acetylcholine receptors formed from linked subunits." *The Journal of Neuroscience : the Official Journal of the Society for Neuroscience* 23(27): 9004-9015.